JEAN MAYER USDA HUMAN NUTRITION RESEARCH CENTER ON AGING

HNRCA

The Role of Adipocyte Tryptophan Hydroxylase 2 on the Adipose tissue and Systemic Metabolism.

A dissertation presented to
the faculty of the Gerald J. and Dorothy R. Friedman School
of Nutrition Science and Policy
in partial fulfillment of the requirements for the degree of Doctor of Philosophy in
Biochemical and Molecular Nutrition through Tufts University.

By

Brian In-Soon Park

Tufts UNIVERSITY | GERALD J. AND DOROTHY R. Friedman School of Nutrition Science and Policy

Acknowledgements

I am deeply grateful to everyone who has contributed to the successful completion of this thesis. Their support, encouragement, and assistance have been invaluable throughout this challenging journey.

First and foremost, I would like to express my sincere gratitude to my thesis mentor Dr. Andrew S. Greenberg. His guidance, expertise, and patience played a crucial role in shaping this thesis. His insightful feedback and constant encouragement motivated me to strive for excellence.

I extend my heartfelt appreciation to the members of my thesis committee, Dr. Christopher D. Wiley, Dr. Donato A. Rivas, and Dr. Dong Kong, for dedicating their time and expertise to review and provide valuable insights that significantly improved the quality of this work.

I am thankful to the faculties and staffs of both Gerald J. and Dorothy R. Friedman School of Nutrition Science and Policy at Tufts University and Jean Mayer USDA Human Nutrition Research Center on Aging. Their commitment to excellence in education has provided me with a nurturing academic environment and the resources necessary for conducting my research.

I would also like to acknowledge the support of my friends and the members of Obesity and Metabolism laboratory who have been with me every step of the way. Their camaraderie and encouragement made this academic journey more enjoyable and less daunting.

To my loved ones, I owe a debt of gratitude for their unwavering love and support. Their belief in me and their sacrifices have been the driving force behind my achievements.

Lastly, I express my gratitude to my former mentor Dr. Dong-Mi Shin, who recently left us for heavenly abode. She was the first one to recognize my potential as a researcher, and I would have not started the PhD journey without her guidance.

Although it is impossible to mention everyone who has contributed to my growth and the completion of this thesis, please know that your support is deeply appreciated.

Thank you all for being part of this incredible journey.

Table of Contents

Abstract 8

Abbreviations 10

Chapter 1. Introduction 12

1.1. Background 12

Obesity and adipocyte biology 12

Obesity-induced adipocyte dysfunctions 13

Brown and beige adipocytes in obesity 17

Adipocyte oxidative stress in obesity 19

The role of 5-HT in physiology 21

Peripheral 5-HT and obesity 23

1.2. Research Objectives 26

Figure 1. Central Hypothesis and Expected Outcomes in Each Specific Aim. 28

1.3. References 29

Chapter 2. The effect of adipocyte-specific over-expression of TPH2 on adipocyte dysfunction and energy metabolism. 37

2.1. Introduction 37

2.2. Materials & Methods 40

Experimental animals 40

Generation of TPH2 over-expressing AAV 41

AAV injection 41

Metabolic phenotyping 42

Glucose tolerance test 42

Insulin tolerance test 43

Plasma and serum profile analysis 43

5-HT quantification 44

4-HNE quantification 44

Immunohistochemistry and immunofluorescence 45

RNA isolation and real-time quantitative PCR 46

Statistics 46

2.3. Results 47

Epidydimal adipocyte-specific TPH2 over-expression is not sufficient to induce systemic changes in body composition, but significantly increases plasma serotonin level, BAT and eWAT mass. 47

Adipocyte TPH2 over-expression impairs glucose tolerance and insulin sensitivity. 48

TPH2 overexpression increases eWAT adiposity through upregulation of lipogenic gene expression and induced pro-inflammatory and p53 signaling gene expressions. 49

TPH2 over-expression induces eWAT 4-HNE formation and increases circulating 4-HNE level. 50

Epididymal adipocyte-specific TPH2 over-expression increases iWAT adiposity through increased lipogenic signaling and decreased lipolysis. 51

Epididymal adipocyte-specific TPH2 over-expression induces hepatic steatosis through decreased lipogenesis. 51

Epididymal adipocyte-specific TPH2 over-expression induces hepatic 4-HNE accumulation. 52

TPH2 over-expression in epididymal adipocytes decreases systemic energy expenditure. 53

2.4. Discussion 54

2.5. Figures 60

Figure 1. Epididymal Adipocyte-specific TPH2 Over-expression Increases Circulating 5-HT Level and eWAT and BAT mass. 60

Figure 2. Tph2 Oex Mice Exhibit Increases Fasting Insulin Level, Glucose Intolerance and Insulin Resistance. 61

Figure 3. TPH2 Over-expression of Epididymal Adipocyte Induces Changes in eWAT Adiposity and Gene Expression Profile. 62

Figure 4. Elevated 4-HNE Formation in Tph2 Oex eWAT and Circulating 4-HNE level 63

Figure 5. TPH2 Over-expression of Epididymal Adipocyte Induces Changes in iWAT Adiposity and Gene Expression Profile. 64

Figure 6. Epididymal Adipocyte TPH2 Induces Changes in Hepatic Steatosis and Liver Gene Expression Profile. 65

Figure 7. Tph2 Oex Mice Have Increased 4-HNE Accumulation in Liver. ... 66

Figure 8. Epididymal Adipocyte TPH2 Over-expression Increases Systemic Energy Expenditure. 68

Figure 9. Epididymal Adipocyte TPH2 Induces Changes in BAT Gene Expression Profile. 69

Figure S2. No Differences on iWAT 4-HNE Accumulation Between Tph2 Con and Oex Mice. 71

Figure S3. Fasting Plasma Lipid Profile of Each Group. 72

Figure S4. Oxygen Consumption, Carbon Dioxide Production and Total Moving Distance in Indirect Calorimetry Analysis. 74

Supplementary Table 1. Primer sequences used in this study 75

2.6. References 76

Chapter 3. Adipocyte-specific deficiency of TPH2 induced metabolic changes in HFD fed mice. 80

3.1. Introduction 80

3.2. Materials & Methods 83

Experimental animals....83

Metabolic phenotyping....84

BAT Thermal imaging....84

Glucose tolerance test....85

Insulin tolerance test....85

Total gastrointestinal transit time assay....86

Fecal bomb calorimetry....86

Plasma and serum profile analysis....86

5-HT quantification....87

Adipocyte isolation....87

Immunohistochemistry analysis....88

RNA isolation and real-time quantitative PCR....88

Statistics....89

3.3. Results....90

TPH2 is specifically ablated in adipocytes and increased adiposity induces TPH2 upregulation in DIO.....90

Adipocyte-specific ablation of TPH2 improves glucose tolerance and insulin sensitivity in obese mice.....91

Genetic ablation of adipocyte-specific TPH2 reduces eWAT adiposity through upregulation of lipolysis gene expression, and reduces pro-inflammatory and p53 signaling gene expressions.....92

Loss of adipocyte TPH2 derived 5-HT protected mice from DIO induced hepatic steatosis and liver damage.....93

Abolishing TPH2 expression in epididymal adipocytes increases systemic energy expenditure and BAT activation through upregulation of *Ucp-1* and *Prdm16*. 94

Adipocyte-specific loss of TPH2 increases gut transit time, and reduces fecal energy loss, resulting in enhanced energy absorption. 95

3.5. Figures 101

Figure 3. HFD-KO Mice Exhibit Decreased Fasting Blood Glucose and Insulin Level, Glucose Intolerance and Insulin Resistance. 103

Figure 4. Adipocyte-specific Deficiency of TPH2 Induces Changes in eWAT Adiposity and 5-HT level. 104

Figure 5. Adipocyte-specific Deficiency of Tph2 Induces Changes in eWAT Gene Expression Profile. 105

Figure 6. Adipocyte-specific Deficiency of TPH2 Induced Changes in Hepatic Steatosis and Liver Damage. 106

Figure 7. Genetic Ablation of Adipocyte-specific TPH2 Increases Systemic Energy Expenditure. 108

Figure 8. HFD-KO Mice Exhibit Increased BAT Activation and Altered Gene Expression Profile. 109

Figure 9. Adipocyte-specific TPH2 Deletion Reduce Gut Motility and Fecal Energy Loss 110

Figure S1. *Tph2* Gene Expression in Isolated Brown Adipocytes with HFD Feeding and Over-eating 111

Figure S3. Fasting Plasma Lipid Profile of Each Group. 112

Figure S4. Oxygen Consumption, Carbon Dioxide Production and RER in Indirect Calorimetry Analysis. 114

Supplementary Table 1. Primer sequences used in this study. 115

3.6. References 116

Chapter 4. Limitations and future directions 122

4.1. Limitations 122

Chapter 2 122

Chapter 3 123

4.2. Future directions 125

Chapter 2 125

Chapter 3 126

Abstract

The prevalence of obesity is rapidly rising worldwide, reaching a concerning epidemic state with profound socio-economic consequences. Both epidemiological and animal model studies have demonstrated that obesity has a strong association with the development of cardiovascular diseases, non-alcoholic fatty liver and type 2 diabetes mellitus (T2DM). With development of diet-induced obesity (DIO), white adipose tissues (WAT) start to expand their mass by increasing cell number and cell size to store extra calories as fat for the future needs. However, as chronic over-nutrition state prolongs, excessive fat accumulation in WATs alters adipocyte biology and cause dysfunction, such as chronic inflammation, oxidative stress, insulin resistance and adipocyte death. Despite the influence of adipocytes on progression of obesity-induced pathologies and systemic metabolism, underlying molecular mechanisms of how obesity changes adipocyte biology and its impact on metabolic health are still largely unknown.

While multiple mechanisms contribute to metabolic complications in DIO, recent line of evidence highlighted the possible role of peripheral serotonin (5-HT) on regulating both adipocyte and systemic metabolisms. Originally, 5-HT, the tryptophan derived neurotransmitter and hormone, has been found to have primary roles in the brain. However, recent development on the field have discovered that 5-HT in periphery modulates energy metabolism via multifaceted signaling pathways and also contributes to the development of obesity. Genetic deletion of adipocyte-specific tryptophan hydroxylase 1 (TPH1), a rate-limiting enzyme in peripheral 5-HT synthesis, protects against the development of DIO and insulin resistance. Our preliminary data and other studies have demonstrated that high-fat diet (HFD) feeding dramatically increases the gene expression of *Tph2*, a gene encoding isozyme of TPH1 which primarily expressed in the central nervous system (CNS), in epididymal white adipose tissues (eWAT) of mice. However, TPH2 was lowly expressed in the adipocytes from low-fat diet or chow-diet (Chow) fed mice compared to that of HFD fed mice. Although the metabolic regulation by TPH1 in the peripheral tissue has been extensively explored, the peripheral role of adipocyte TPH2 remains elusive. Therefore, the specific aims of this project are: Aim 1) To investigate the effect of adipocyte-specific over-expression of TPH2 on adipocyte dysfunction and energy metabolism; Aim 2) To determine the effect of adipocyte-specific TPH2 deficiency on regulating adipocyte and systemic metabolism in HFD-fed mice.

In Aim 1, to investigate the effect of adipocyte-specific over-expression of TPH2 on adipocyte dysfunction and energy metabolism, we used adeno-associated virus (AAV) to constitutively over-express TPH2 only in epididymal adipocytes in the absence of HFD feeding. Body composition analysis revealed that epididymal adipocyte-specific TPH2 over-expression did not alter whole body composition, however, eWAT and brown adipose tissue (BAT) mass were significantly increased. Mice with TPH2 over-expression exhibited increased fasting insulin level, glucose intolerance and insulin resistance. With over-expression of TPH2, eWAT adipocyte

sizes were enlarged, and also expression levels of lipogenesis, inflammation and p53 signaling associated genes were highly upregulated, demonstrating adipocyte dysfunction. We found increased 4-HNE formation and accumulation in eWAT, liver and plasma, suggesting the association between TPH2 derived 5-HT and lipid peroxidation. Over-expression of TPH2 also contributed to the development of hepatic steatosis. Finally, upregulation of epididymal adipocyte TPH2 expression significantly reduced systemic energy expenditure by inhibiting BAT activation. Overall, these data suggest the crucial role of adipocyte TPH2 derived 5-HT in developing obesity-induced adipocyte dysfunctions and metabolic complications.

In Aim 2, to determine the effect of adipocyte-specific TPH2 deficiency on regulating adipose tissues and systemic metabolism in HFD-fed mice, we generated an adipocyte-specific knockout mouse model of TPH2 and fed either Chow or HFD. We found that adipocyte- specific loss of TPH2 did not prevent the development of DIO. However, HFD fed adipocyte TPH2 knockout mice exhibited significantly reduced fasting insulin levels, improved glucose tolerance and insulin resistance compared to HFD fed control mice. eWAT adiposity was also decreased with adipocyte-specific deficiency of TPH2 in HFD fed mice, and expression levels of lipolysis, inflammation and p53 related genes were significantly downregulated. Furthermore, DIO induced hepatic steatosis and liver damage was significantly improved with the ablation of adipocyte-specific TPH2. Mice without adipocyte TPH2 exhibited increased BAT activation and systemic energy expenditure. Adipocyte-specific deletion of TPH2 decreased gut motility which increased total gut transit time, resulting in significant reduction in fecal energy loss and compensation of increased energy expenditure. Collectively, these data indicate that the possible role of adipocyte TPH2 in regulating whole body energy homeostasis, which encompasses both energy expenditure and harvesting.

Through the completion of this thesis project, we demonstrated that the contribution of adipocyte-specific TPH2 to the development of DIO is a multifaceted and complex process that includes both 5-HTR mediated signaling and intracellular molecular pathways. Our results provide a novel insight into how adipocyte-specific TPH2 induces significant changes in adipocyte biology that could result in the progression of obesity and its associated dysfunctions.

Abbreviations

5-HT	Serotonin
5-HTR	Serotonin receptor
ATM	Adipose tissue macrophages
ATP	Adenosine triphosphate
Atgl	Adipose triglyceride lipase
ALT	Alanine transaminase
AST	Aspartate aminotransferase
BBB	Blood brain barrier
BAT	Brown adipose tissue
Cidea	cell death inducing DFFA like effector a
CNS	Central nervous system
DIO	Diet-induced obesity
ETC	Electron transport chain
eWAT	Epididymal white adipose tissue
Fasn	Fatty acid synthase
GLUT	Glucose transporter
Hsl	Hormone sensitive lipase
HIF-1α	Hypoxia-inducible factor 1 alpha
IL-1β	Interleukin-1 beta
IL-6	Interleukin-6
IRS	Insulin receptor substrates
iWAT	Inguinal white adipose tissue
mWAT	Mesenteric white adipose tissue
Maoa	Monoamine oxidase A
Mcp-1	Monocyte chemoattractant protein-1
NEFA	Non-esterified fatty acid
NF-κB	Nuclear factor-kappa B
Ppargc1a	Peroxisome proliferator-activated receptor-gamma coactivator-1 alpha

PI3K Phosphatidylinositol 3-kinase

PIP3 Phosphatidylinositol (3,4,5)-trisphosphate

PKB Protein kinase B

Ppar Peroxisome proliferator-activated receptor

PUFA Polyunsaturated fatty acid

RER Respiratory Exchange Ratio

ROS Reactive oxygen specie

SEM Standard error of the mean

Srebp1c Sterol Regulatory Element-binding Protein-1c

T2DM Type 2 diabetes mellitus

TG Triglyceride

Tnfa Tumor necrosis factor-alpha

Ucp1 Uncoupling protein-1

WAT White adipose tissue

Chapter 1. Introduction

1.1. Background

Obesity and adipocyte biology

Global incidence of obesity is rising at alarming rate, and obesity is becoming an epidemic as well as a socio-economic burden[1,2]. Being overweight or obese is associated with the development of non-communicable diseases including atherosclerosis, nonalcoholic fatty liver, hypertension and T2DM[3,4]. While, many factors, such as sedentary life style, gut microbiome profile and genetic differences promote the development of obesity, chronic energy imbalance between calorie intake and energy expenditure is undoubtedly a major contributor[5]. Consuming high-fat and high-sugar diet, such as Western diet (high in fat and refined carbohydrate with low vegetables and fruits), could easily overthrow the balance between calorie intake and energy expenditure. Western diet has much higher calorie content than regular balanced diet, but it also stimulates appetite and increases the amount of food consumed[6,7]. This vicious cycle further reinforces the over-nutrition state and if prolonged, excessive energy will be ultimately converted and stored as fat, which will lead to the development of obesity.

Storage of surplus calorie as fat is a core homeostatic process that is crucial for survival of the organism[8]. Adipocytes, a major component of adipose tissue, are a type of cell that specializes in converting the excess energy into triglyceride (TG)[9]. This process is called lipogenesis, and TG is primarily synthesized from glucose and fatty acids obtained from the diet[10]. Synthesized TGs are then packaged into lipid

droplets within the adipocytes. As energy is stored in lipid droplets, the adipocytes expand in size (hypertrophy) and can also proliferate (hyperplasia) to accommodate additional TGs[11]. In obesity, adipose tissue undergoes both hypertrophy and hyperplasia, however the relative contributions of hypertrophy and hyperplasia to adipose tissue expansion in obesity can vary among individuals due to factors such as genetics, age, and the duration and severity of obesity[12]. In some cases, hypertrophy may be the predominant mechanism, while in others, hyperplasia may play a more significant role. The balance between hypertrophy and hyperplasia can have implications for metabolic health. Previous studies demonstrated that adipocyte hypertrophy is associated with increased inflammation, insulin resistance, and metabolic dysfunction[13,14]. In contrast, adipocyte hyperplasia, when it occurs in a healthy manner, has been suggested to have a more favorable metabolic profile[15].

Obesity-induced adipocyte dysfunctions

As adipocytes expand in size due to excess lipid accumulation in obesity, the level of oxygen and nutrient demands also increase. However, the expansion of adipose tissue vasculature cannot keep pace with adipocyte growth, resulting in inadequate blood supply to meet oxygen needs of enlarged adipocytes[16,17]. Prolonged insufficient oxygen supply leads to local hypoxia within the adipose tissue, and hypoxic state of adipocytes has been implicated with the development of multiple adipocyte dysfunctionality, such as chronic inflammation, altered adipokine secretion, impaired insulin sensitivity and adipocyte death. Hypoxia in adipose tissue leads to the activation of a transcription factor called hypoxia-inducible factor 1 alpha (HIF-1α).

Hypoxia-induced HIF-1α activation promotes the expression and activity of Nuclear Factor-Kappa B (NF-κB) by directly interacting with NF-κB subunits or regulating the expression of genes involved in NF-κB activation[18,19]. With NF-κB activation, adipocytes secrete cytokines, such as tumor necrosis factor-alpha (TNF-α), interleukin-6, interleukin-1 beta (IL-1β) and monocyte chemoattractant protein-1 (MCP-1) [20,21]. Elevated levels of pro-inflammatory cytokines in adipose tissue has been associated with the infiltration of immune cells (mast cells, dendritic cells and macrophages) into adipose tissue, and contribute to chronic low-grade inflammation within adipose tissue[22]. In both obese rodents and humans, strong positive correlation has been observed between the adipose tissue infiltration of macrophages and adiposity[22]. These adipose tissue macrophages (ATM) further reinforce the recruitment of other immune cells by secreting pro-inflammatory mediators[23]. Furthermore, ATMs initiate the apoptosis of morbidly enlarged adipocytes by surrounding them and a forming crown-like structure to maintain homeostasis of the adipose tissue[24]. This process causes adipocyte death, which has been demonstrated to induce adipokine dysregulation, insulin resistance, dyslipidemia and hepatic steatosis[25].

Adipocytes secrete various bioactive substances called adipokines. In obesity, disruption of adipokine secretion occurs, such as leptin, the first adipokine that was discovered in 1994[26]. Leptin is primarily secreted by adipocytes and acts as a hormone to regulate energy balance and appetite[27]. In obesity, circulating leptin levels are generally elevated in obesity due to increased adiposity. Nevertheless, obese individuals often develop leptin resistance, where the brain becomes less responsive

to the satiety signals of leptin[28]. This resistance contributes to increased appetite, reduced energy expenditure, and a positive energy balance, exacerbating obesity[29]. Additionally, secretion of other adipokines, such as adiponectin, chemerin and resistin is altered in obese adipocytes. Adiponectin has been shown to increase insulin sensitivity, energy expenditure and exert anti-inflammatory properties[30,31]. Chemerin and resistin have been linked to adipocyte insulin resistance and inflammation[32–34]. Overall, the dysregulation of adipokine secretion in obesity contributes to altered metabolic and inflammatory processes, ultimately leading to insulin resistance, systemic inflammation, and increased risks of metabolic disorders. Although the underlying molecular mechanism of adipokine dysregulation in obesity is not fully elucidated, understanding the role of adipokines in obesity development and progression is important for unraveling potential therapeutic targets for managing obesity and its associated health risks.

Insulin resistance is one of the key pathophysiology of DIO. Not all obese individuals with insulin resistance develop T2DM, however it is evident that insulin resistance plays a significant role on impairing glucose homeostasis[35]. Insulin is a hormone secreted by pancreatic β-cells[36]. The vital role of insulin is maintaining adequate blood glucose level preventing the occurrence of hypoglycemia or hyperglycemia[36]. Persistent abnormalities in glucose homeostasis, either due to the insulin resistance or other factors, have been implicated with the development and progression of multiple pathologies such as atherosclerosis, neuropathy, retinopathy and T2DM[37].

Obesity induced insulin resistance is a very complex multifactorial pathophysiology which involves multiple tissue dysfunctions. Circulating insulin regulates systemic metabolism of macronutrients (carbohydrate, protein and fat) through multiple signaling pathways via activation of insulin receptors[38]. The binding of insulin to its receptor triggers a series of intracellular events. The insulin receptor undergoes a conformational change, leading to autophosphorylation of specific tyrosine residues within the receptor[39]. The phosphorylated insulin receptor recruits and phosphorylates insulin receptor substrates (IRS), specifically IRS-1 and IRS-2. Phosphorylated IRS proteins serve as docking sites for downstream signaling molecules. Activated IRS proteins bind and activate phosphatidylinositol 3-kinase (PI3K), which leads to the generation of phosphatidylinositol (3,4,5)-trisphosphate (PIP3). PIP3 activates protein kinase B (PKB/Akt), a key mediator of insulin signaling. Akt phosphorylates and activates various downstream targets, including AS160 (Akt substrate of 160 kDa). Phosphorylated AS160 facilitates the translocation of glucose transporter 4 (GLUT4) vesicles from intracellular compartments to the cellular membrane of adipocytes[40–42]. Once translocated to the plasma membrane, GLUT4 proteins enable the facilitated diffusion of glucose into adipocytes. The increased presence of GLUT4 on the adipocyte surface enhances the capacity of adipocytes to uptake glucose from the bloodstream, helping to regulate blood glucose levels and store excess glucose as energy reserves[43]. Impairments in insulin signaling, such as insulin resistance, can disrupt this process and contribute to metabolic disorders.

However, with the onset of obesity, adipocytes become less responsive to insulin, and this alters adipocyte physiology and energy metabolism. Lack of insulin

signaling inhibits lipogenesis, while promotes lipolysis[44]. As a result, adipocyte increases breakdown intracellular lipid droplets and release FFA to circulation. Increased level of circulating FFA contribute to ectopic fat deposition and cause lipotoxicity and insulin resistance in liver and muscle tissues[45]. Liver and muscle tissues could uptake and convert glucose into glycogen to use them as rapid energy source and maintain glucose homeostasis[46,47]. In the human body, the liver is the only organ capable of *de novo* glucose synthesis (gluconeogenesis) and orchestrates the whole body glucose metabolism through complex process[48]. Unlike adipocytes, both hepatocytes and myocytes are not specialized in accumulating intracellular lipid, the presence of lipid droplets in these cells are associated with metabolic dysfunction. Notably, hepatic and myocytic lipid depositions are strongly associated with insulin resistance in obese individuals[49–51]. Collectively, liver plays a central role in regulating blood glucose levels through balancing glucose uptake and output. In contrast, muscles primarily utilize glucose to generate glycogen for their own energy needs during physical activity. The coordinated glucose metabolism between the liver and muscles helps to maintain stable blood glucose levels and meet the energy demands of the body under different physiological conditions.

Brown and beige adipocytes in obesity

Alongside aforementioned obesity mediated dysfunctionalities, obesity affects adipocyte energy metabolism, contributing to altered energy balance[52]. Brown adipocyte is a distinctive type of adipocyte, which has much higher content of mitochondria compared to regular white adipocytes. Mitochondria-rich adipocytes

were found to have a unique capacity for thermogenesis, specifically non-shivering thermogenesis, the process of generating heat without cold-induced shivering[53]. Because brown adipocyte mitochondria express protein called uncoupling protein 1 (UCP1), which dissipates the inner mitochondrial electrochemical gradient to generate heat without producing Adenosine triphosphate (ATP)[54]. Previous studies demonstrated that obese individuals have less BAT mass as well as their BAT thermogenic activity is lower compared to lean personlas[55,56]. The activity of key thermogenic protein UCP1 is downregulated in BAT of obese individuals, and this decrease limits the ability of brown adipocytes to serve as a 'metabolic sink' for burning excess calories[57]. Furthermore, the recent discovery of beige adipocytes challenged the traditional view that the human brown adipocytes were only present in specific depots and restricted to early life stages[58]. WAT in mice and humans can undergo a process called "browning" or "beiging" when exposed to certain stimuli, such as cold temperature or β3-adrenergic signaling[59–61]. Browning of WAT involves the induction of brown-like characteristics, including the expression of UCP1, cell death inducing DFFA like effector a (CIDEA) and peroxisome proliferator-activated receptor-gamma coactivator-1 alpha (PGC-1α) and increased thermogenic capacity[62]. In obesity, the beiging process is inhibited because of increase in molecules such as transforming growth factor beta and Notch signaling, resulting in a reduced number and activity of beige adipocytes within WAT depots[63,64]. Promoting beiging of white adipocytes may hold therapeutic potential for combating obesity and metabolic disorders by harnessing the thermogenic capacity of brown and beige adipocytes to increase energy expenditure.

Adipocyte oxidative stress in obesity

In addition to dysregulation of brown and beige adipocytes, obesity also has been associated with increased oxidative stress in adipose tissue. Cellular oxidative stress is caused by imbalance between reactive oxygen species (ROS) and antioxidant defense mechanisms[65]. The majority of cellular ROS originates from mitochondrial electron transport chain (ETC), especially complex I and III[66]. Chronic over-nutrition state provides excess material for generation of ATP in mitochondria, which exceeds the demand, and leads to increased ROS production from ETC[67]. Furukawa et al. reported that WAT of obese individuals had increased level of ROS, insulin resistance and decreased antioxidant activity[66]. Frohnert et al. also found the association between obesity induced oxidative stress and insulin resistance in humans[68]. Prolonged oxidative stress has been associated with dysregulation of metabolic enzymes, such as aconitase and pyruvate dehydrogenase kinase 2[69,70]. Furthermore, ROS, such as superoxide or hydrogen peroxide, could undergo Fenton reaction in the presence of proteins with Fe^{-} to form hydroxyl radicals[71]. Hydroxyl radicals readily “attack” intracellular polyunsaturated fatty acids (PUFA), arachidonic and linoleic acids, and increase the rate of lipid peroxidation causing oxidative stress [72,73]. Lipid peroxidation of PUFA produces lipid metabolites, such as 4-HNE a particularly toxic molecule due to its high reactivity and abundance[74,75]. 4-HNE can covalently bind to protein residues and form stable adducts, altering the functions and structures of proteins[74]. Previous studies reported that the production of 4-HNE in obese adipose tissue is increased and it can either bind to proteins within the mitochondria or cellular Akt to reduce rates of cellular oxygen consumption and

promote insulin resistance, respectively [76–78]. Furthermore, 4-HNE can activate tumor protein 53 (p53), a master regulator of the DNA damage response, by inducing DNA damage and phosphorylating its serine residue. Multiple studies demonstrated that the activation of p53 can increase pro-inflammatory cytokine levels and insulin resistance, and ultimately result in apoptosis, which can also lead to increased inflammation and insulin resistance in adipocytes. Minamino et al. found that mice with adipocyte-specific p53 deficiency were more insulin sensitive and had lower levels of pro-inflammatory cytokine expressions[79]. Moreover, it has been demonstrated that lipid peroxidation products such as 4-HNE generated in adipocytes could be bound to high density lipoprotein and transported to liver and skeletal muscle thus promoting insulin resistance in DIO[80].

Overall, obesity induces significant changes in adipose tissue biology, leading to adipocyte hypertrophy, increased adipogenesis, inflammation, altered adipokine secretion, insulin resistance, and decreased tissue remodeling such as beiging. These changes collectively contribute to the metabolic disturbances associated with obesity and increase the risk of developing obesity-related complications. Understanding the obesity induced molecular changes in adipocytes is crucial for developing strategies to improve metabolic profile and obesity-related diseases. Given the severity of obesity epidemic in United States and other nations, wide varieties of potential therapeutic targets, such as leptin, glucagon-like peptide-1 and 5-HT, were discovered and utilized to develop pharmacological interventions[81].

The role of 5-HT in physiology

Among many candidates for treating obesity, 5-HT, a biogenic monoamine that acts as a neurotransmitter as well as a hormone, has been a target of interest for developing obesity drugs. Originally, in 1918, the existence of 5-HT was first described as a vasoconstricting molecule in serum[82]. A few decades later, Rapport et al. successfully isolated 5-HT from bovine serum and characterized its molecular details[83]. Furthermore, both 5-HT and 5-HTRs were found to be present in various tissue types, including lung, kidney, gastrointestinal tract and brain[84]. With the discovery of high level of 5-HT in the CNS, researchers proposed the possible role of 5-HT as a neurotransmitter. Indeed, Fuxe identified a cluster of neurons that has high level of 5-HT, which is later named as serotonergic neuron[85]. Through this serotonergic neuronal system, 5-HT modulates various functions of CNS, such as mood, cognitive function, behaviors and appetite[86,87]. Appetite regulation is a very complex multifaceted homeostatic process that includes both CNS and peripheral interactions[88,27]. 5-HT promotes satiation, while reduce carbohydrate craving and emotional eating through cascades of signaling in the CNS[73]. Lam et al. demonstrated that 5-HT could directly suppress appetite by stimulating hypothalamic pro-opiomelanocortin neurons through serotonin receptor 2c (5-HTR_{2c})[90]. Based on this observation, 5-HTR_{2C} antagonist, Lorcaserin, was developed and tested for its efficacy and safety as an obesity drug. In the large randomized-control trial, Lorcaserin significantly reduced amount of food intake of participants, decreased body weight and improved glycemic profile[91,92]. Lorcaserin was approved as a prescribed drug for treating severe obesity and T2DM

by FDA, but later it was withdrew from the market because of the potential risk of cancer[93,94].

In addition to regulation of food intake, CNS 5-HT also has been implicated in modulation of energy expenditure. 5-HT, along with norepinephrine, is involved in the regulation of the sympathetic nervous system. 5-HT can modulate the activity of sympathetic neurons and influence their release of neurotransmitters, including norepinephrine[95]. Activation of serotonin receptors, such as 5-HTR_{2a} and 5-HTR_{2c} receptors in sympathetic nerve terminals that innervate brown adipose tissue, modulate the release of norepinephrine onto brown adipocytes[96]. When the released norepinephrine binds to these receptors, it triggers a signaling cascade that leads to the activation of thermogenesis by increasing Ucp-1 expression[97]. McGlashon et al. demonstrated that the specific ablation of serotonergic neurons significantly reduces the thermogenic capacity of mouse brown fat and caused steatosis and hyperglycemia[98]. Even though, central 5-HT plays crucial roles as a metabolism modulator, utilizing it as a therapeutic target has been unsuccessful, including Lorcaserin. Because, CNS 5-HT based medications may be associated with rare but serious side effects, such as pulmonary hypertension, cardiac valvulopathy or depression[81]. While the overall risk-benefit profile of central 5-HT based obesity drugs is unbalanced, the recent discovery of energy metabolism regulation via peripheral 5-HT suggests a new possible therapeutic target for treating obesity.

Peripheral 5-HT and obesity

Peripheral 5-HT has been appreciated for its role in vasoconstriction, platelet aggregation and gut motility modulation[99]. Most of the circulating 5-HT is stored at platelets and released upon stimulation to induce vasoconstriction, enhance platelet aggregation and blood coagulation[100]. However, recent evidence highlighted the role of 5-HT in affecting obesity development due to its ability to regulate both adipocyte and systemic metabolic signaling related to energy intake and expenditure[101–103]. Considering the completely different 5-HT functions on both CNS and periphery, it suggests the existence of two distinctive 5-HT pools for regulating each system. As a matter fact, the CNS and peripheral 5-HT systems is separated by the blood brain barrier (BBB), the tight junction of endothelial cells that divides blood circulation and extracellular fluid of the CNS, and protects the CNS from toxins and pathogens[104,105]. Since, 5-HT is a neurotransmitter, it cannot readily cross the BBB and enter either the CNS or peripheral body[106]. Thus, to maintain two different pools of 5-HT, there are two isoforms of 5-HT synthesizing enzyme, TPH1 and TPH2. TPH1 is mainly expressed in peripheral system, whereas Tph2 predominates the brainstem of CNS and enteric nerve system[107]. Almost 90% of 5-HT in human system is synthesized by TPH1 in peripheral system, mainly from gut-enterochromaffin cells[108]. 5-HT is synthesized from tryptophan, an essential amino acid. Tryptophan is hydroxylated by Tph to produce 5-hydroxytryptophan, and subsequently converted to 5-HT by amino acid decarboxylase[109]. The synthesis of 5-HT is tightly regulated by availability of tryptophan and TPH, which is a rate-limiting enzyme[101]. However, duodenal or colonic carbohydrates (glucose, fructose or sucrose) have been shown to increase the

synthesis and secretion of 5-HT from enterochromaffin cells, resulting in elevated level of circulating 5-HT[110]. This highlights the possible link between 5-HT and nutrient availability, which could modulate energy harvesting.

Released 5-HT can be taken up by cells via the serotonin transporter (SERT) and then metabolized by monoamine oxidase A (MAOA) located at the outer membrane of mitochondria, into 5-hydroxyindole aldehyde, ammonia and hydrogen peroxide[111]. Then, 5-hydroxyindole aldehyde further degraded into 5-hydroxyindoleacetic acid, which could be excreted in urine[112].

The functionality of peripheral 5-HT has been investigated by utilizing various transgenic mice models. Gut-specific ablation of the TPH1 expression in mice reduced circulating 5-HT level and increased insulin sensitivity in chow fed mice, even though they still gained body weight and became obese with HFD feeding[113,114]. Unexpectedly, global knockout of TPH1 in mice induced glucose intolerance and mild diabetes in mice with chow feeding, because of impaired insulin secretion from pancreas[115]. Genetic ablation of TPH1 in pancreatic β-cells caused impairment in insulin secretion and glucose homeostasis, demonstrating 5-HT is a crucial factor in pancreatic insulin secretion[116]. In liver, 5-HT has been associated with increased lipogenesis and liver fat deposition[117]. Injection of 5-HTR_3 agonist *to ob/ob* mice reduced liver lipid accumulation, and genetic deficiency of liver 5-HTR_{2a} prevented HFD induced NAFLD development[118,119]. Adipocyte-specific ablation of TPH1 protected mice from developing DIO and its metabolic complications[120,121]. With HFD feeding, TPH1 deficient mice gained less weight and were more insulin sensitive as compared to the wild type mice. Injection of a peripheral TPH1 inhibitor, LP-533401, to HFD fed mice

also showed similar effect with *Tph1* adipocyte-specific knockout[120]. In mice with adipocyte-specific TPH1 deficiency, increased BAT thermogenesis was observed, as well as decreased lipogenesis in WATs, and the proposed underlying molecular mechanisms for these changes were decreased 5-HT signaling through 5-HTR_3 and 5-HTR_{2a} in BAT and WAT, respectively[120]. While, inhibition of adipocyte derived 5-HT production protected mice from developing DIO, total level of circulating 5-HT was not altered[120]. Also, significant reduction in circulating 5-HT level did not protect mice from developing DIO[113]. Based on these observations, it is possible to hypothesize that not all metabolic effects of peripheral 5-HT could be induced via 5-HTR signaling pathways, and there may be other factors that play a role in peripheral 5-HT effect.

1.2. Research Objectives

Although 5-HT functions as a neurotransmitter with vital roles in the CNS, more than 90% of the body's serotonin is actually located peripherally and modulates energy metabolism. 5-HT synthesis is tightly regulated by two isoforms of TPH: TPH1 is mainly expressed peripherally while TPH2 is predominantly located in the CNS. Interestingly, our lab and others have found that HFD feeding leads to massive upregulation of *Tph2* in mouse WATs. Despite the importance of adipocyte-derived 5-HT, very little is known about the role of adipocyte-specific TPH2 functionality. Our preliminary data demonstrates that gonadal adipocyte-specific over-expression of *Tph2* was sufficient to increase mouse eWAT adiposity without feeding a HFD to mouse. Moreover, both p53 and pro-inflammatory cytokine gene expression were increased with TPH2 over-expression, suggesting ongoing adipose tissue inflammation and dysfunction. Based upon these compelling observations, I hypothesized that adipocyte TPH2 will increase intracellular 5-HT synthesis, which may play a critical role in contributing to adipocyte dysfunction and the overall development of obesity. To comprehensively evaluate these ideas, I used an AAV induced adipocyte-specific *Tph2* over-expression method and a complimentary knockout transgenic mouse model to address the following two specific aims:

Aim 1. To investigate the effect of adipocyte-specific over-expression of Tph2 on adipocyte dysfunction and energy metabolism.

We hypothesized that AAV induced increased epididymal adipocyte 5-HT can be subsequently degraded by MAOA into hydrogen peroxide (H_2O_2), which induces adipocyte dysfunction, inflammation and oxidative stress by forming 4-HNE and activating p53 signaling (Fig.1).

Aim 2. To determine the effect of adipocyte-specific Tph2 deficiency on regulating adipocyte and systemic metabolism in HFD-fed mice.

We hypothesized that adipocyte-specific *Tph2* knockout mice have reduced production of adipocyte 5-HT, which decreases inflammatory cytokine production and oxidative stress, ultimately protecting against HFD-induced obesity (Fig.1).

Impact: To the best our knowledge, the role of adipocyte-specific TPH2 has never been investigated. This project explored novel pathways and how the expression of adipocyte-specific TPH2 regulates adipocyte energy metabolism and the development of DIO and associated metabolic complications. The completion of these aims contributed to a deeper understanding of the role of adipocyte-specific 5-HT and TPH2 in obesity development and pathophysiology, which may prove to be a potential therapeutic target.

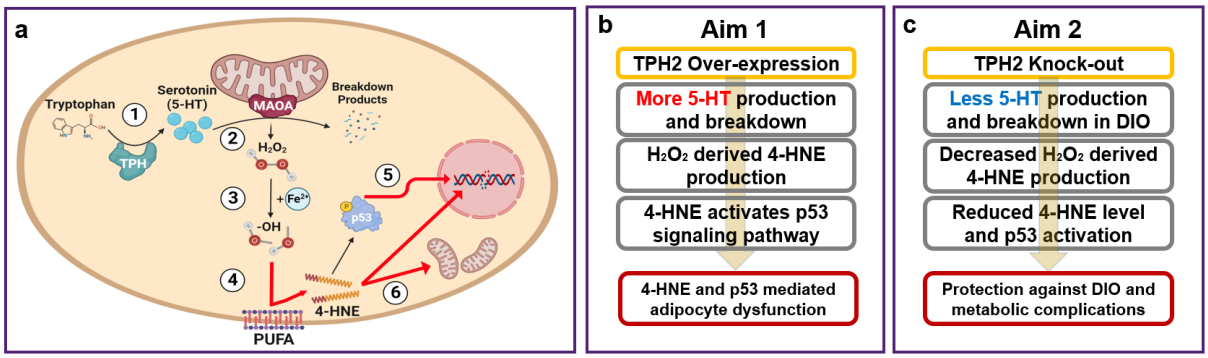

Figure 1. Central Hypothesis and Expected Outcomes in Each Specific Aim. **(a)** Possible role of adipocyte 5-HT in inducing inflammation, oxidative stress, DNA damage and mitochondrial dysfunction. ① Tph synthesizes 5-HT from tryptophan. ② MAOA metabolizes 5-HT into H2O2. ③ With $Fe2^{+}$, H_2O_2 will be degraded into –OH by Fenton reaction. ④ -OH causes oxidative stress and oxidizes PUFA to 4-HNE. ⑤4-HNE activates p53 signaling, which will induce pro-inflammatory cytokine gene transcription and adipocyte death. ⑥ 4-HNE induces DNA damage and mitochondrial dysfunction. **(b)** Expected Outcomes in Aim 1. **(c)** Expected Outcomes in Aim 2.

1.3. References

1. Wang, Y., Beydoun, M. A., Liang, L., Caballero, B. & Kumanyika, S. K. Will all Americans become overweight or obese? Estimating the progression and cost of the US obesity epidemic. *Obesity* **16**, 2323–2330 (2008).
2. James, W. P. T. The epidemiology of obesity: The size of the problem. *J. Intern. Med.* **263**, 336–352 (2008).
3. Lega, I. C. & Lipscombe, L. L. Review: Diabetes, Obesity, and Cancer-Pathophysiology and Clinical Implications. *Endocr. Rev.* **41**, (2020).
4. Lim, S. S. *et al.* A comparative risk assessment of burden of disease and injury attributable to 67 risk factors and risk factor clusters in 21 regions, 1990-2010: A systematic analysis for the Global Burden of Disease Study 2010. *Lancet* **380**, 2224–2260 (2012).
5. Franks, P. W. & McCarthy, M. I. Exposing the exposures responsible for type 2 diabetes and obesity. *Science (80-.).* **354**, 69–73 (2016).
6. Hill, J. O. & Prentice, A. M. Sugar and body weight regulation. *Am. J. Clin. Nutr.* **62**, (1995).
7. Stubbs, R. J., Mazlan, N. & Whybrow, S. Carbohydrates, appetite and feeding behavior in humans. *J. Nutr.* **131**, 2775S-2781S (2001).
8. Redinger, R. N. Fat storage and the biology of energy expenditure. *Transl. Res.* **154**, 52–60 (2009).
9. Cohena, P. & Spiegelmanb, B. M. Cell biology of fat storage. *Mol. Biol. Cell* **27**, 2523–2527 (2016).
10. Kersten, S. Mechanisms of nutritional and hormonal regulation of lipogenesis. *EMBO Rep.* **2**, 282–286 (2001).
11. Choe, S. S., Huh, J. Y., Hwang, I. J., Kim, J. I. & Kim, J. B. Adipose tissue remodeling: Its role in energy metabolism and metabolic disorders. *Front. Endocrinol. (Lausanne).* **7**, 1–16 (2016).
12. Muir, L. A. *et al.* Adipose tissue fibrosis, hypertrophy, and hyperplasia: Correlations with diabetes in human obesity. *Obesity* **24**, 597–605 (2016).
13. Gustafson, B. *et al.* Inflammation and impaired adipogenesis in hypertrophic obesity in man. *Am. J. Physiol. - Endocrinol. Metab.* **297**, (2009).
14. Drolet, R. *et al.* Hypertrophy and hyperplasia of abdominal adipose tissues in women. *Int. J. Obes.* **32**, 283–291 (2008).
15. Jang, H. *et al.* Adipose tissue hyperplasia with enhanced adipocyte-derived stem cell activity in Tc1(C8orf4)-deleted mice. *Sci. Rep.* **6**, 1–10 (2016).

16. Trayhurn, P. Hypoxia and adipose tissue function and dysfunction in obesity. *Physiol. Rev.* **93**, 1–21 (2013).

17. Choe, S. S., Huh, J. Y., Hwang, I. J., Kim, J. I. & Kim, J. B. Adipose tissue remodeling: Its role in energy metabolism and metabolic disorders. *Front. Endocrinol. (Lausanne).* **7**, 30 (2016).

18. Halberg, N. *et al.* Hypoxia-Inducible Factor 1α Induces Fibrosis and Insulin Resistance in White Adipose Tissue. *Mol. Cell. Biol.* **29**, 4467–4483 (2009).

19. Rius, J. *et al.* NF-κB links innate immunity to the hypoxic response through transcriptional regulation of HIF-1α. *Nature* **453**, 807–811 (2008).

20. Sewter, C. P., Digby, J. E., Blows, F., Prins, J. & O'Rahilly, S. Regulation of tumour necrosis factor-alpha release from human adipose tissue in vitro. *J. Endocrinol.* **163**, 33–38 (1999).

21. Baker, R. G., Hayden, M. S. & Ghosh, S. NF-κB, inflammation, and metabolic disease. *Cell Metab.* **13**, 11–22 (2011).

22. Weisberg, S. P. *et al.* Obesity is associated with macrophage accumulation in adipose tissue. *J. Clin. Invest.* **112**, 1796–1808 (2003).

23. Klover, P. J., Clementi, A. H. & Mooney, R. A. Interleukin-6 depletion selectively improves hepatic insulin action in obesity. *Endocrinology* **146**, 3417–3427 (2005).

24. Strissel, K. J. *et al.* Adipocyte death, adipose tissue remodeling, and obesity complications. *Diabetes* **56**, 2910–2918 (2007).

25. Alkhouri, N. *et al.* Adipocyte apoptosis, a link between obesity, insulin resistance, and hepatic steatosis. *J. Biol. Chem.* **285**, 3428–3438 (2010).

26. Friedman, J. & Friedman, J. The long road to leptin The long road to leptin. **126**, 4727–4734 (2016).

27. Dhillo, W. S. Appetite regulation: An overview. *Thyroid* **17**, 433–445 (2007).

28. Li, M., Coleman, D. & Fried-, J. Leptin and Beyond : An odyssey to the central control of Body Weight. **84**, 1–7 (2011).

29. Gruzdeva, O. & Borodkina, D. Leptin resistance : underlying mechanisms and diagnosis. 191–198 (2019).

30. Ma, Y. *et al.* 5-HT2A Receptor and 5-HT Degradation Play a Crucial Role in Atherosclerosis by Modulating Macrophage Foam Cell Formation, Vascular Endothelial Cell Inflammation, and Hepatic Steatosis. *J. Atheroscler. Thromb.* **29**, 322–336 (2022).

31. Straub, L. G. & Scherer, P. E. Metabolic Messengers: adiponectin. *Nat. Metab.* **1**, 334–339 (2019).

32. Bozaoglu, K. *et al.* Chemerin Is a Novel Adipokine Associated with Obesity and Metabolic Syndrome. **148**, 4687–4694 (2007).

33. Ding, E. L. & Dam, R. M. Van. Adiponectin Levels and Risk of Type 2 Diabetes. **302**, 179–188 (2009).

34. Recinella, L. *et al.* Adipokines : New Potential Therapeutic Target for Obesity and Metabolic , Rheumatic , and Cardiovascular Diseases. **11**, 1–32 (2020).

35. Kolb, H., Stumvoll, M., Kramer, W., Kempf, K. & Martin, S. Insulin translates unfavourable lifestyle into obesity. *BMC Med.* **16**, 1–10 (2018).

36. Wondmkun, Y. T. Obesity, insulin resistance, and type 2 diabetes: Associations and therapeutic implications. *Diabetes, Metab. Syndr. Obes.* **13**, 3611–3616 (2020).

37. Plum, L., Belgardt, B. F. & Brüning, J. C. Central insulin action in energy and glucose homeostasis. *J. Clin. Invest.* **116**, 1761–1766 (2006).

38. Petersen, M. C. & Shulman, G. I. Mechanisms of insulin action and insulin resistance. *Physiol. Rev.* **98**, 2133–2223 (2018).

39. Kahn, R. THE MOLECULAR MECHANISM OF INSULIN ACTION. *Annu. Rev.* **36**, 429–451 (1985).

40. Yaribeygi, H., Farrokhi, F. R., Butler, A. E. & Sahebkar, A. Insulin resistance: Review of the underlying molecular mechanisms. *J. Cell. Physiol.* **234**, 8152–8161 (2019).

41. Rains, J. L. & Jain, S. K. Oxidative stress, insulin signaling, and diabetes. *Free Radic. Biol. Med.* **50**, 567–575 (2011).

42. White, M. F. & Kahn, C. R. The insulin signaling system. *J. Biol. Chem.* **269**, 1–4 (1994).

43. Smith, U. & Kahn, B. B. Adipose tissue regulates insulin sensitivity : role of adipogenesis , de novo lipogenesis and novel lipids. 465–475 (2016) doi:10.1111/joim.12540.

44. Lumeng, C. N., DeYoung, S. M., Bodzin, J. L. & Saltiel, A. R. Increased inflammatory properties of adipose tissue macrophages recruited during diet-induced obesity. *Diabetes* **56**, 16–23 (2007).

45. Prentki, M., Joly, E., El-Assaad, W. & Roduit, R. Malonyl-CoA Signaling, Lipid Partitioning, and Glucolipotoxicity. *Diabetes* **51**, S405–S413 (2002).

46. Richter, E. A. & Hargreaves, M. Exercise, GLUT4, and skeletal muscle glucose uptake. *Physiol. Rev.* **93**, 993–1017 (2013).

47. Bechmann, L. P. *et al.* The interaction of hepatic lipid and glucose metabolism in liver diseases. *J. Hepatol.* **56**, 952–964 (2012).

48. Zhang, X., Yang, S., Chen, J. & Su, Z. Unraveling the Regulation of Hepatic Gluconeogenesis. **9**, 1–17 (2019).

49. Samuel, V. T., Petersen, K. F. & Shulman, G. I. Lipid-induced insulin resistance : unravelling the mechanism. *Lancet* **375**, 2267–2277 (2010).

50. Khan, R. S., Bril, F., Cusi, K. & Newsome, P. N. Modulation of Insulin Resistance in Nonalcoholic Fatty Liver Disease. **70**, (2019).

51. Waddell, T. *et al.* Greater ectopic fat deposition and liver fibroinflammation and lower skeletal muscle mass in people with type 2 diabetes. *Obesity* **30**, 1231–1238 (2022).

52. Chouchani, E. T. & Kajimura, S. Metabolic adaptation and maladaptation in adipose tissue. *Nat. Metab.* **1**, 189–200 (2019).

53. Mulya, A. & Kirwan, J. P. Brown and Beige Adipose Tissue. *Endocrinol. Metab. Clin. North Am.* **45**, 605–621 (2016).

54. Kajimura, S., Spiegelman, B. M. & Seale, P. Brown and beige fat: Physiological roles beyond heat generation. *Cell Metab.* **22**, 546–559 (2015).

55. Cypess, A. M. *et al.* Identification and Importance of Brown Adipose Tissue in Adult Humans. 1509–1517 (2009).

56. Saito, M. *et al.* High incidence of metabolically active brown adipose tissue in healthy adult humans: Effects of cold exposure and adiposity. *Diabetes* **58**, 1526–1531 (2009).

57. Wang, W. & Seale, P. Control of brown and beige fat development. *Nat. Rev. Mol. Cell Biol.* **17**, 691–702 (2016).

58. Harms, M. & Seale, P. Brown and beige fat: Development, function and therapeutic potential. *Nat. Med.* **19**, 1252–1263 (2013).

59. Rogers, N. H., Landa, A., Park, S. & Smith, R. G. Aging leads to a programmed loss of brown adipocytes in murine subcutaneous white adipose tissue. *Aging Cell* **11**, 1074–1083 (2012).

60. Merlin, J. *et al.* Rosiglitazone and a β3-adrenoceptor agonist are both required for functional browning of white adipocytes in culture. *Front. Endocrinol. (Lausanne).* **9**, 1–17 (2018).

61. Sanchez-Gurmaches, J. *et al.* Brown Fat AKT2 Is a Cold-Induced Kinase that Stimulates ChREBP-Mediated De Novo Lipogenesis to Optimize Fuel Storage and Thermogenesis. *Cell Metab.* **27**, 195-209.e6 (2017).

62. Lehr, L. *et al.* The control of UCP1 is dissociated from that of PGC-1α or of mitochondriogenesis as revealed by a study using β-less mouse brown adipocytes in culture. *FEBS Lett.* **580**, 4661–4666 (2006).

63. Bi, P. *et al.* Inhibition of Notch signaling promotes browning of white adipose tissue and ameliorates obesity. *Nat. Med.* **20**, 911–918 (2014).

64. Sidossis, L. & Kajimura, S. Brown and beige fat in humans: Thermogenic adipocytes that control energy and glucose homeostasis. *J. Clin. Invest.* **125**, 478–486 (2015).

65. Masschelin, P. M., Cox, A. R., Chernis, N. & Hartig, S. M. The Impact of Oxidative Stress on Adipose Tissue Energy Balance. *Front. Physiol.* **10**, 1638 (2020).

66. Furukawa, S. *et al.* Increased oxidative stress in obesity and its impact on metabolic syndrome. *J. Clin. Invest.* **114**, 1752–1761 (2004).

67. Murphy, M. P. How mitochondria produce reactive oxygen species. *Biochem. J.* **417**, 1–13 (2009).

68. Liesa, M. & Shirihai, O. S. Mitochondrial dynamics in the regulation of nutrient utilization and energy expenditure. *Cell Metab.* **17**, 491–506 (2013).

69. Hurd, T. R. *et al.* Inactivation of pyruvate dehydrogenase kinase 2 by mitochondrial reactive oxygen species. *J. Biol. Chem.* **287**, 35153–35160 (2012).

70. Quijano, C., Trujillo, M., Castro, L. & Trostchansky, A. Interplay between oxidant species and energy metabolism. *Redox Biol.* **8**, 28–42 (2016).

71. Ahmed, B., Sultana, R. & Greene, M. W. Adipose tissue and insulin resistance in obese. *Biomed. Pharmacother.* **137**, 111315 (2021).

72. Schöneich, C., Asmus, K. D., Dillinger, U. & Bruchhausen, F. v. Thiyl radical attack on polyunsaturated fatty acids: A possible route to lipid peroxidation. *Biochem. Biophys. Res. Commun.* **161**, 113–120 (1989).

73. Ramsay, R. R. & Albreht, A. Kinetics, mechanism, and inhibition of monoamine oxidase. *J. Neural Transm.* **125**, 1659–1683 (2018).

74. Castro, J. P., Jung, T., Grune, T. & Siems, W. 4-Hydroxynonenal (HNE) modified proteins in metabolic diseases. *Free Radic. Biol. Med.* **111**, 309–315 (2017).

75. Dalleau, S., Baradat, M., Guéraud, F. & Huc, L. Cell death and diseases related to oxidative stress:4-hydroxynonenal (HNE) in the balance. *Cell Death and Differentiation* vol. 20 1615–1630 (2013).

76. Shearn, C. T., Reigan, P. & Petersen, D. R. Inhibition of Hydrogen peroxide signaling by 4-hydroxynonenal due to differential regulation of Akt1 and Akt2 contributes to decreases in cell survival and proliferation in hepatocellular carcinoma cells. *Free Radic. Biol. Med.* **53**, 1–11 (2012).

77. Shearn, C. T., Fritz, K. S., Reigan, P. & Petersen, D. R. Modification of Akt2 by 4-hydroxynonenal inhibits insulin-dependent Akt signaling in HepG2 cells. *Biochemistry* **50**, 3984–3996 (2011).

78. Pillon, N. J. *et al.* The lipid peroxidation by-product 4-hydroxy-2-nonenal (4-HNE) induces insulin resistance in skeletal muscle through both carbonyl and oxidative stress. *Endocrinology* **153**, 2099–2111 (2012).

79. Minamino, T. *et al.* A crucial role for adipose tissue p53 in the regulation of insulin resistance. *Nat. Med.* **15**, 1082–1087 (2009).

80. Cai, J. *et al.* Autophagy Ablation in Adipocytes Induces Insulin Resistance and Reveals Roles for Lipid Peroxide and Nrf2 Signaling in Adipose-Liver Crosstalk. *Cell Rep.* **25**, 1708-1717.e5 (2018).

81. Müller, T. D., Blüher, M., Tschöp, M. H. & DiMarchi, R. D. Anti-obesity drug discovery: advances and challenges. *Nat. Rev. Drug Discov.* **21**, 201–223 (2022).

82. On, E., Action, V. & Serum, O. F. B. EXPERIMENTS ON THE VASOCONSTRICTOR ACTION of Blood Serum. (2023).

83. Rapport, M. M., Green, A. A. & Page, I. H. Crystalline serotonin. *Science (80-.).* **108**, 329–330 (1948).

84. Yabut, J. M. *et al.* Emerging Roles for Serotonin in Regulating Metabolism: New Implications for an Ancient Molecule. *Endocrine Reviews* vol. 40 1092–1107 (2019).

85. Fuxe, K. Evidence for the existence of monoamine neurons in the central nervous system - III. The monoamine nerve terminal. *Zeitschrift für Zellforsch. und Mikroskopische Anat.* **65**, 573–596 (1965).

86. Amin, Z., Canli, T. & Epperson, C. N. Effect of estrogen-serotonin interactions on mood and cognition. *Behav. Cogn. Neurosci. Rev.* **4**, 43–58 (2005).

87. Canli, T. & Lesch, K. P. Long story short: The serotonin transporter in emotion regulation and social cognition. *Nat. Neurosci.* **10**, 1103–1109 (2007).

88. Delzenne, N. *et al.* Gastrointestinal targets of appetite regulation in humans: ILSI Supplement. *Obes. Rev.* **11**, 234–250 (2010).

89. Halford, J. C. G. & Blundell, J. E. Separate systems for serotonin and leptin in appetite control. *Ann. Med.* **32**, 222–232 (2000).

90. Lam, D. D. & Heisler, L. K. Serotonin and energy balance: Molecular mechanisms and implications for type 2 diabetes. *Expert Rev. Mol. Med.* **9**, 1–24 (2007).

91. O'Neil, P. M. *et al.* Randomized placebo-controlled clinical trial of lorcaserin for weight loss in type 2 diabetes mellitus: The BLOOM-DM study. *Obesity* **20**, 1426–1436 (2012).

92. Fidler, M. C. *et al.* A one-year randomized trial of lorcaserin for weight loss in obese and overweight adults: The BLOSSOM Trial. *J. Clin. Endocrinol. Metab.* **96**, 3067–3077 (2011).

93. Brashier, D. B. S., Sharma, A. K., Dahiya, N., Singh, S. K. & Khadka, A. Lorcaserin: A novel antiobesity drug. *J. Pharmacol. Pharmacother.* **5**, 175–178 (2014).

94. Administration, U. S. F. and D. FDA requests the withdrawal of the weight-loss drug Belviq, Belviq XR (lorcaserin) from the market | FDA. *Fda* 3–5 (2020).

95. Nakamura, K. *et al.* Identification of sympathetic premotor neurons in medullary raphe regions mediating fever and other thermoregulatory functions. *J. Neurosci.* **24**, 5370–5380 (2004).

96. Nakamura, K. & Morrison, S. F. Central efferent pathways for cold-defensive and febrile shivering. *J. Physiol.* **589**, 3641–3658 (2011).

97. Townsend, K. L. & Tseng, Y. H. Brown fat fuel utilization and thermogenesis. *Trends in Endocrinology and Metabolism* vol. 25 168–177 (2014).

98. McGlashon, J. M. *et al.* Central Serotonergic Neurons Activate and Recruit Thermogenic Brown and Beige Fat and Regulate Glucose and Lipid Homeostasis. *Cell Metab.* **21**, 692–705 (2015).

99. Mohammad-Zadeh, L. F., Moses, L. & Gwaltney-Brant, S. M. Serotonin: A review. *J. Vet. Pharmacol. Ther.* **31**, 187–199 (2008).

100. Lopez-Vilchez, I., Diaz-Ricart, M., White, J. G., Escolar, G. & Galan, A. M. Serotonin enhances platelet procoagulant properties and their activation induced during platelet tissue factor uptake. *Cardiovasc. Res.* **84**, 309–316 (2009).

101. El-Merahbi, R., Löffler, M., Mayer, A. & Sumara, G. The roles of peripheral serotonin in metabolic homeostasis. *FEBS Letters* vol. 589 1728–1734 (2015).

102. Namkung, J., Kim, H. & Park, S. Peripheral serotonin: A new player in systemic energy homeostasis. *Mol. Cells* **38**, 1023–1028 (2015).

103. Lund, M. L. *et al.* Enterochromaffin 5-HT cells – A major target for GLP-1 and gut microbial metabolites. *Mol. Metab.* **11**, 70–83 (2018).

104. Keaney, J. & Campbell, M. The dynamic blood-brain barrier. *FEBS J.* **282**, 4067–4079 (2015).

105. Abbott, N. J., Patabendige, A. A. K., Dolman, D. E. M., Yusof, S. R. & Begley, D. J. Structure and function of the blood-brain barrier. *Neurobiol. Dis.* **37**, 13–25 (2010).

106. Sharma, H. S., Olsson, Y. & Kumar Dey, P. Changes in blood-brain barrier and cerebral blood flow following elevation of circulating serotonin level in anesthetized rats. *Brain Res.* **517**, 215–223 (1990).

107. Walther, D. J. *et al.* Synthesis of serotonin by a second tryptophan hydroxylase isoform. *Science (80-.).* **299**, 76 (2003).

108. Lund, M. L. *et al.* Enterochromaffin 5-HT cells – A major target for GLP-1 and gut microbial metabolites. *Mol. Metab.* **11**, 70–83 (2018).

109. Berger, M., Gray, J. A. & Roth, B. L. The expanded biology of serotonin. *Annu. Rev. Med.* **60**, 355–366 (2009).

110. Gifford, C. a. *et al.* Transcriptional and epigenetic dynamics during specification of human embryonic stem cells. *Cell* **153**, 1149–1163 (2013).

111. Ostadkarampour, M. & Putnins, E. E. Monoamine Oxidase Inhibitors: A Review of Their Anti-Inflammatory Therapeutic Potential and Mechanisms of Action. *Front. Pharmacol.* **12**, 1–17 (2021).

112. Keszthelyi, D., Troost, F. J. & Masclee, A. A. M. Understanding the role of tryptophan and serotonin metabolism in gastrointestinal function. *Neurogastroenterol. Motil.* **21**, 1239–1249 (2009).

113. Sumara, G., Sumara, O., Kim, J. K. & Karsenty, G. Gut-derived serotonin is a multifunctional determinant to fasting adaptation. *Cell Metab.* **16**, 588–600 (2012).

114. Martin, A. M. *et al.* The gut microbiome regulates host glucose homeostasis via peripheral serotonin. *Proc. Natl. Acad. Sci. U. S. A.* **116**, 19802–19804 (2019).

115. Paulmann, N. *et al.* Intracellular serotonin modulates insulin secretion from pancreatic β-cells by protein serotonylation. *PLoS Biol.* **7**, 1–10 (2009).

116. Kim, K. *et al.* Functional role of serotonin in insulin secretion in a diet-induced insulin-resistant state. *Endocrinol. (United States)* **156**, 444–452 (2015).

117. Osawa, Y. *et al.* L-tryptophan-mediated enhancement of susceptibility to nonalcoholic fatty liver disease is dependent on the mammalian target of rapamycin. *J. Biol. Chem.* **286**, 34800–34808 (2011).

118. Choi, W. *et al.* Serotonin signals through a gut-liver axis to regulate hepatic steatosis. *Nat. Commun.* **9**, 1–9 (2018).

119. Haub, S. *et al.* Serotonin receptor type 3 antagonists improve obesity-associated fatty liver disease in mice. *J. Pharmacol. Exp. Ther.* **339**, 790–798 (2011).

120. Oh, C. M. *et al.* Regulation of systemic energy homeostasis by serotonin in adipose tissues. *Nat. Commun.* **6**, (2015).

121. Crane, J. D. *et al.* Inhibiting peripheral serotonin synthesis reduces obesity and metabolic dysfunction by promoting brown adipose tissue thermogenesis. *Nat. Med.* **21**, 166–172 (2015).

Chapter 2. The effect of adipocyte-specific over-expression of TPH2 on adipocyte dysfunction and energy metabolism.

2.1. Introduction

The incidence of obesity is rapidly rising in all around the world[1]. But we have limited understanding of the underlying molecular details that promote obesity and its complications. In obese animals and humans, adipocytes become dysfunctional, which is strongly associated with the progression of obesity and its metabolic complications[2,3]. Beyond being an essential reservoir of energy, adipose tissue plays an integral role in regulating systemic metabolism through complex endocrine signaling[4–6]. However, obesity disrupts crucial metabolic functions of adipocytes, such as insulin sensitivity, adipokine secretion, lipogenesis, lipolysis and thermogenesis[7]. Although, obesity-mediated adipocyte dysfunction is extensively explored, the underlying molecular mechanisms of how obesity changes adipocyte biology and its impact on metabolic health has not been fully elucidated.

Recent lines of evidence highlight the contribution of peripheral 5-HT in developing adipocyte dysfunction, obesity, insulin resistance and NAFLD[8–10]. 5-HT acts as a neurotransmitter and a hormone and ubiquitously exists in both peripheral system and CNS. As a neurotransmitter in the CNS, 5-HT regulates mood, sleep cycle and appetite[11]. The activation of central serotonergic system stimulates hypothalamic feeding circuits to suppress appetite and promote satiety[12]. While as a hormone, it modulates reproductive function, hemostasis, vascular tone and energy metabolism[13].

Though 5-HT is present in both the CNS and periphery, more than 90% of 5-HT is synthesized from tryptophan by TPH1 in gut-enterochromaffin cells[14,15]. Since 5-HT cannot readily cross the blood brain barrier, two distinctive 5-HT pools are needed for each system and involve different enzymes for biosynthesis. TPH1 is predominantly expressed in the periphery and responsible for producing peripheral 5-HT, while TPH2 is the main enzyme in the CNS[16]. In contrast to the anorectic effects of the CNS 5-HT, peripheral 5-HT actually induces pleiotropic effects on peripheral tissues, especially on liver, BAT and WATs.

In individuals with obesity, circulating level of 5-HT is elevated, which is associated with body weight gain and impaired glycemic control[17]. In rodent models, pharmacological inhibition of peripheral 5-HT synthesis improved HFD-induced hepatic lipid accumulation[18]. Sumara et al. demonstrated that genetic ablation of intestine-specific TPH1 expression on mice significantly decreased circulating 5-HT level, and prevented HFD induced liver steatosis and glucose intolerance[19]. Additionally, mice lacking adipocyte expression of TPH1 showed increased activation of BAT thermogenesis compared to that of control mice, and were protected against DIO, fatty liver and insulin resistance[8,9]. Also, Oh et al. reported that either pharmacological or genetic inhibition of 5-HTR_{3a} increased the BAT thermogenesis and systemic energy expenditure, preventing HFD-induced weight gain[8]. Moreover, incubating 3T3-L1 cells with 5-HT significantly increased the lipid uptake and accumulation[8]. Other studies have also reported that the activation of liver 5-HTR_{2a} increases hepatic lipogenesis and lipid accumulation in mice, providing further evidence that peripheral 5-HT regulates metabolism through 5-HTR signaling[20,21].

However, adipocyte-specific deficiency of TPH1 did not reduce the total circulating level of 5-HT, while significant reduction of serum 5-HT level with intestine-specific TPH1 knockout did not prevent the development of DIO in mice[8,10]. These conflicting findings underscore the significance of elucidating the intracellular effects of adipocyte-derived 5-HT, which remains poorly understood.

The majority of previous studies have primarily investigated the metabolic role of peripheral 5-HT by focusing on Tph1. However, multiple studies have reported a significant upregulation of adipose tissue *Tph2* expression in mice fed a HFD[22,23]. Our lab also found that HFD feeding increases *Tph2* expression in epididymal adipocytes by ~20-fold compared to that of chow fed mice. Furthermore, in epididymal adipocytes from mice fed a HFD, a significant upregulation was observed in the gene expression level of *Maoa*, the enzyme responsible for metabolizing 5-HT into 5-hydroxyindoleacetic acid, ammonia, and hydrogen peroxide. Interestingly, these molecular changes were only observed in obese mice, but not in lean mice. Considering the links between peripheral 5-HT and metabolic regulation, adipocyte Tph2 mediated production of 5-HT may play a crucial role in promoting obesity and adipocyte dysfunction.

To test the hypothesis that adipocyte TPH2 derived 5-HT can shape adipocyte biology towards the development and progression of obesity induced adipocyte and metabolic dysfunction, we utilized Cre-loxP and AAV mediated over-expression method, called FLEx switch, to generate mice constitutively over-express epididymal adipocyte-specific *Tph2* in the absence of HFD feeding, and investigated whether adipocyte TPH2 derived 5-HT promotes obesity and its metabolic complications[24]. We

found that over-expression of TPH2 in mice epididymal adipocytes instigatedobesity associated adipocyte dysfunction and metabolic complications such as increased adiposity, insulin resistance, WAT inflammation and reduced systemic energy expenditure without developing obesity.

2.2. Materials & Methods

Experimental animals

All experimental animals, C57BL6/J background mice carrying Adipoq-Cre transgene were purchased from The Jackson Laboratory. Mice were housed at Comparative Biological Unit in Jean Mayer U.S. Department of Agriculture Human Nutrition Research Center on Aging, and all the experimental procedures were in accordance with standards and guidelines approved by Institutional Animal Care and Use Committee of Tufts University. Mice were kept at 22–24 °C with a 12:12 hours light/dark cycle, and had unrestricted access to water and chow diet, (Teklad, 2016S, Chow) during whole experimental period, unless stated otherwise. At week 24 of the experiment, mice were fasted for 6 hours and sacrificed to collect specimens (blood, liver, iWAT, eWAT, BAT and brain). Under continuous isoflurane anesthesia, cardiac puncture was carried out to collect blood. Collected blood was transferred to both ethylenediaminetetraacetic acid (EDTA) coated tubes and non-coated 2mL tubes for plasma and serum isolation, respectively. All collected tissues were weighed for their mass and immediately snap-frozen in liquid nitrogen. All collected specimens were stored at -80°C for further analysis.

Generation of TPH2 over-expressing AAV

Plasmid construct pAAV-CAG-DIO-Tph2 (anti-sense orientation)-WPRE was acquired from Vector Biolabs (Fig.S1A). The plasmid vector was amplified using chemically competent *E. coli* system (OneShot Stbl3, Invitrogen). Briefly, the construct was incubated on ice with OneShot *E. coli*. After short cold exposure, cells were heat-shocked (42°C), then incubated on 37°C with gentle shaking. The transformant was spread on pre-warmed Luria broth (LB) agar plate Containing ampicillin (100μg/mL). Single colony was isolated and inoculated in LB Containing ampicillin on 37°C with gentle shaking for overnight. After overnight incubation, amplified plasmid was purified using column method (QIAGEN, Plasmid Maxi kit). To validate the presence of Tph2 gene in purified plasmid, restriction enzyme based diagnostic test was performed. In the plasmid construct, PmeI and EcoRV sites are flanking the inserted *Tph2* cDNA sequence, thus restriction enzymes for both sites were used to verify the size of plasmid with PCR after digestion (Fig. S1b). Verified plasmid was sent to Boston Children's Hospital Viral Core and packaged into AAV8 serotype (AAV-Tph2), and the final titer of AAV-Tph2 was 3.0 x 10^{13} GC/mL.

AAV injection

To directly inject AAV into eWAT, laparotomies were performed. Mice with or without Adiponectin-Cre expression (Tph2 Oex and Tph2 Con, respectively) were anesthetized with isoflurane. Small vertical incision was made on mouse abdomen skin, and exposed peritoneal cavity. Each epididymal adipose depot was carefully brought out, and a total of 20μl of AAV (titer: 3.0 x 10^{13} GC/mL) was injected 5 different

points throughout each epididymal fat pad (2µl per point of injection). Peritoneal cavity was closed with absorbable-sutures and wound clips were used to close outer skin wound. For post-operative pain, mice got slow-releasing buprenorphine (0.1 mg/kg) by intraperitoneal injection after the procedure. Mice were individually caged, and closely monitored for any signs of infection or distress. Wound clips were removed from mice after 10 days from the procedure. All surgical procedures were carried out by skilled veterinarians from Tufts Comparative Medicine Services.

Metabolic phenotyping

The mouse body composition (lean, fat and body mass) was analyzed by using magnetic resonance instrument (EchoMRI-700, EchoMRI) every 3 week. Diet intake was determined daily by measuring the weight of remaining diet pellets on feeders at 10 am. By utilizing indirect calorimetry system (Promethion BX1, Sable systems), systemic energy expenditure was analyzed. Mice were placed in individual metabolic chamber to collect oxygen consumption, carbon dioxide production, spontaneous activity (total distance moved and locomotion) and food intake for 96 hours. First 24 hours of collected data was excluded from analysis for acclimation purpose. Collected metabolic data was analyzed by CalR as previously described[25].

Glucose tolerance test

Glucose tolerance test was performed at week 16 after the AAV injection. Mice were transferred to new cages without food pellets as soon as light cycle started and

fasted for 6 hours. After fasting, tail bit was snipped to measure baseline blood glucose level with glucometer (Autocode, Prodigy). The glucose concentration of the solution (D-glucose, Sigma, diluted with sterile phosphate-buffered saline) was 1.5g/kg lean mass. Glucose solution was intraperitoneally injected and blood glucose level was measured at 10, 20, 30, 60, 90 and 120 minutes after the injection. Area under the curve (AUC) was calculated based on average glucose level on each time point.

Insulin tolerance test

Insulin tolerance test was performed at week 19 after the AAV injection. Mice were transferred to new cages without food pellets as soon as light cycle started and fasted for 6 hours. After fasting, tail bit was snipped to measure baseline blood glucose level with glucometer (Autocode, Prodigy). The insulin concentration of the solution (Humulin R U-100, Eli Lily, diluted with sterile PBS) was 0.85IU/kg lean mass. Insulin solution was intraperitoneally injected and blood glucose level was measured at 10, 20, 30, 60, 90 and 120 minutes after the injection. AUC was calculated based on average glucose level on each time point.

Plasma and serum profile analysis

Total cholesterols, triglycerides, alanine transaminase (ALT), and aspartate aminotransferase (AST) in fasting plasma were analyzed using Beckman Coulter Diagnostic reagents on a chemistry analyzer (Beckman Coulter AU480, Beckman Coulter). Non-Esterified Fatty Acid (NEFA) and TG were analyzed using the Wako

NEFA-HR test kit and analyzed on the chemistry analyzer (Beckman Coulter AU480, Beckman Coulter). Serum insulin was measured by ELISA (Ultra Sensitive Mouse Insulin ELISA, Crystal Chem) with the wide-range standard curve (0.1-12.8 ng/mL standard curve option) and read on the Epoch plate reader.

5-HT quantification

Plasma 5-HT level was quantified using enzyme-linked immunosorbent assay (ELISA, IM1749, Beckman Coulter) according to manufacturer's instructions. For tissue 5-ht quantification, pulverized tissues were transferred to 0.2N perchloric acid and mechanically homogenized (Tissue lyzer II, Qiagen). After homogenization, samples were centrifuged at 10,000 x g to pellet insoluble debris and draw off supernatant. Transferred supernatant was neutralized with 1M borate buffer. With neutralized tissue extracts, ELISA was performed to quantify 5-HT (IM1749, Beckman Coulter).

4-HNE quantification

Plasma 4-HNE adduct level was quantified by ELISA (HNE Adduct Competitive ELISA, Cell biolabs) according to manufacturer's instructions. Tissue protein extract was prepared by mechanical homogenization of pulverized tissues in ice cold RIPA buffer with phosphatase and protease inhibitors (Halt™ Protease and Phosphatase Inhibitor Cocktail, Invitrogen). BCA assay was performed to determine protein Concentration. For tissue 4-HNE adduct quantification, ELISA (HNE Adduct

Competitive ELISA, Cell biolabs) was performed using total protein extract, and 4-HNE adduct level was normalized by protein concentration of the extract.

Immunohistochemistry and immunofluorescence

Dissected iWAT, eWAT and liver tissue were fixed in 10% aqueous buffered zinc formalin (Z-fix, Anatech), embedded in paraffin, sectioned (5μm), and stained with hematoxylin and eosin (H&E). Digital images were acquired at 20X or 40 X magnification (DX51 light microscope, Olympus). Average adipocyte size or lipid droplet percentage were quantified using Image J software. For immunofluorescence, paraffin-embedded sections were deparaffinized with xylene and rehydrated with ethanol. Citrate buffer (Antigen unmasking solution, Vector Laboratories) was used for antigen retrieval. Sections were blocked with the solution Containing 5% bovine serum albumin (BSA) and 0.1% Tween20 for 1 hour at room temperature. After blocking, slides were washed with PBS and incubated with primary antibody for 4-HNE (1: 200, 4 Hydroxynonenal Polyclonal Antibody, Bioss USA) for overnight at 4°C. Following 3 times of PBS washing, sections were incubated with goat-anti rabbit AlexaFluor 488 (1:500, Invitrogen) Conjugated secondary antibody for 1 hour at room temperature. After multiple PBS washings, Slides were counterstained with the nuclei marker 4′-6-diamindino-2-phenylindole (DAPI, ProLong™ Gold Antifade Mountant with DAPI) and mounted with glass coverslip. Digital images were acquired on either 20X or 40X magnification (Axiovert 200, Zeiss).

RNA isolation and real-time quantitative PCR

iWAT, eWAT, BAT and liver tissue (20~100mg) were submerged in Qiazol (Qiagen) and mechanically homogenized (Tissue lyzer II, Qiagen). From tissues, total RNA was extracted (RNeasy Mini columns, Qiagen) and RNA purity and Concentration was quantified with spectrophotometer (Nanodrop 100, Thermofisher). With 1 μg of RNA, cDNA was generated by reverse transcription (High Capacity cDNA Reverse Transcription Kit, Applied Biosystems). Quantitative real-time PCR (qPCR) was performed using SYBR Green (PowerUp™ SYBR™ Green Master Mix, Applied Biosystems) on an QuantStudio 6 Flex real-time PCR systems PCR (Applied Biosystems). RT-PCR cycle threshold (Ct) values were normalized and analyzed with 2-delta delta Ct method[26]. Both forward and reverse primer sequences are listed in Supplementary Table 1.

Statistics

All statistical analyses were Conducted using GraphPad Prism 9 software and R Studio. False discovery rate adjusted (FDR) Student's t-test was performed to determine statistical differences between groups. A p-value under 0.05 was Considered to be significant. All data were expressed as mean ± standard error of the mean (SEM).

2.3. Results

Epidydimal adipocyte-specific TPH2 over-expression is not sufficient to induce systemic changes in body composition, but significantly increases plasma serotonin level, BAT and eWAT mass.

To investigate the role of adipocyte Tph2 derived 5-HT in developing adipocyte dysfunction and obesity, we generate mice that constitutively over-express *Tph2* in adipocytes in the absence of HFD feeding. AAV-Tph2 was directly injected into the eWAT of mice with or without adiponectin-Cre recombinase expression. With a double-floxed inverse orientation in the AAV Construct, the target mouse *Tph2* sequence will be inserted in reverse/antisense orientation (3'-> 5') and this reversed sequence will be flanked by loxP and lox2272 sites. Cre-recombinase excises loxP and lox2272 sites and flips the transgene from antisense orientation into sense orientation (5'->3'), which initiates the translation of *Tph2* (Fig. S1c). To verify whether AAV induced epididymal adipocyte-specific *Tph2* over-expression was successful, we determined *Tph2* gene expression level on eWAT, BAT and iWAT. In Tph2 Oex eWAT, relative expression of *Tph2* was increased more than 4-fold compared to that of Tph2 Con, while there were no differences in BAT and iWAT (Fig.1a).

After injection of AAV-Tph2, body composition of mice was analyzed to determine the impact of TPH2 over-expression on weight gain and adiposity. During the experimental period, mice body weight and lean mass were not statistically different in any time points (Fig.1b & d). Total fat mass of Tph2 Oex trended higher

than that of Tph2 Con on week 12 and 20, but none of them were statistically significant (Fig.1c).

At 24 weeks after the AAV-Tph2 injection, experimental animals were euthanized and specimens were collected. To explore whether adipocyte TPH2 over-expression increased the circulating 5-HT level, plasma 5-HT level was quantified. Indeed, Tph2 OEX mice had significantly higher plasma 5-HT level than Tph2 Con mice (Fig.1e). Interestingly, TPH2 overexpression resulted in a significant increase in both BAT and eWAT mass, while other tissues did not show such changes (Fig.1f & g). These findings demonstrate that epididymal adipocyte TPH2 induce lipid accumulation in BAT and contributes to increased adiposity in eWAT.

Adipocyte TPH2 over-expression impairs glucose tolerance and insulin sensitivity.

To evaluate whether adipocyte TPH2-derived 5-HT changes systemic metabolism, food intake and blood glucose level were quantified. Food intake was monitored for 5 weeks, and there were no significant differences in weekly food intake (Fig. 2a). Additionally, fed-state and 6-hour fasting state blood glucose levels were measured, and both Tph2 Oex and Tph2 Con showed similar levels of blood glucose in both states (Fig. 2b & c). Even though both fed and fasting blood glucose levels are not different, this does not necessarily mean that glucose tolerance and insulin sensitivity are not altered. Thus, we evaluated serum insulin level, and Tph2 Oex mice demonstrated a significant elevation in serum insulin levels, suggesting reduced insulin sensitivity due to adipocyte TPH2 over-expression (Fig.2d). We also performed

IPGTT and IPITT at week 16 and 19, to further confirm glucose intolerance and insulin resistance, respectively. Tph2 Oex mice exhibited significantly higher blood glucose levels than Tph2 Con at 20 and 30 minutes after IP glucose injection, indicating impaired glucose tolerance (Fig.2e & f). Furthermore, following IP insulin injection, Tph2 Oex mice exhibited a significantly slower decline in blood glucose levels compared to Tph2 Con mice. Moreover, the blood glucose levels remained significantly elevated throughout the process in Tph2 Oex mice (Fig. 2g & h). Taken together, over-expressing Tph2 only in epididymal adipocytes was sufficient to induce glucose intolerance and insulin resistance without affecting food intake and HFD feeding.

TPH2 overexpression increases eWAT adiposity through upregulation of lipogenic gene expression and induced pro-inflammatory and p53 signaling gene expressions.

Consistent with increased eWAT mass in Tph2 Oex, H&E stainings of eWAT revealed that adipocytes in Tph2 Oex eWAT were significantly bigger than that of Tph2 CON mice (Fig. 3a & b). To further assess the molecular changes with TPH2 over-expression, we analyzed gene expression profile of eWATs from both groups of mice. AAV-Tph2 significantly increased *Tph2* mRNA level in Tph2 OEX mice, but had no effects on *Tph1* and *Maoa* (Fig. 3c). Since Tph2 over-expression increased eWAT adiposity, we investigated the mRNA levels of lipid metabolism related genes. We found that mRNA of fatty acid synthase (*Fasn*), a critical enzyme for de novo synthesis of fatty acids was highly upregulated, while, mRNA levels of adipose triglyceride lipase

(*Atgl*) and hormone sensitive lipase (*Hsl*) responsible for lipolysis were significantly down (Fig. 3d). Surprisingly, eWAT of Tph2 Oex mice exhibited elevated expressions of pro-inflammatory genes, including *Tnfa*, *Il-1b*, and *F4/80*, indicating signs of inflammation (Fig. 3e). We also measured the expression of p53 signaling related genes that induce adipocyte death, and p53 and its downstream target genes *Cdkn1a* and *Igfbp1* were upregulated with Tph2 over-expression (Fig. 3f). However, there were no significant differences in adiponectin mRNA levels between Tph2 Con and Oex mice (Fig. 3e).

TPH2 over-expression induces eWAT 4-HNE formation and increases circulating 4-HNE level.

Previous studies demonstrated that 4-HNE, a lipid peroxidation product, activates p53 signaling and causes cellular stress and adipocyte death[27]. Furthermore, cellular hydrogen peroxide is a potent ROS that can propagate lipid peroxidation and form 4-HNE[27,28]. We hypothesized that adipocyte TPH2-synthesized 5-HT could be metabolized by MAOA and produce hydrogen peroxide. Based on our observation of increased eWAT 5-HT level and eWAT p53 signaling gene expression profile in Tph2 Oex mice, we investigated the 4-HNE levels in eWAT and plasma. Immunohistochemical staining of eWAT slides revealed stronger immunofluorescence signal of 4-HNE from Tph2 OEX eWAT (Fig. 4a). We also quantified the 4-HNE adduct levels in eWAT and plasma, and both eWAT and plasma from Tph2 Oex mice had significantly elevated levels of 4-HNE adduct, indicating the possible conversion of 5-HT to 4-HNE (Fig. 4b & c).

Epididymal adipocyte-specific TPH2 over-expression increases iWAT adiposity through increased lipogenic signaling and decreased lipolysis.

To explore the systemic impact of epididymal adipocyte-specific TPH2 over-expression, we also processed iWAT samples for H&E staining and qPCR. H&E staining revealed that Tph2 Oex mice had significantly increased adipocyte size in iWAT (Fig. 5a & b). This was unexpected, because there was no statistical difference in iWAT weights between groups (Fig. 1f). There were no changes in gene expression of 5-HT related, pro-inflammatory cytokine or p53 signaling, while Tph2 Oex iWAT had increased *Fasn*, *Srebp-1c* and decreased *Atgl* expression (Fig. 5c & d & e). We also checked thermogenesis related gene expression, such as *Ucp1* and *Ppargc1a* but there were no differences between Tph2 Oex and Con mice (Fig. 5f). Unlike eWAT, immunostaining revealed no differences of 4-HNE accumulation in iWAT (Fig. S2a).

Epididymal adipocyte-specific TPH2 over-expression induces hepatic steatosis through decreased lipogenesis.

Tph2 Oex mice showed increased insulin resistance and glucose intolerance compared to Tph2 Con mice. Thus, we investigated the molecular details of liver, the central organ that modulates glucose homeostasis and systemic metabolism. H&E staining sections of liver showed significantly higher lipid accumulation in Tph2 Oex mice (Fig. 6a & b). Additionally, to further investigate the impact of TPH2 over-expression on whole body physiology, we assayed the serum metabolic profile of experimental animals. Adipocyte TPH2 over-expression did not significantly increase the serum ALT and AST levels (Fig. 6a & b). Since, Tph2 Oex mice showed increased

liver lipid accumulation, we analyzed the serum lipid profile to check whether adipocyte TPH2 contributes to the development of dyslipidemia. However, total cholesterol level in serum was not different between Tph2 Oex and Con (Fig. S3a). Also, both serum NEFA and TG levels were not affected by adipocyte TPH2 over-expression (Fig. S3b & c).

Further qPCR analysis revealed that Tph2 Oex mice had elevated glucokinase mRNA level, while other glucose metabolism related genes, such as Glucose 6-phosphate (*G6P*), phosphoenolpyruvate carboxykinase 1 (*Pck1*) or glucose transporter 2 (*Glut2*) were not altered (Fig. 6c). As we expected, hepatic mRNA level of lipogenesis related genes *Fasn* and *Srebp-1c* were significantly upregulated in Tph2 Oex mice without altering *Ppara* or *Pparg* expression level (Fig. 6d). The mRNA levels of pro-inflammatory cytokine were also measured. *Tnfa* was highly upregulated in Tph2 Oex liver, while *Il1b* and *F4/80* trended higher without statistical significance (Fig. 6e).

Epididymal adipocyte-specific TPH2 over-expression induces hepatic 4-HNE accumulation.

Previous studies reported that 4-HNE could be taken up by hepatocytes and contributes to insulin resistance and liver injury[29–31]. Since, circulating level of 4-HNE adduct was increased in Tph2 Oex mice, liver sections were immunostained for 4-HNE. Tph2 Oex liver sections showed more 4-HNE signaling than Tph2 Con sections, indicating higher 4-HNE accumulation in hepatocytes (Fig.7a).

TPH2 over-expression in epididymal adipocytes decreases systemic energy expenditure.

The over-expression of adipocyte TPH2 contributed to the increased WAT adiposity, hepatic liver accumulation and insulin resistance. However, between Tph2 Oex and Con mice there was no difference in energy intake. Tph2 Oex mice still showed obesity-associated pathologies, thus we hypothesized that Tph2 Oex mice may have reduced energy expenditure. To determine the systemic energy expenditure and metabolic profile, both groups of mice were put in indirect calorimetry for 96 hours. During the experiment, oxygen consumption and carbon dioxide production were measured to determine energy expenditure (Fig. S4a & b). Systemic energy expenditure was analyzed with regression and generalized linear model by CalR, and Tph2 Oex mice had significantly lower energy expenditure[25] (Fig. 8a & b). Interestingly, Tph2 Oex mice displayed a significantly lower respiratory exchange ratio (RER) compared to Tph2 Con mice, indicating a higher utilization of lipids than carbohydrate to generate energy (Fig. 8c). Also, we did not observe significant difference in physical activity between groups of mice (Fig. S4c). Previous studies reported the impact of adipocyte-derived peripheral 5-HT in regulating BAT thermogenesis, therefore we analyzed gene expression profile of BAT in both groups. qPCR analysis revealed no alterations in 5-HT related genes, however mRNA level of *Fasn* was increased with TPH2 over-expression (p-value: 0.068) (Fig. 9a & b). Furthermore, thermogenesis related genes such as *Ucp1*, *Ppargc1a* and *Cidea* were significantly downregulated in Tph2 Oex BAT, while BAT *Adipoq* level was significantly reduced (Fig.9c & d).

2.4. Discussion

HFD feeding to experimental animals promotes obesity, and both HFD and obesity spontaneously affects all organs, altering energy metabolism, behavior, gut microbiome, immune system and etc.[32–35]. This is a major obstacle for exploring the role of a target molecule or gene that upregulated in adipocytes with DIO, because HFD confounds the biology of adipocytes by altering whole body physiology. In this study, we bypassed this obstacle by using AAV FLEx conditional Cre-Switch gene expression vector method to investigate the role of epididymal adipocyte in developing adipocyte dysfunction and obesity associated metabolic complications. Direct AAV-Tph2 injection into eWAT of Adipoq-cre mice successfully induced eWAT specific over-expression of TPH2, and altered adipocyte biology and contributed to the development of obesity-associated pathologies without HFD feeding. Epididymal adipocyte-specific *Tph2* over-expression provides a niche approach to delineate the role of TPH2 on adipocyte dysfunction without altering TPH1, another enzyme that produces 5-HT.

Epididymal adipocyte-specific *Tph2* over-expression did not result in significant differences in body composition of mice. However, *Tph2* Oex mice had significantly increased eWAT and BAT mass, and also H&E staining showed enlarged adipocytes in eWAT and iWAT. Although, epipdydimal adipocyte-specific *Tph2* over-expression was not enough to change whole body composition, it still increased adiposity in eWAT and iWAT, and contributed to BAT whitening. Recent studies reported the adipocyte 5-HT mediated upregulation of WAT lipogenesis and downregulation of BAT thermogenesis via 5-HTRs in DIO[8,9]. Indeed, in our mice,

TPH2 over-expression significantly upregulated lipogenesis genes, while downregulated lipolysis genes. However, in aforementioned studies, circulating 5-HT level was not altered with genetic ablation or inhibition of adipocyte *Tph1*, while our epididymal adipocyte-specific *Tph2* over-expression significantly increased plasma 5-HT level[8,9]. Oh et al. reported that 2-week of HFD feeding to mice increased 5-HT level in eWAT more than 8-fold, also Crane et al. showed that HFD fed mice lacks *Tph1* in BAT had significantly decreased BAT 5-HT level[8,9]. This may due to the DIO-induced dramatic increase in adipocyte *Tph2* expression, resulting in compensation of reduced 5-HT production by adipocyte TPH1 with TPH2 derived 5-HT. This raises an important question: if 5-HT modulates WAT physiology through extracellular membrane-bound 5-HTRs, why do adipocyte TPH1 deficient mice exhibit protection against DIO despite no differences in systemic 5-HT levels, but only variations in 5-HT levels within WATs?

Based on this fundamental question, we hypothesized that 5-HT could modulates adipocyte biology via an alternate intracellular pathway in which encompasses both adipocyte TPH1 and TPH2 derived 5-HT. Previously, multiple studies demonstrated the role of MAOA on inducing oxidative stress in various tissues by degrading biogenic monoamines such as 5-HT[36–38]. MAOA derived ROS such as hydrogen peroxide propagates lipid peroxidation of PUFA and produces 4-HNE. In mice, development of obesity increased 4-HNE level in eWAT, while decreased in iWAT[39]. Thus, we injected AAV-Tph2 into eWAT to test whether adipocyte TPH2-derived 5-HT could modulate adipocyte physiology and systemic metabolism by generating 4-HNE and contributing to adipocyte dysfunctions. Tph2 Oex eWAT showed stronger 4-HNE fluorescence with immunostaining, which verified with

increased formation of 4-HNE adduct in eWAT. Furthermore, we also detected higher level of 4-HNE in plasma, suggesting that epididymal adipocyte derived 4-HNE may leak into the circulation. However, immunostaining of iWAT sections revealed no differences in 4-HNE fluorescence, demonstrating induction of 4-HNE formation with adipocyte TPH2-derived 5-HT. 4-HNE has been positively associated with activation of p53 signaling, which is known to induce adipocyte dysfunction and apoptosis[5,27,40]. In eWAT of Tph2 Oex mice, p53 and its downstream target gene expression levels were significantly increased compared to eWAT of Tph2 Con. In iWAT, there was no difference in *p53* expression level between Tph2 Oex and Tph2 Con mice, suggesting p53 activation of eWAT is associated with increased 4-HNE formation. Adipocyte p53 activation has been implicated with obesity induced inflammation and insulin resistance[41,42]. We also found the increased expression of pro-inflammatory cytokine related genes in Tph2 Oex eWAT, while no changes in iWAT, implying increased inflammation with Tph2 over-expression. Additionally, Tph2 Oex mice exhibited impaired insulin sensitivity, glucose tolerance and increased circulating insulin level, which further supports our hypothesis that intracellular degradation of adipocyte 5-HT leads to p53 activation induced adipocyte dysfunction and insulin resistance.

Although Tph2 over-expression was epididymal adipocyte specific, increase in circulating 5-HT altered iWAT and liver biology. Mice with genetic adipocyte-specific ablation of 5-HTR_{2a} gained significantly less fat mass with HFD feeding, demonstrating 5-HT induced lipogenesis via 5-HTR_{2a}[21]. On the contrary, in Tph2 Oex mice, average adipocyte size of iWAT was increased through increased lipogenic signaling from 5-HT. Moreover, hepatocytes express 5-$HTR_{2a,}$ and 5-HT signaling induces de novo

lipogenesis in hepatocytes[43]. Hepatocyte-specific 5-HTR_{2a} knockout mice accumulated significantly less lipid, and were protected against hepatic steatosis[44]. H&E staining of Tph2 Oex liver slides revealed increased hepatic lipid content. Furthermore, Tph2 Oex mice demonstrated increased liver mRNA levels of *Fasn* and *Srebp1c*, indicating upregulated hepatic lipogenesis. However, there were no significant changes observed in the mRNA level of *Cd36*, a fatty acid transporter, suggesting that hepatic lipid is coming from de novo lipogenesis, not fatty acid uptake. This is consistent with our serum metabolic markers of Tph2 Oex mice. Epididymal Tph2 over-expression did not alter serum lipid profile, such as total cholesterol, NEFA and TG. Previous study noted the possible adipocytes derived 4-HNE trafficking into hepatocyte, thus we also immunostained liver sections for 4-HNE[45]. In Tph2 Oex mice, we observed higher 4-HNE fluorescence in liver sections than Tph2 Con liver slides. Even though hepatic 4-HNE level was higher in Tph2 Oex mice, liver functional markers ALT and AST were not altered, suggesting 4-HNE induced liver damages was not substantial. However, previous studies reported that increased hepatic 4-HNE level could contribute to the development and progression of NAFLD and alcoholic liver disease[29,46,47].

Since Tph2 Oex mice exhibited insulin resistance and glucose intolerance, we also analyzed liver glucose metabolism related genes. We found that glucokinase gene expression was significantly increased in Tph2 Oex mice. While the reason why hepatic glucokinase is increased with adipocyte TPH2 over-expression is unclear, glucokinase has been associated with increased insulin resistance and impairment of

BAT thermogenesis[48,49]. This may further reinforce the unfavorable metabolic profile of Tph2 Oex mice.

As would be expected from increased circulating 5-HT level, BAT of Tph2 Oex mice displayed whitening and decreased thermogenic potential. Both systemic energy expenditure and RER was significantly reduced in Tph2 Oex mice. 5-HT could inhibit BAT thermogenesis by binding to 5-HTR_{3a}, and genetic deletion or pharmacological inhibition of 5-HTR_{3a} resulted in increased BAT thermogenesis and energy expenditure[8,9]. Tph2 Oex mice also exhibited decreased expression of thermogenesis related genes such as *Ucp1*, *Ppargc1a* and *Cidea*, which lead to decreased systemic energy expenditure. Also increased *Fasn* expression was observed, consistent with increased lipid accumulation in BAT. Interestingly, mRNA level of *Adipoq* was significantly decreased in Tph2 Oex BAT. Similar to white adipocytes, brown adipocytes also secrete adipokines and other factors to regulate and crosstalk with other tissues[50–52]. Recently, single-cell RNA sequencing analysis has uncovered the presence of a heterogeneous cell population within BAT, consisting of both low thermogenic potential cells and high thermogenic brown adipocytes[53]. Brown adipocytes with low thermogenic potential have lower mRNA levels of *Adipoq* and *Ucp1*, and larger lipid droplets compared to high thermogenic brown adipocytes[53]. Considering the phenotype of Tph2 Oex BAT, peripheral 5-HT may favor the conversion of high thermogenic brown adipocytes to low thermogenic ones.

In conclusion, our study provides novel finding that eWAT derived 5-HT regulates metabolic physiology of various tissues, and ultimately impact systemic metabolism. Furthermore, we demonstrated that adipocyte-derived 5-HT not only

modulates metabolism via extracellular membrane 5-HTR signaling, but also induce metabolic dysfunction through intracellular pathways that produces 4-HNE and activation of p53 signaling. To further delineate the underlying mechanisms in which TPH2 induces adipocyte dysfunctions, insulin signaling, crown-like structures, tissue-specific level of 5-HT and the effect of 4-HNE reduction or p53 inhibition should be assessed. These data contribute to a deeper understanding of the role of adipocyte-specific 5-HT and TPH2 in obesity development and pathophysiology, which may prove to be a potential therapeutic target.

2.5. Figures

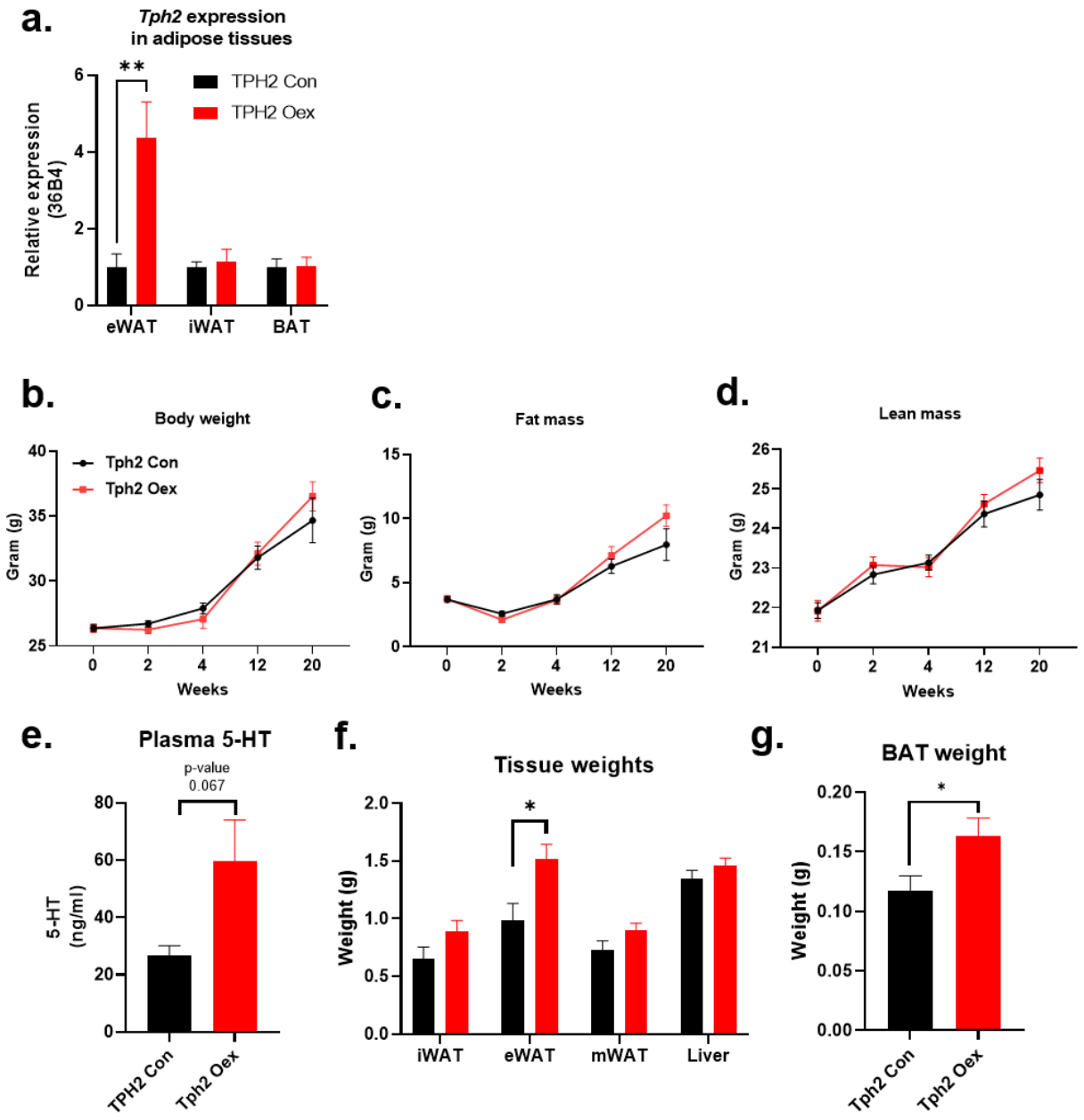

Figure 1. Epididymal Adipocyte-specific TPH2 Over-expression Increases Circulating 5-HT Level and eWAT and BAT mass. **(a)** *Tph2* gene expression levels in adipose tissues 24-week following AAV injection, n=8~9 per group. **(b)** Body weight, **(c)** fat mass and **(d)** lean mass during the experimental period, n=8~9 per group. **(e)** Plasma 5-HT level 24-week following AAV injection, n=4. **(f)** Weights of dissected and collected tissues 24-week following AAV injection, n=8~9 per group. **(g)** Weight of BAT after dissection 24-week following AAV injection, n=8~9 per group. All data are expressed as mean ± SEM via Student's t-test. *p<0.05

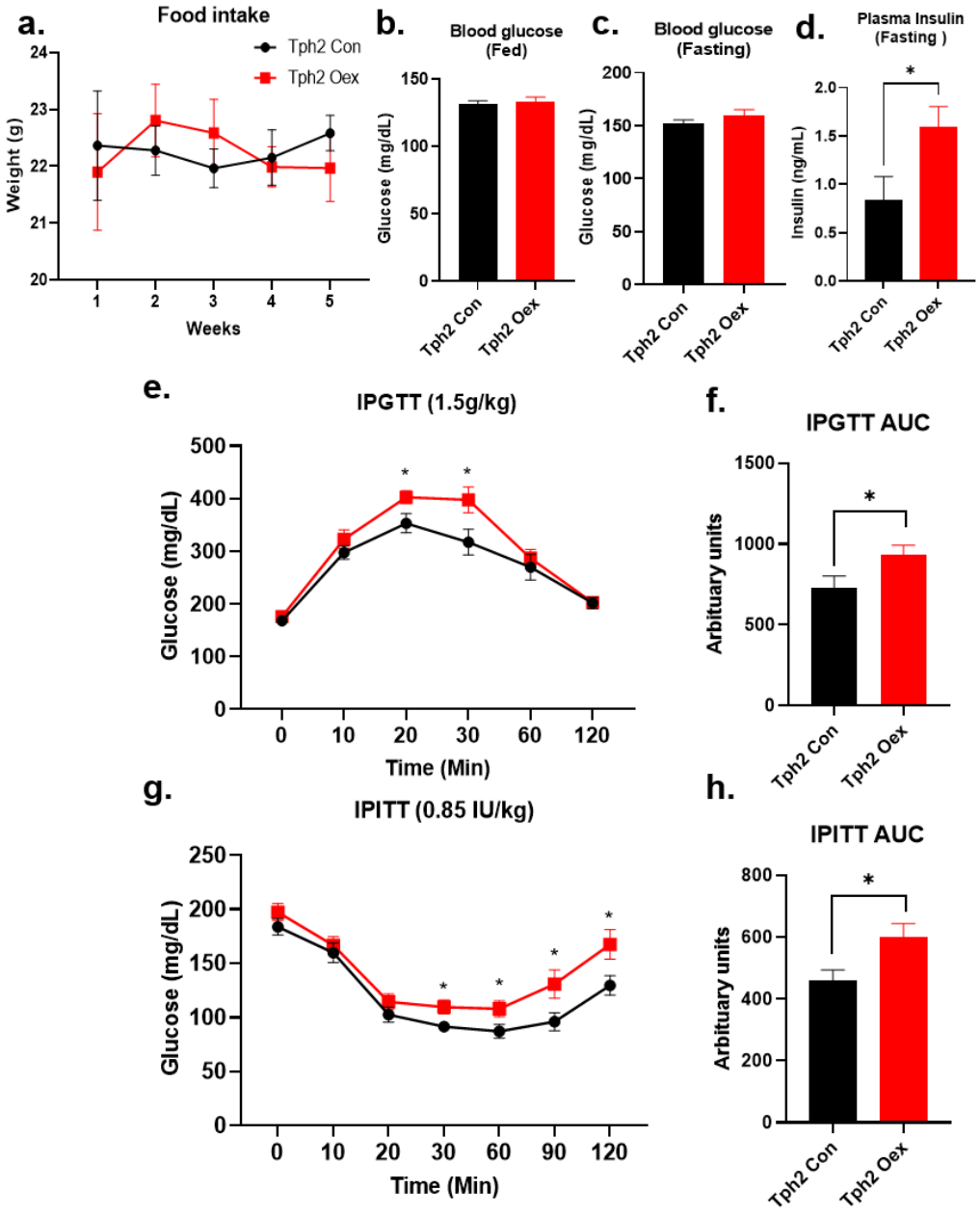

Figure 2. Tph2 Oex Mice Exhibit Increases Fasting Insulin Level, Glucose Intolerance and Insulin Resistance. **(a)** Average weekly food intake in *Tph2* Con and Oex mice, n=8~9 per group. **(b)** Fed state blood glucose level, **(c)** fasting state blood glucose level and **(d)** fasting plasma insulin level 24-week following AAV injection, n=8~9 per group. **(e)** IPGTT in mice after 6-h fasting period at week 16. Each data point represents mean glucose level at each time point, n=8 per group. **(f)** AUC for IPGTT was calculated after normalization with the lowest glucose level. **(g)** IPITT in mice after 6-h fasting period at week 19. **(h)** AUC for IPITT was calculated after normalization with the lowest glucose level. Each data point represents mean glucose level at each time point., n=8 per group. All data are expressed as mean ± SEM via Student's t-test. *p<0.05

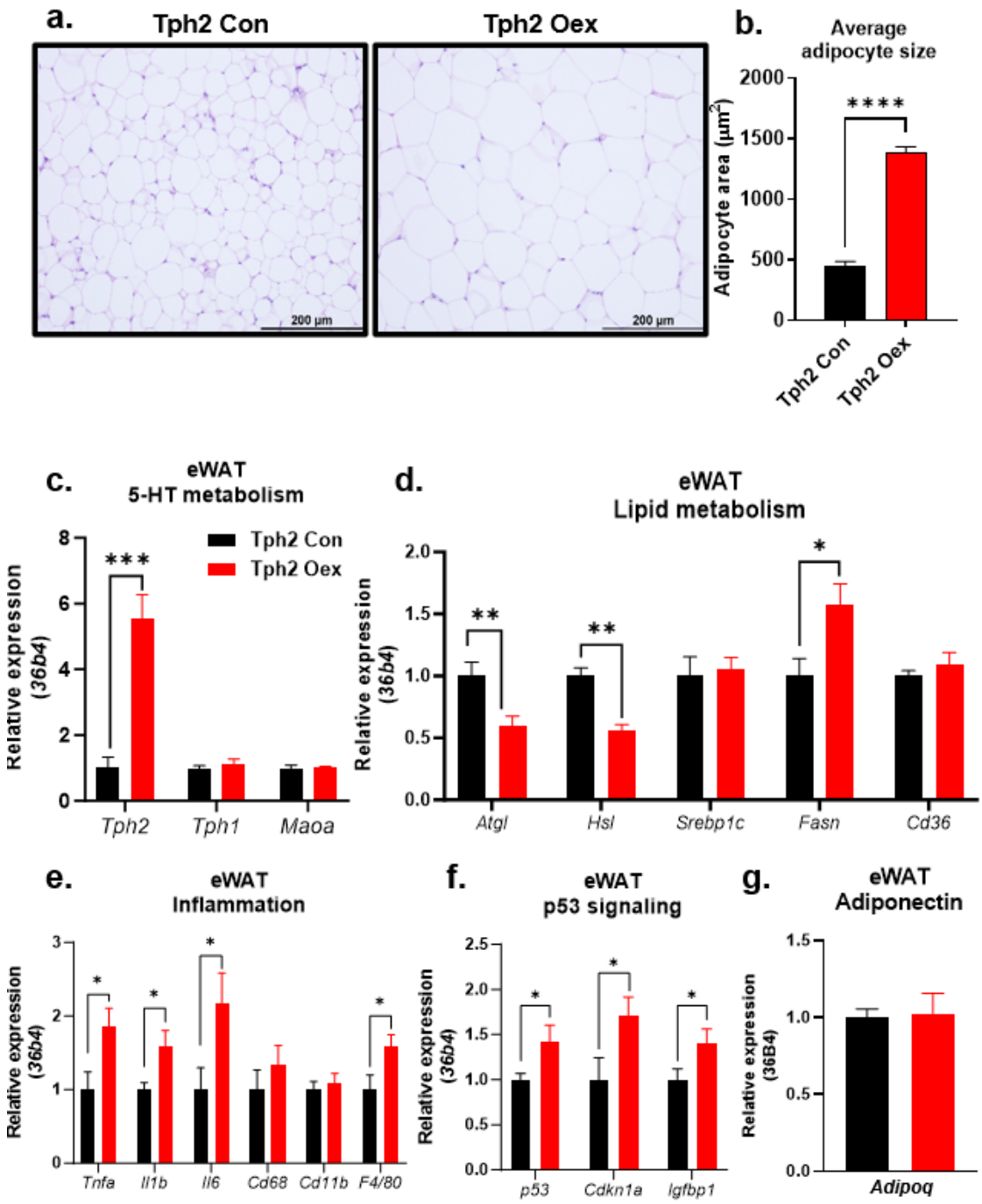

Figure 3. TPH2 Over-expression of Epididymal Adipocyte Induces Changes in eWAT Adiposity and Gene Expression Profile. **(a)** Representative images of H&E staining of eWAT from Tph2 Con and Oex mice. **(b)** Average adipocyte size calculated from eWAT H&E staining images, n=5 per group **(c)** Expression profile of 5-HT metabolism related genes in eWAT, n=8~9 per group. **(d)** Expression profile of lipid metabolism related genes in eWAT, n=8~9 per group **(e)** Expression profile of inflammation related genes in eWAT, n=8~9 per group **(f)** Expression profile of p53 signaling related genes in eWAT, n=8~9 per group. **(g)** Adiponectin mRNA level in eWAT, n=8~9 per group. All data are expressed as mean ± SEM via Student's t-test. *p<0.05; **p<0.01; ***p<0.001; ****p<0.0001.

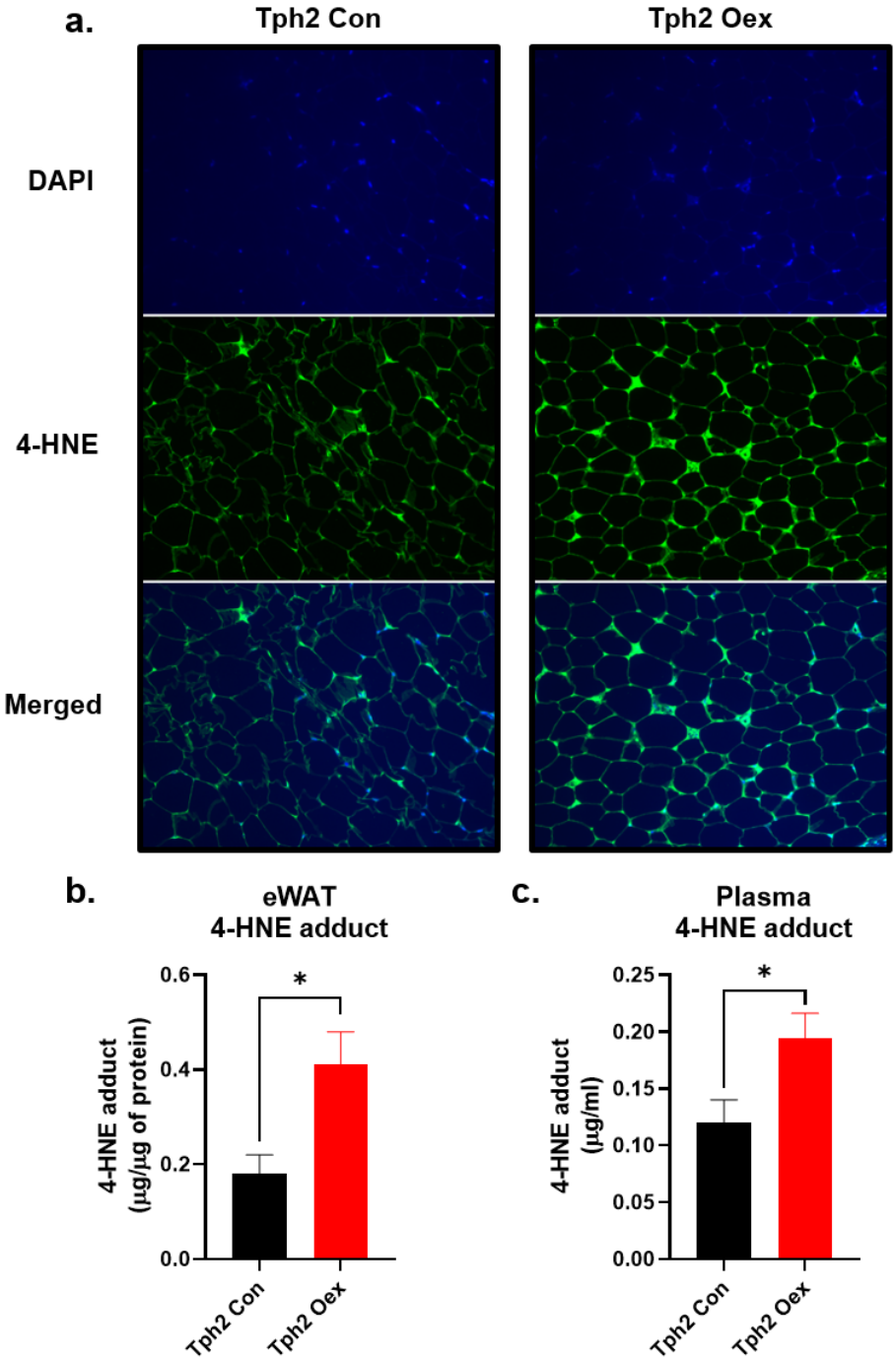

Figure 4. Elevated 4-HNE Formation in Tph2 Oex eWAT and Circulating 4-HNE level (a) Representative images of Immunofluorescence on eWAT with antibodies against 4-HNE and DAPI counterstaining. **(b)** 4-HNE adduct level in eWAT of Tph2 Con and Oex mice, n=5 per group. **(d)** 4-HNE adduct level in plasma of Tph2 Con and Oex mice, n=5 per group. All data are expressed as mean ± SEM via Student's t-test. *p<0.05.

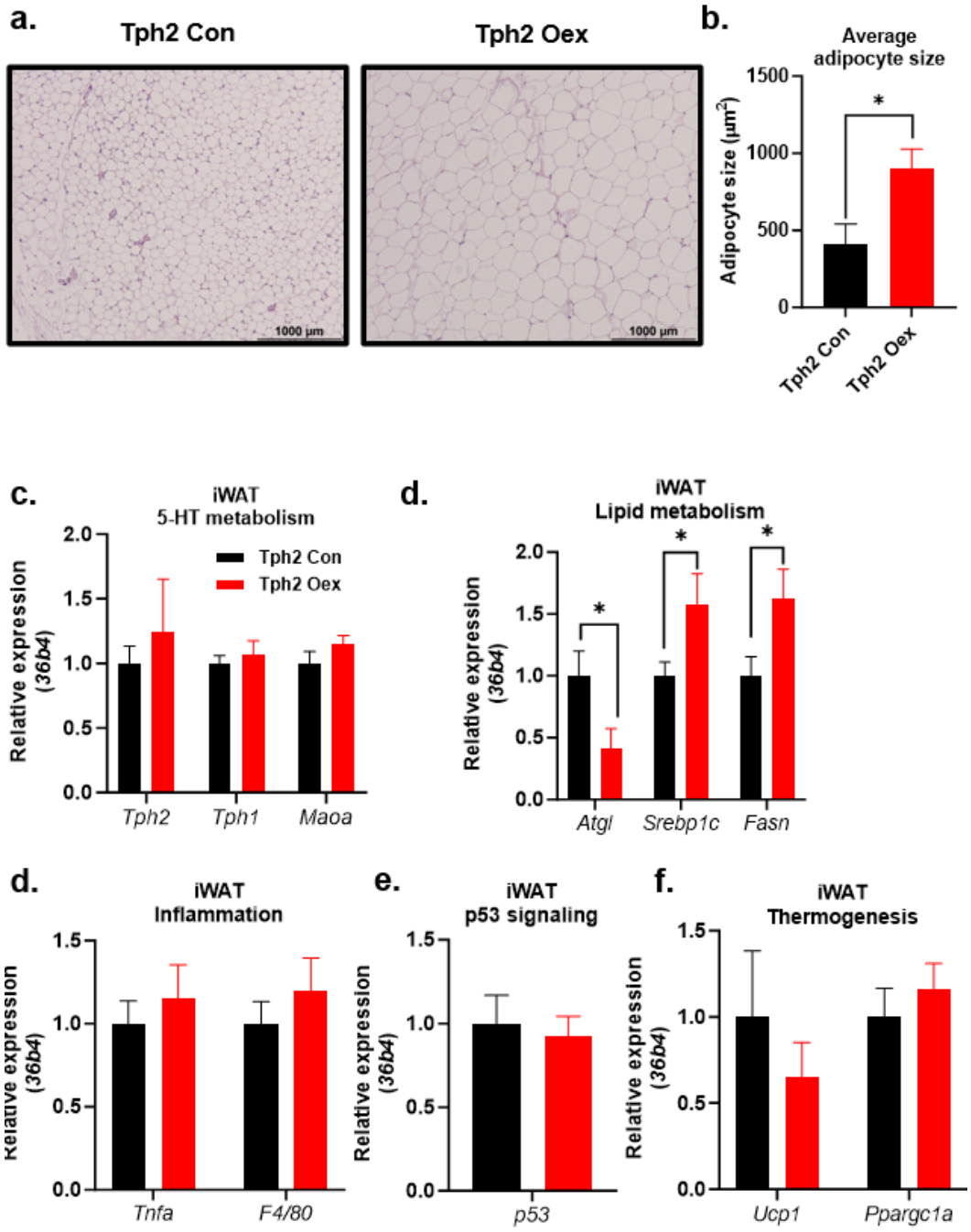

Figure 5. TPH2 Over-expression of Epididymal Adipocyte Induces Changes in iWAT Adiposity and Gene Expression Profile. **(a)** Representative images of H&E staining of iWAT from Tph2 Con and Oex mice. **(b)** Average adipocyte size calculated from eWAT H&E staining images, n=5 per group **(c)** Expression profile of 5-HT metabolism related genes in iWAT, n=8~9 per group. **(d)** Expression profile of lipid metabolism related genes in iWAT, n=8~9 per group **(e)** Expression profile of inflammation related genes in iWAT, n=8~9 per group **(f)** Expression profile of p53 signaling related genes in iWAT, n=8~9 per group. **(g)** Expression profile of thermogenesis related genes in iWAT, n=8~9 per group. All data are

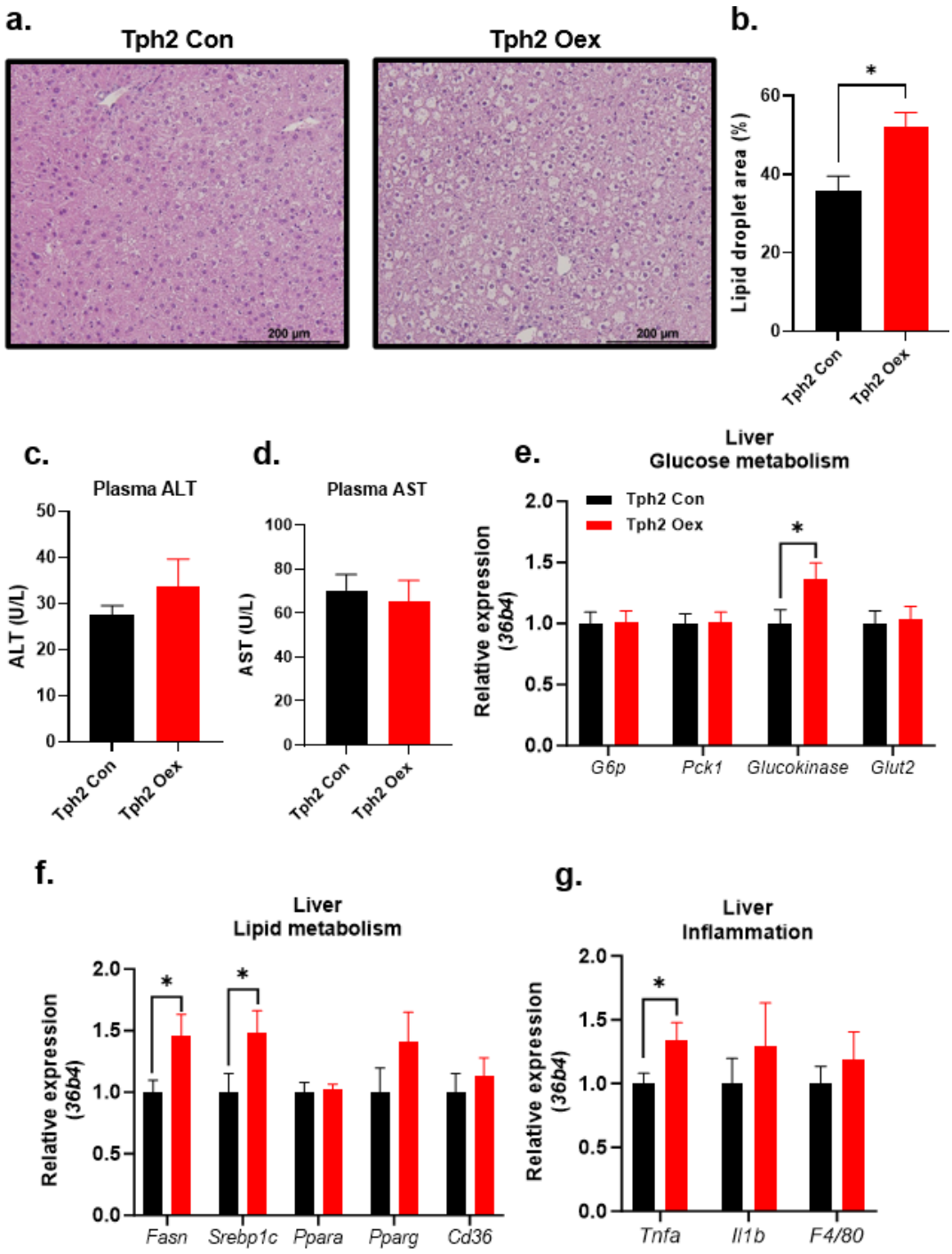

Figure 6. Epididymal Adipocyte TPH2 Induces Changes in Hepatic Steatosis and Liver Gene Expression Profile. **(a)** Representative images of H&E staining of liver from Tph2 Con and Oex mice. **(b)** Average lipid droplet area calculated from liver H&E staining images, n=5 per group **(c)** Plasma ALT and **(d)** plasma AST levels in Tph2 Con and Oex mice, n=5~7 per group. **(e)** Expression profile of glucose metabolism related genes in liver, n=8~9 per group **(f)** Expression profile of lipid metabolism related genes in liver, n=8~9 per group. **(g)**

Expression profile of inflammation related genes in liver, n=8~9 per group. All data are expressed as mean ± SEM via Student's t-test. *p<0.05

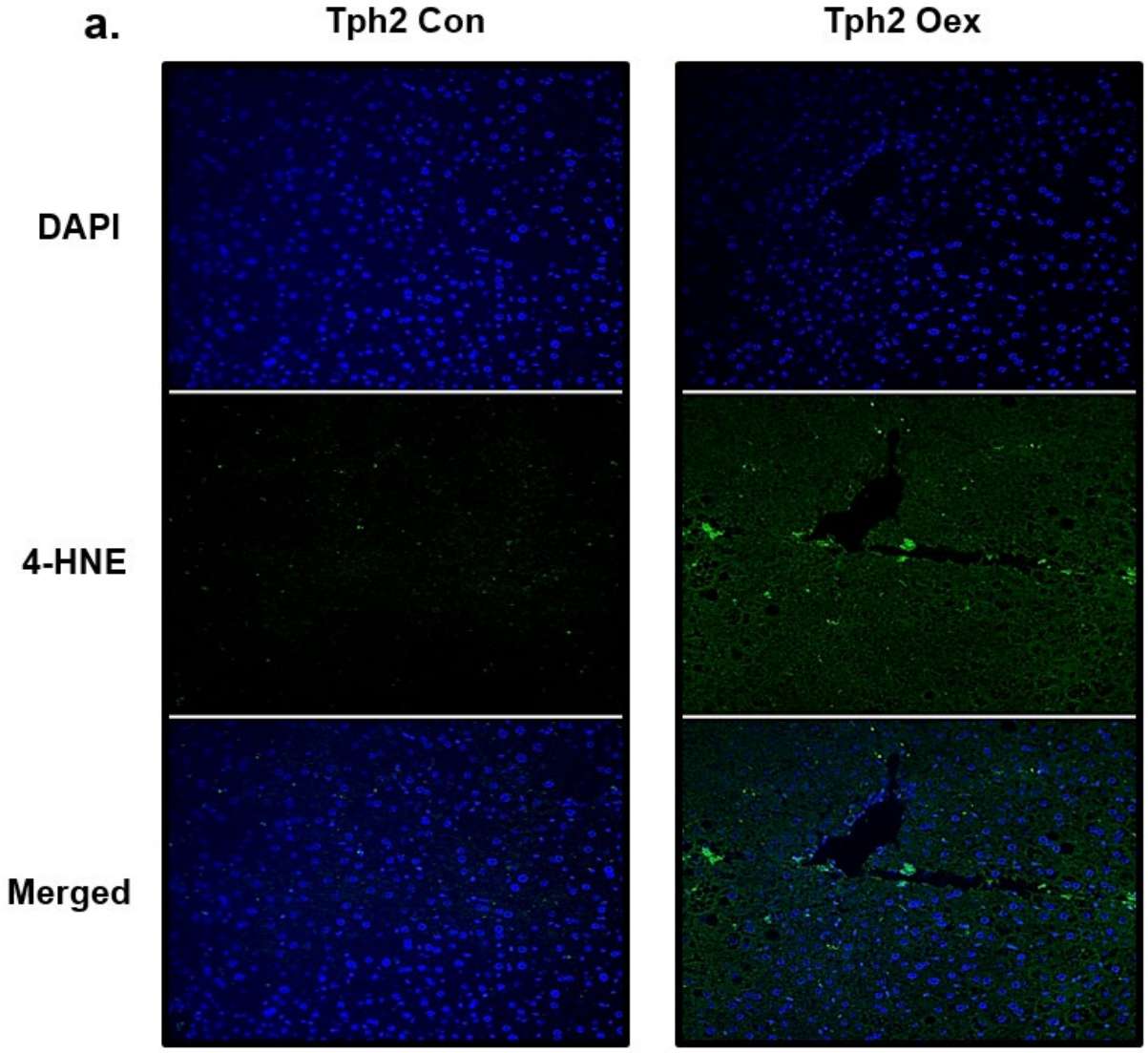

Figure 7. Tph2 Oex Mice Have Increased 4-HNE Accumulation in Liver.
(a) Representative images of Immunofluorescence on liver with antibodies against 4-HNE and DAPI counterstaining.

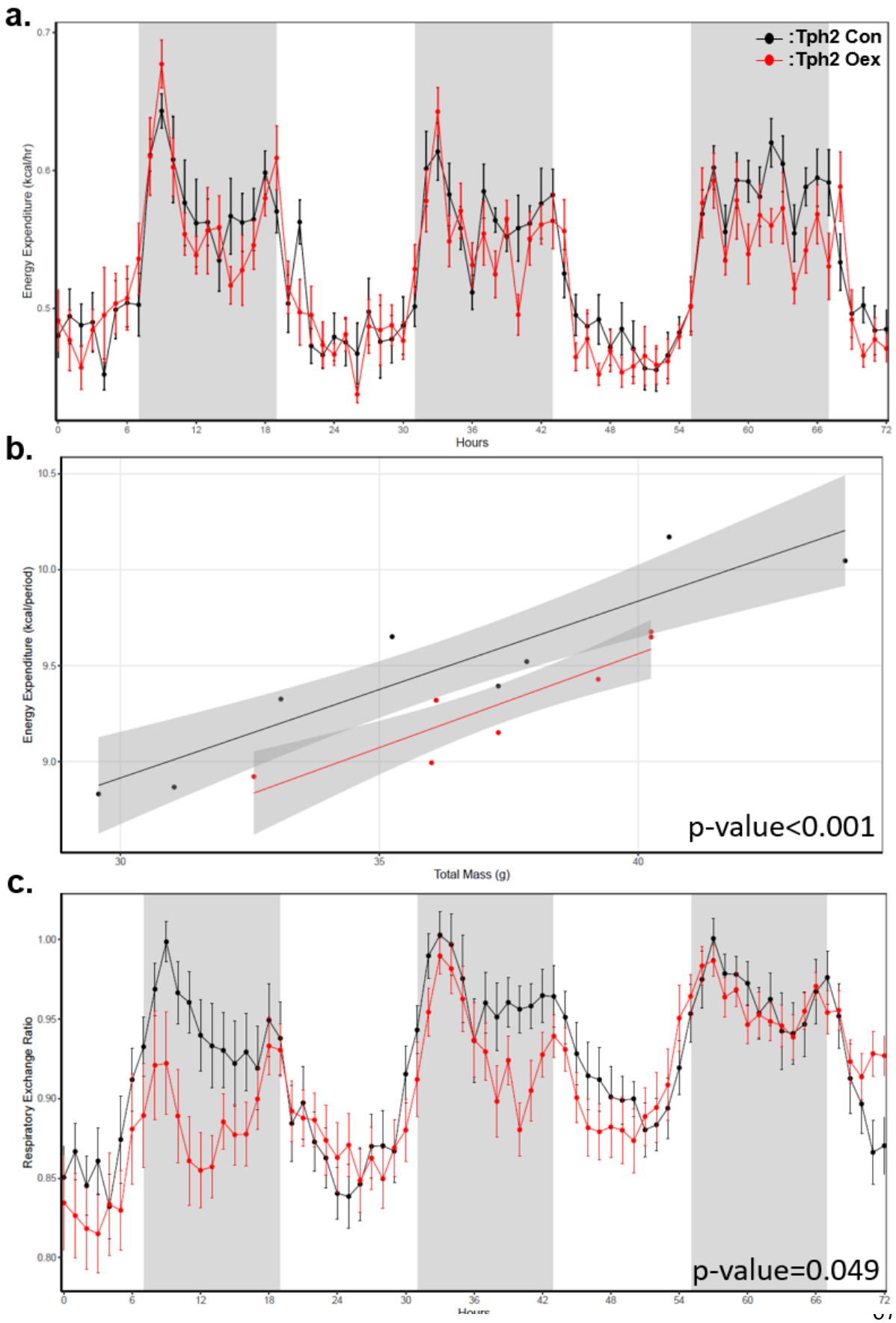
a.
:Tph2 Con
:Tph2 Oex
Energy Expenditure (kcal/hr)
Hours
b.
Energy Expenditure (kcal/period)
Total Mass (g)
p-value<0.001
c.
Respiratory Exchange Ratio
p-value=0.049

Figure 8. Epididymal Adipocyte TPH2 Over-expression Increases Systemic Energy Expenditure. **(a)** Time course energy expenditure during the indirect calorimetry analysis **(b)** Regression model of average energy expenditure for 72-hour, analyzed by the generalized linear model using body mass as a covariate, n=7~8 per group. **(c)** Time course RER during the indirect calorimetry analysis, n=7~8. All data are expressed as mean ± SEM.

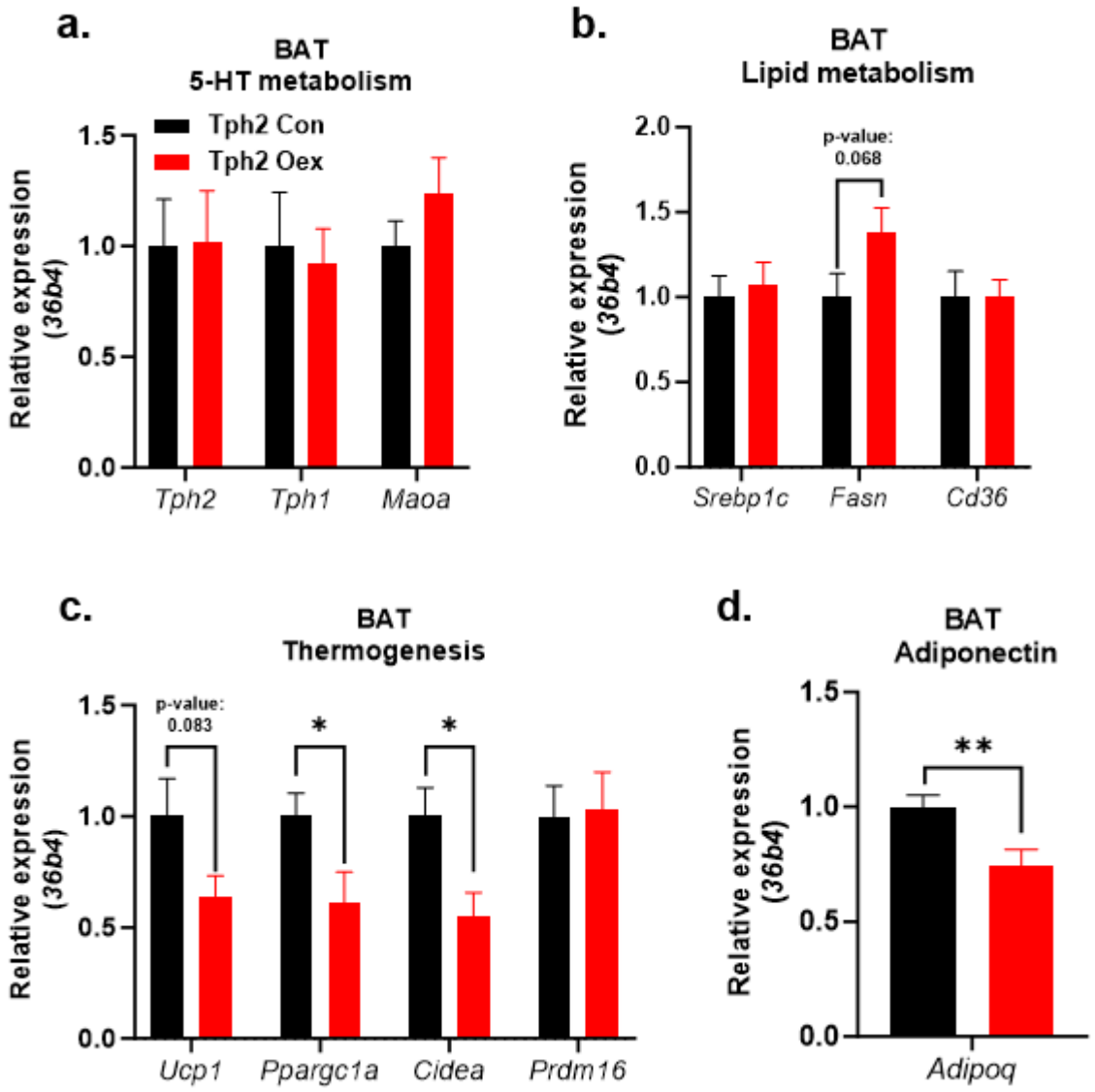

Figure 9. Epididymal Adipocyte TPH2 Induces Changes in BAT Gene Expression Profile. (a) Expression profile of 5-HT metabolism related genes in BAT, n=8~9 per group **(b)** Expression profile of lipid metabolism related genes in BAT, n=8~9 per group. **(c)** Expression profile of thermogenesis related genes in BAT, n=8~9 per group. **(d)** Adiponectin mRNA level in BAT, n=8~9 per group. All data are expressed as mean ± SEM via Student's t-test. *p<0.05.

a.

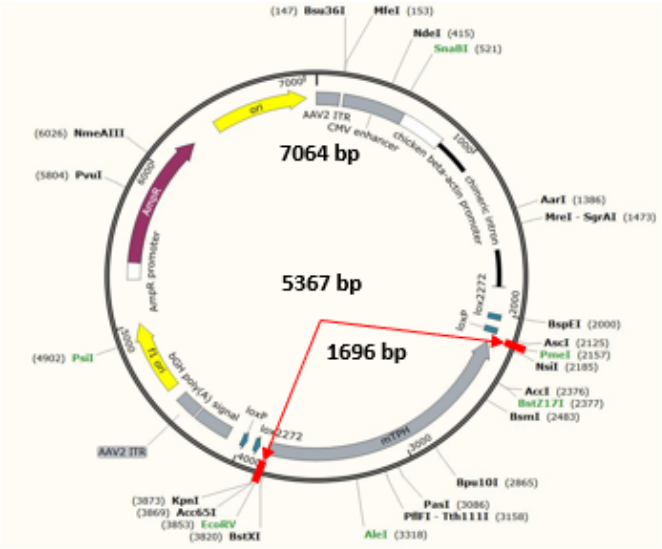

b.

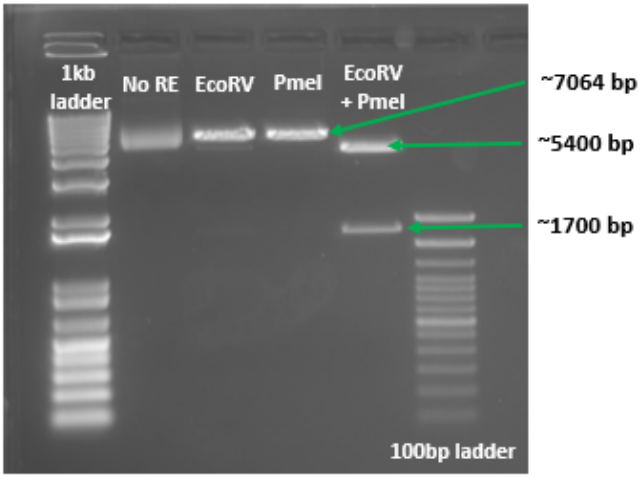

c.

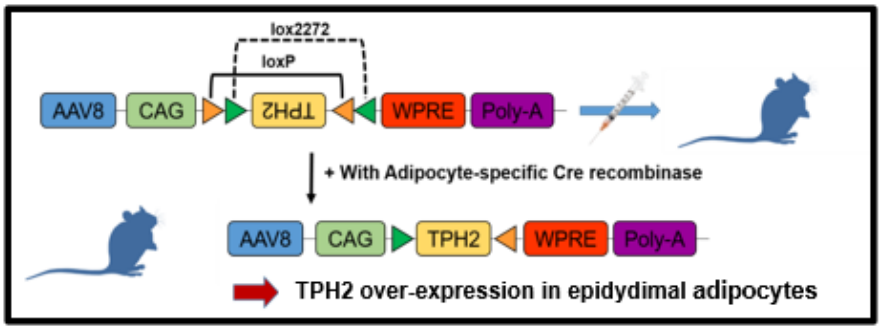

Figure S1. TPH2 Over-expressing AAV Plasmid Vector Map and Experimental Scheme. **(a)** Plasmid vector map of AAV-Tph2. **(b)** Plasmid size after each restriction enzyme treatment. **(c)** Experimental scheme of Tph2-AAV induced over-expression.

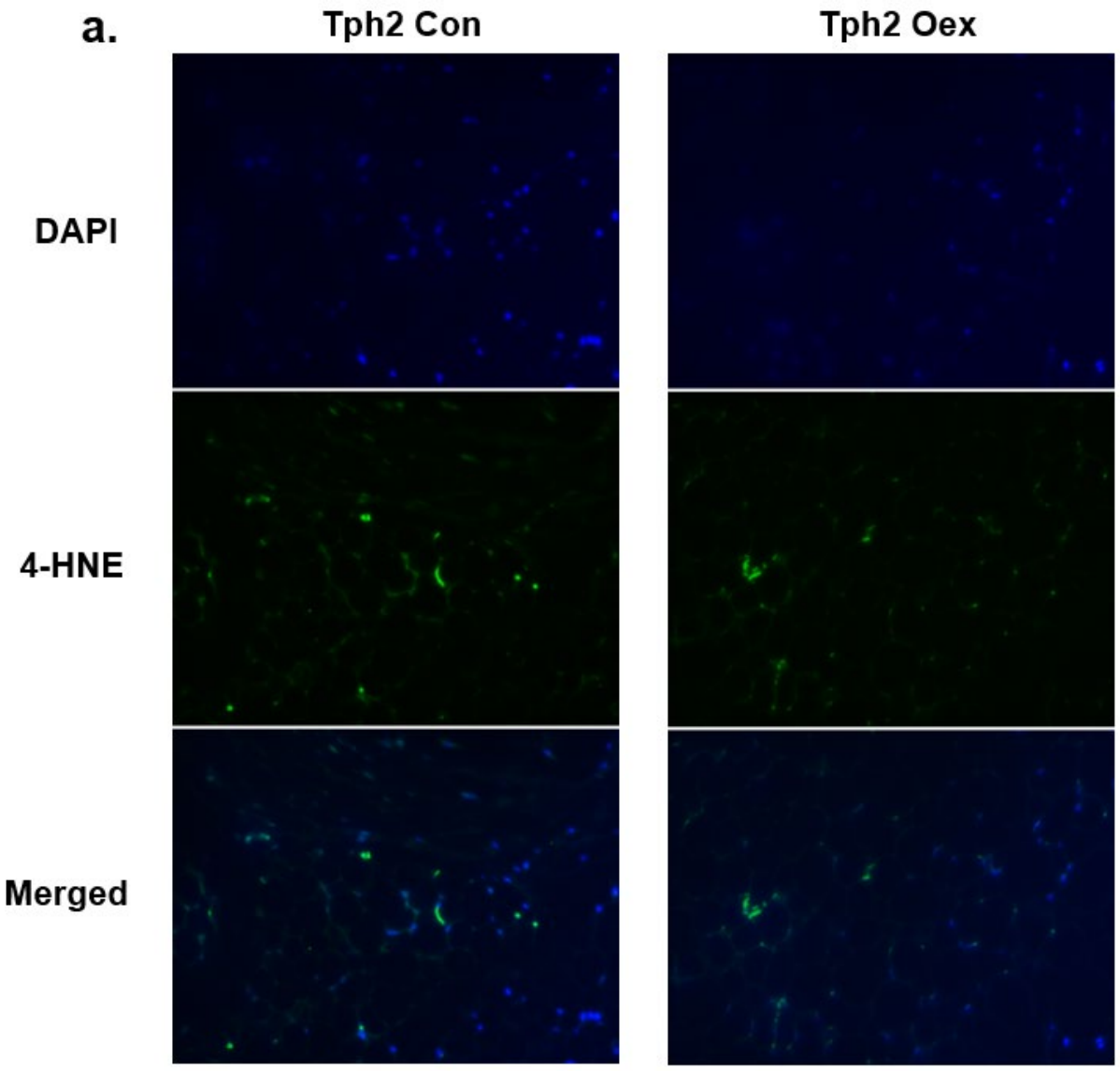

Figure S2. No Differences on iWAT 4-HNE Accumulation Between Tph2 Con and Oex Mice. (a) Representative images of Immunofluorescence on iWAT with antibodies against 4-HNE and DAPI counterstaining.

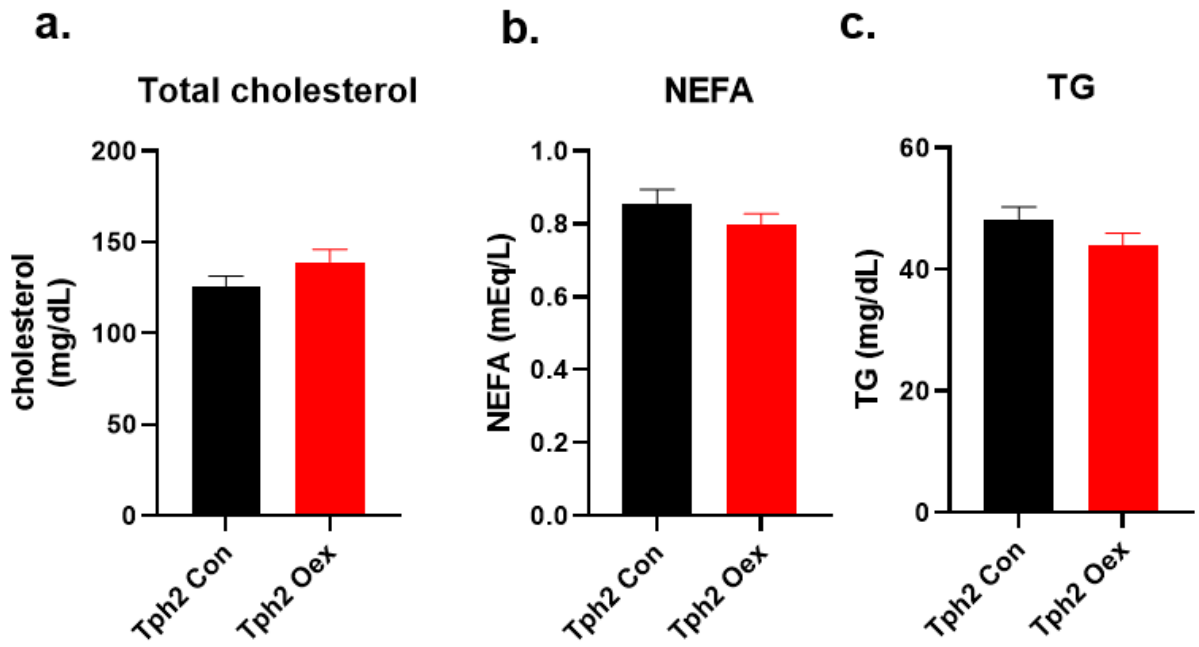

Figure S3. Fasting Plasma Lipid Profile of Each Group. **(a)** Plasma total cholesterol level in Tph2 Con and Oex mice, n=5~7. **(b)** Plasma NEFA level in Tph2 Con and Oex mice, n=5~7. **(c)** Plasma TG level in Tph2 Con and Oex mice, n=5~7. All data are expressed as mean ± SEM via Student's t-test.

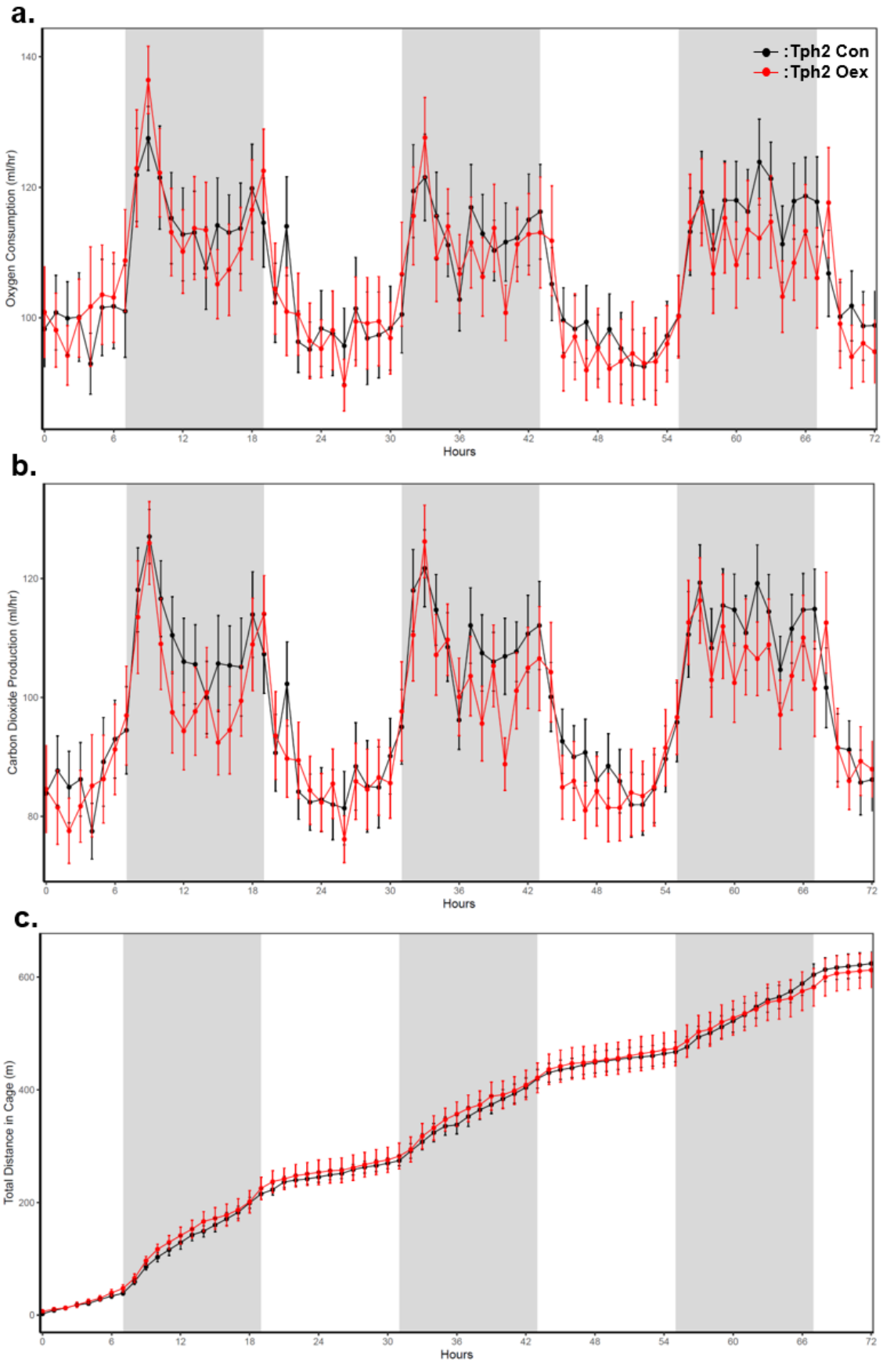
a.
:Tph2 Con
:Tph2 Oex
Oxygen Consumption (ml/hr)
Hours
b.
Carbon Dioxide Production (ml/hr)
Hours
c.
Total Distance in Cage (m)
Hours

Figure S4. Oxygen Consumption, Carbon Dioxide Production and Total Moving Distance in Indirect Calorimetry Analysis. (a) Time course oxygen consumption during the indirect calorimetry analysis, n=7~8. **(b)** Time course carbon dioxide production during the indirect calorimetry analysis, n=7~8. **(c)** Cumulative moving distance of mice during the indirect calorimetry analysis, n=7~8. All data are expressed as mean ± SEM.

Supplementary Table 1. Primer sequences used in this study.

Gene	Forward	Reverse
36b4	GAGGAATCAGATGAGGATATGGGA	AAGCAGGCTGACTTGGTTGC
Adipoq	CTCCACCCAAGGGAACTTGT	GGACCAAGAAGACCTGCATC
Atgl	TGTGGCCTCATTCCTCCTAC	TCGTGGATGTTGGTGGAGCT
Cdkn1a	CACAGCTCAGTGGACTGGAA	ACCCTAGACCCACAATGCAG
Cidea	GCCGTGTTAAGGAATCTGCTG	TGCTCTTCTGTATCGCCCAGT
Cd11b	CACTCAGTGACTGCCCAAAA	CCTCAAGACAGGACATCGCT
Cd36	TGGCCAAGCTATTGCGACAT	ACACAGCGTAGATAGACCTGC
Cd68	ACCGCCATGTAGTCCAGGTA	ATCCCCACCTGTCTCTCTCA
Fasn	GCTGCGGAAACTTCAGGAAAT	AGAGACGTGTCACTCCTGGACTT
F4/80	CTTTGGCTATGGGCTTCCAGTC	GCAAGGAGGACAGAGTTTATCGTG
Hsl	GGAGCACTACAAACGCAACGA	TCGGCCACCGGTAAAGAG
Igfbp3	TGTTTTCTGGTCCAGCCTCT	CAAGCCACTCCTCTTTCCTG
Il1b	CTGGTGTGTGACGTTCCCATT	CCGACAGCACGAGGCTTT
Maoa	GCGGTACAAGGGTCTGTTCC	CAGCCAATCCTGAGATGCCG
Mcp1	AGGTCCCTGTCATGCTTCTG	TCTGGACCCATTCCTTCTTG
Ppargc1a	GCCCAGGTACGACAGCTATG	ACGGCGCTCTTCAATTGCTT
Ppara	AGAAGTTGCAGGAGGGGATT	TCGGACTCGGTCTTCTTGAT
Pparg	GGTGTGATCTTAACTGCCGGA	GCCCAAACCTGATGGCATTG
Prdm16	AGCCCTCGCCCACAACTTGC	TGACCCCCGGCTTCCGTTCA
p53	TGGCTCCTCCCCAACATCTTATC	CTTCCTCTGTCCGACGGTCTCTC
Srebp1c	GGAGGGGTAGGGCCAACGGCCT	CATGTCTTCGAAAGTGCAATCC
Tnf-α	ATGGGCTTTCCGAATTCAC	GAGGCAACCTGACCACTCTC
Tph1	ACCATGATTGAAGACAACAAGGAG	TCAACTGTTCTCGGCTGATG
Tph2	GCCATGCAGCCCGCAATGATGATG	CAACTGCTGTCTTGCTGCTC
Ucp1	CTTTGCCTCACTCAGGATTGG	CTTTGCCTCACTCAGGATTGG

2.6. References

1. Wondmkun, Y. T. Obesity, insulin resistance, and type 2 diabetes: Associations and therapeutic implications. *Diabetes, Metab. Syndr. Obes.* **13**, 3611–3616 (2020).
2. Cypess, A. M. *et al.* Identification and Importance of Brown Adipose Tissue in Adult Humans. 1509–1517 (2009).
3. Samuel, V. T., Petersen, K. F. & Shulman, G. I. Lipid-induced insulin resistance : unravelling the mechanism. *Lancet* **375**, 2267–2277 (2010).
4. Ahmed, B., Sultana, R. & Greene, M. W. Adipose tissue and insulin resistance in obese. *Biomed. Pharmacother.* **137**, 111315 (2021).
5. Masschelin, P. M., Cox, A. R., Chernis, N. & Hartig, S. M. The Impact of Oxidative Stress on Adipose Tissue Energy Balance. *Front. Physiol.* **10**, 1–8 (2020).
6. Sonne, S. B. *et al.* Obesity is associated with depot-specific alterations in adipocyte DNA methylation and gene expression. *Adipocyte* **6**, 124–133 (2017).
7. Rosen, E. D. & Spiegelman, B. M. Adipocytes as regulators of energy balance and glucose homeostasis. *Nature* vol. 444 847–853 (2006).
8. Oh, C. M. *et al.* Regulation of systemic energy homeostasis by serotonin in adipose tissues. *Nat. Commun.* **6**, (2015).
9. Crane, J. D. *et al.* Inhibiting peripheral serotonin synthesis reduces obesity and metabolic dysfunction by promoting brown adipose tissue thermogenesis. *Nat. Med.* **21**, 166–172 (2015).
10. Sumara, G., Sumara, O., Kim, J. K. & Karsenty, G. Gut-derived serotonin is a multifunctional determinant to fasting adaptation. *Cell Metab.* **16**, 588–600 (2012).
11. Namkung, J., Kim, H. & Park, S. Peripheral serotonin: A new player in systemic energy homeostasis. *Molecules and Cells* vol. 38 1023–1028 (2015).
12. Halford, J. C. G. & Blundell, J. E. Separate systems for serotonin and leptin in appetite control. *Ann. Med.* **32**, 222–232 (2000).
13. Spohn, S. N. & Mawe, G. M. Non-conventional features of peripheral serotonin signalling-the gut and beyond. *Nat. Rev. Gastroenterol. Hepatol.* **14**, 412–420 (2017).
14. Walther, D. J. *et al.* Synthesis of serotonin by a second tryptophan hydroxylase isoform. *Science (80-.).* **299**, 76 (2003).
15. Yabut, J. M. *et al.* Emerging Roles for Serotonin in Regulating Metabolism: New Implications for an Ancient Molecule. *Endocr. Rev.* **40**, 1092–1107 (2019).

16. Mohammad-Zadeh, L. F., Moses, L. & Gwaltney-Brant, S. M. Serotonin: A review. *J. Vet. Pharmacol. Ther.* **31**, 187–199 (2008).

17. Young, R. L. *et al.* Augmented capacity for peripheral serotonin release in human obesity. *Int. J. Obes.* **42**, 1880–1889 (2018).

18. Wang, L. *et al.* Gut-Derived Serotonin Contributes to the Progression of Non-Alcoholic Steatohepatitis via the Liver HTR2A/PPARγ2 Pathway. *Front. Pharmacol.* **11**, 553 (2020).

19. Sumara, G., Sumara, O., Kim, J. K. & Karsenty, G. Gut-derived serotonin is a multifunctional determinant to fasting adaptation. *Cell Metab.* **16**, 588–600 (2012).

20. Namkung, J. *et al.* Inhibition of serotonin synthesis induces negative hepatic lipid balance. *Diabetes Metab. J.* **42**, 233–243 (2018).

21. Shong, K. E., Oh, C. M., Namkung, J., Park, S. & Kim, H. Serotonin regulates de novo lipogenesis in adipose tissues through serotonin receptor 2a. *Endocrinol. Metab.* **35**, 470–479 (2020).

22. Hageman, R. S. *et al.* High-fat diet leads to tissue-specific changes reflecting risk factors for diseases in DBA/2J mice. *Physiol Genomics* **42**, 55–66 (2010).

23. Choi, M. S. *et al.* High-fat diet decreases energy expenditure and expression of genes controlling lipid metabolism, mitochondrial function and skeletal system development in the adipose tissue, along with increased expression of extracellular matrix remodelling- and inflammation-related genes. *Br. J. Nutr.* **113**, 867–877 (2015).

24. Atasoy, D. *et al.* A directional strategy for monitoring Cre-mediated recombination at the cellular level in the mouse. *Nat. Biotechnol.* **21**, 562–565 (2003).

25. Mina, A. I. *et al.* CalR: A Web-Based Analysis Tool for Indirect Calorimetry Experiments. *Cell Metab.* **28**, 656-666.e1 (2018).

26. Livak, K. J. & Schmittgen, T. D. Analysis of relative gene expression data using real-time quantitative PCR and the 2-ΔΔCT method. *Methods* **25**, 402–408 (2001).

27. Pillon, N. J. *et al.* The lipid peroxidation by-product 4-hydroxy-2-nonenal (4-HNE) induces insulin resistance in skeletal muscle through both carbonyl and oxidative stress. *Endocrinology* **153**, 2099–2111 (2012).

28. Castro, J. P., Jung, T., Grune, T. & Siems, W. 4-Hydroxynonenal (HNE) modified proteins in metabolic diseases. *Free Radic. Biol. Med.* **111**, 309–315 (2017).

29. Zheng, R. *et al.* Differential metabolism of 4-hydroxynonenal in liver, lung and brain of mice and rats. *Toxicol. Appl. Pharmacol.* **279**, 43–52 (2014).

30. Qiao, H. *et al.* Protective effects of an anti-4-HNE monoclonal antibody against liver injury and lethality of endotoxemia in mice. *Eur. J. Pharmacol.* **950**, 175702 (2023).

31. Rains, J. L. & Jain, S. K. Oxidative stress, insulin signaling, and diabetes. *Free Radic. Biol. Med.* **50**, 567–575 (2011).

32. Kakimoto, P. A. & Kowaltowski, A. J. Effects of high fat diets on rodent liver bioenergetics and oxidative imbalance. *Redox Biol.* **8**, 216–225 (2016).

33. Rohr, M. W., Narasimhulu, C. A., Rudeski-Rohr, T. A. & Parthasarathy, S. Negative Effects of a High-Fat Diet on Intestinal Permeability: A Review. *Adv. Nutr.* **11**, 77–91 (2020).

34. Ribaroff, G. A., Wastnedge, E., Drake, A. J., Sharpe, R. M. & Chambers, T. J. G. Animal models of maternal high fat diet exposure and effects on metabolism in offspring: a meta-regression analysis. *Obes. Rev.* **18**, 673–686 (2017).

35. Arnold, S. E. *et al.* High fat diet produces brain insulin resistance, synaptodendritic abnormalities and altered behavior in mice. *Neurobiol. Dis.* **67**, 79–87 (2014).

36. Soto-Otero, R. *et al.* Inhibition of brain monoamine oxidase activity by the generation of hydroxyl radicals potential implications in relation to oxidative stress. *Life Sci.* **69**, 879–889 (2001).

37. Umbarkar, P. *et al.* Monoamine oxidase-A is an important source of oxidative stress and promotes cardiac dysfunction, apoptosis, and fibrosis in diabetic cardiomyopathy. *Free Radic. Biol. Med.* **87**, 263–273 (2015).

38. Sturza, A. *et al.* Monoamine oxidase is a source of oxidative stress in obese patients with chronic inflammation. *Can. J. Physiol. Pharmacol.* **97**, 844–849 (2019).

39. Long, E. K., Olson, D. M. & Bernlohr, D. A. High-fat diet induces changes in adipose tissue trans-4-oxo-2-nonenal and trans-4-hydroxy-2-nonenal levels in a depot-specific manner. *Free Radic. Biol. Med.* **63**, 390–398 (2013).

40. Shearn, C. T., Reigan, P. & Petersen, D. R. Inhibition of Hydrogen peroxide signaling by 4-hydroxynonenal due to differential regulation of Akt1 and Akt2 contributes to decreases in cell survival and proliferation in hepatocellular carcinoma cells. *Free Radic. Biol. Med.* **53**, 1–11 (2012).

41. Vergoni, B. *et al.* DNA damage and the activation of the p53 pathway mediate alterations in metabolic and secretory functions of adipocytes. *Diabetes* **65**, 3062–3074 (2016).

42. Minamino, T. *et al.* A crucial role for adipose tissue p53 in the regulation of insulin resistance. *Nat. Med.* **15**, 1082–1087 (2009).

43. Li, T. *et al.* Important role of 5-hydroxytryptamine in glucocorticoid-induced insulin resistance in liver and intra-abdominal adipose tissue of rats. *J. Diabetes Investig.* **7**, 32–41 (2016).

44. Choi, W. *et al.* Serotonin signals through a gut-liver axis to regulate hepatic steatosis. *Nat. Commun.* **9**, (2018).

45. Cai, J. *et al.* Autophagy Ablation in Adipocytes Induces Insulin Resistance and Reveals Roles for Lipid Peroxide and Nrf2 Signaling in Adipose-Liver Crosstalk. *Cell Rep.* **25**, 1708-1717.e5 (2018).

46. Smathers, R. L., Galligan, J. J., Stewart, B. J. & Petersen, D. R. Overview of lipid peroxidation products and hepatic protein modification in alcoholic liver disease. *Chem. Biol. Interact.* **192**, 107–112 (2011).

47. Linhart, K.-B. *et al.* The generation of carcinogenic etheno-DNA adducts in the liver of patients with nonalcoholic fatty liver disease. *Hepatobiliary Surg. Nutr.* **4**, 117–23 (2015).

48. Ferre, T., Riu, E., Franckhauser, S., Agudo, J. & Bosch, F. Long-term overexpression of glucokinase in the liver of transgenic mice leads to insulin resistance. *Diabetologia* **46**, 1662–1668 (2003).

49. Tsukita, S. *et al.* Hepatic glucokinase modulates obesity predisposition by regulating BAT thermogenesis via neural signals. *Cell Metab.* **16**, 825–832 (2012).

50. Sidossis, L. & Kajimura, S. Brown and beige fat in humans: Thermogenic adipocytes that control energy and glucose homeostasis. *J. Clin. Invest.* **125**, 478–486 (2015).

51. Harms, M. & Seale, P. Brown and beige fat: Development, function and therapeutic potential. *Nat. Med.* **19**, 1252–1263 (2013).

52. Shinde, A. B., Song, A. & Wang, Q. A. Brown Adipose Tissue Heterogeneity, Energy Metabolism, and Beyond. *Front. Endocrinol. (Lausanne).* **12**, 333 (2021).

53. Viengchareun, S., Zennaro, M. C., Tallec, L. P. Le & Lombes, M. Brown adipocytes are novel sites of expression and regulation of adiponectin and resistin. *FEBS Lett.* **532**, 345–350 (2002).

Chapter 3. Adipocyte-specific deficiency of TPH2 induced metabolic changes in HFD fed mice.

3.1. Introduction

Obesity has become a significant global health challenge, with its prevalence reaching epidemic proportions in many countries[1,2]. It is a multifactorial condition characterized by the excessive accumulation of body fat, leading to an increased risk of numerous chronic diseases, including cardiovascular disorders, certain types of cancer and T2DM[3,4]. Understanding the underlying mechanisms contributing to obesity is essential for the development of effective prevention and management strategies.

In recent years, there has been increasing interest in the role of 5-HT, a neurotransmitter with diverse physiological functions, in the development and regulation of obesity. 5-HT is mainly synthesized in enterochromaffin cells which are specialized cells found in the lining of the gastrointestinal tract[5]. The synthesis of 5-HT is initiated by an enzyme called Tph, which exists in two isoforms. While TPH1 and TPH2 share similar enzymatic activity in catalyzing the rate-limiting step of 5-HT synthesis, their distinct expression patterns and locations result in differential regulation and contribute to the diverse roles of serotonin in both peripheral and central systems[6,7]. The association between 5-HT and obesity is multifaceted and involves intricate interactions between central nervous system signaling, peripheral tissues, and hormonal pathways. 5-HT is primarily known for its involvement in mood regulation, sleep, and various cognitive processes[8,9]. However, emerging evidence

suggests that 5-HT also plays a critical role in the complex regulation of gut motility and energy balance[10,11]. Obese individuals have increased level of plasma 5-HT which also showed positive correlation with increased BMI and hemoglobin A1C level[12]. Interestingly, obesity also has been associated with increased gastrointestinal motility which could induce more frequent eating[13,14]. Previous studies demonstrated that 5-HT could promote smooth muscle contraction and increase gut motility. 5-HT binds to specific receptors, mainly 5-HTR$_3$ and 5-HTR$_4$, located on enteric neurons and smooth muscle cells in the gastrointestinal tract, triggering peristaltic contractions and facilitating the movement of food through the digestive system[15,16]. Furthermore, chronic usage of selective 5-HT reuptake inhibitors (SSRI) increases circulating 5-HT level and also induces weight gain, insulin resistance and alterations in gut motility, demonstrating the clinical relevance of peripheral 5-HT in regulating the energy metabolism and progression of obesity.[15,17–19].

Additionally, 5-HT has been implicated in the regulation of carbohydrate and fat metabolism. Recent lines of evidences highlighted that 5-HT can influence insulin secretion and sensitivity, glucose homeostasis, and lipolysis in adipose tissue[20,21]. Peripheral 5-HT has been also implicated with the progression of fatty liver and impairment of thermogenesis in rodents[20–22]. Moreover, our lab and previous studies found the dramatic increase of *Tph2* expression on WATs in obese mice (data unpublished)[23,24]. WATs of obese mice have elevated intracellular level of 5-HT which could be derived from both TPH1 and TPH2[25]. Interestingly, genetic ablation of adipocyte-specific TPH1 protected mice from DIO, however circulating 5-HT level was not altered, implying intracellular effect of 5-HT in modulating energy metabolism,

demonstrating possible, but crucial role of TPH2 on regulating adipocyte 5-HT metabolism[20,21]. Dysregulation of energy metabolism by peripheral 5-HT can contribute to metabolic disturbances associated with DIO. Thus, understanding the intricate association between 5-HT and obesity has significant implications for the management of obesity.

To test the hypothesis that DIO-induced increases in adipocyte-specific *Tph2* contributes to the development of obesity and its metabolic complications, we generated mice deficient in adipocyte-specific *Tph2* expression. Both control and Tph2 deficient mice were fed a HFD and closely monitored for any physiological changes and tested to determine metabolic profile. With completion of this project, we provided deeper understanding on complex relationship between 5-HT and obesity that could provide valuable insights into the underlying mechanisms and may contribute to the development of novel therapeutic strategies for the prevention and management of obesity-related complications.

3.2. Materials & Methods

Experimental animals

Adipocyte-specific TPH2 deficient mice were generated by mating mice possessing *loxP* sites flanking exon 5 of the *Tph2* ($TPH2^{loxP/loxP}$) and Adipoq-Cre transgene expressing mice purchased from The Jackson Laboratory. From the first round of mating, heterozygous floxed mice with hemizygous Adipoq-Cre were mated again with *Tph2* loxP heterozygotes to generate $TPH2^{loxP/loxP}$ mice with hemizygous Adipoq-Cre gene. Mice were housed at Comparative Biological Unit in Jean Mayer U.S. Department of Agriculture Human Nutrition Research Center on Aging, and all the experimental procedures were in accordance with standards and guidelines approved by Institutional Animal Care and Use Committee of Tufts University. Mice were kept at 22–24 °C with a 12:12 hours light/dark cycle, and had unrestricted access to water and Chow (Teklad, 2016S) till experimental period. At the age of week 9, mice were randomized into 4 groups; Chow fed $TPH2^{loxP/loxP}$ lacking Adipoq-Cre (Chow-Fl), Chow fed $TPH2^{loxP/loxP}$ with Adipoq-Cre (Chow-Ko), HFD fed $TPH2^{loxP/loxP}$ lacking Adipoq-Cre (HFD-Fl) and HFD fed $TPH2^{loxP/loxP}$ with Adipoq-Cre (HFD-Ko). *Ob/ob* mice, 8-week-old, were purchased from the Jackson Laboratory and housed under same environment with other mice. Mice had unrestricted access to either Chow or HFD (D12492, Research Diets) according to their groups during whole experimental period. Prior to sacrifice, mice were fasted for 6 hours to collect specimens (blood, liver, iWAT, eWAT, BAT and brain). Under continuous isoflurane anesthesia, cardiac puncture was carried out to collect blood. Collected blood was transferred to both EDTA covered tubes and non-coated 2mL tubes for plasma and serum isolation,

respectively. All collected tissues were weighed for their mass and immediately snap-frozen in liquid nitrogen. All collected specimens were stored at -80°C for further analysis.

Metabolic phenotyping

The mouse body composition (lean, fat and body mass) was analyzed by using magnetic resonance instrument (EchoMRI-700, EchoMRI) every 3 week. Diet intake was determined daily by measuring the weight of remaining diet pellets on feeders at 10 am. By utilizing indirect calorimetry system (Promethion BX1, Sable systems), systemic energy expenditure was analyzed. Mice were placed in individual metabolic chamber to collect oxygen consumption, carbon dioxide production, spontaneous activity (total distance moved and locomotion) and food intake for 96 hours. First 24 hours of collected data was excluded from analysis for acclimation purpose. Collected metabolic data was analyzed by CalR as previously described[26].

BAT Thermal imaging

The temperature of interscapular region was measured with thermal camera (FLIR One Pro LT iOS, FLIR). Within 2 hours after light cycle begins, mice were carefully brought from the cages (without directly touching them), and thermal images of mice were taken without shaving their back hair for 3 days. Both average temperature of interscapular region and highest temperature were analyzed with FLIR thermal studio suite (FLIR).

Glucose tolerance test

Glucose tolerance test (IPGTT) was performed after 6 week of diet feeding. Mice were transferred to new cages without food pellets as soon as light cycle started and fasted for 6 hours. After fasting, tail bit was snipped to measure baseline blood glucose level with glucometer (Autocode, Prodigy). The glucose concentration of the solution (D-glucose, Sigma, diluted with sterile PBS) was 2g/kg lean mass. Glucose solution was intraperitoneally injected and blood glucose level was measured at 15, 30, 45, 60, 90 and 120 minutes after the injection. Area under the curve (AUC) was calculated based on average glucose level on each time point.

Insulin tolerance test

Insulin tolerance test (IPITT) was performed at week 8 of diet feeding. Mice were transferred to new cages without food pellets as soon as light cycle started and fasted for 6 hours. After fasting, tail bit was snipped to measure baseline blood glucose level with glucometer (Autocode, Prodigy). The insulin concentration of the solution (Humulin R U-100, Eli Lily, diluted with sterile PBS) was 1IU/kg lean mass. Insulin solution was intraperitoneally injected and blood glucose level was measured at 15, 30, 45, 60, 90 and 120 minutes after the injection. AUC was calculated based on average glucose level on each time point.

Total gastrointestinal transit time assay

6% carmine red solution was prepared by mixing 0.5% methylcellulose (Sigma) solution with carmine red powder (Sigma), and autoclaved. Mice were transferred to clean cages without beddings right after dark cycle ended. To determine total gastrointestinal transit time, mice were gavaged with prepared carmine red solution, and observed until they produce first red feces with carmine red.

Fecal bomb calorimetry

Mice were transferred to wire-bottom cages (LabCorp) and given 3 days for acclimation to new environment. After acclimation, fecal samples were collected in 50 mL tubes for 5 days. During the collection, mice body mass, diet intake and fecal weight were measured every day. Fecal samples were freeze-dried for 4 hours, and calorie content in dried feces were analyzed by bomb calorimetry (Parr 1261 bomb calorimeter, Parr Instruments) with benzoic acid standard[27].

Plasma and serum profile analysis

Total Cholesterols, Triglycerides, ALT, and AST were analyzed using Beckman Coulter Diagnostic reagents on a chemistry analyzer (Beckman Coulter AU480, Beckman Coulter). NEFA was analyzed using the Wako NEFA-HR test kit and analyzed on the chemistry analyzer (Beckman Coulter AU480, Beckman Coulter). Serum Insulin was measured by ELISA (Ultra Sensitive Mouse Insulin ELISA, Crystal

Chem) with the Wide-range standard curve (0.1-12.8 ng/mL standard curve option) and read on the Epoch plate reader.

5-HT quantification

Plasma 5-HT level was quantified using ELISA (IM1749, Beckman Coulter) according to manufacturer's instructions. For tissue 5-ht quantification, pulverized tissues were transferred to 0.2N perchloric acid and mechanically homogenized (Tissue lyzer II, Qiagen). After homogenization, samples were centrifuged at 10,000 x g to pellet insoluble debris and draw off supernatant. Transferred supernatant was neutralized with 1M borate buffer. With neutralized tissue extracts, ELISA was performed to quantify 5-HT (IM1749, Beckman Coulter).

Adipocyte isolation

Dissected single depot of eWAT were minced with razor blades and immediately put in Dulbecco's modified eagle medium (DMEM) with high glucose and HEPES (Gibco) with 4% bovine serum albumin and 500nM adenosine. eWAT homogenates were digested with collagenase type 1 (1mg/mL) for 30 minutes on shaking incubator (37C°). Digested adipocytes were filtered through a 250-mm nylon mesh and washed with DMEM. After short 500g centrifugation, adipocytes were washed again with DMEM, then centrifuged at 1000g for 15 minutes to separate adipocytes and stromal vascular fraction (SVF). Separated adipocytes and SVFs were transferred to Qiazol and frozen at 80 C° for subsequent RNA analysis.

Immunohistochemistry analysis

Dissected eWAT and liver tissue were fixed in 10% aqueous buffered zinc formalin (Z-fix, Anatech), embedded in paraffin, sectioned (5μm), and stained with hematoxylin and eosin (H&E). Digital images were acquired at 20X or 40 X magnification (DX51 light microscope, Olympus). Average adipocyte size or lipid droplet percentage were quantified using Image J software.

RNA isolation and real-time quantitative PCR

Isolated adipocytes, eWAT, mesenteric white adipose tissue (mWAT) and BAT (20~100mg) were submerged in Qiazol (Qiagen) and mechanically homogenized (Tissue lyzer II, Qiagen). From tissues, total RNA was extracted (RNeasy Mini columns, Qiagen) and RNA purity and concentration was quantified with spectrophotometer (Nanodrop 100, Thermofisher). With 1 μg of RNA, cDNA was generated by reverse transcription (High Capacity cDNA Reverse Transcription Kit, Applied Biosystems). Quantitative real-time PCR (qPCR) was performed using SYBR Green (PowerUp™ SYBR™ Green Master Mix, Applied Biosystems) on an QuantStudio 6 Flex real-time PCR systems PCR (Applied Biosystems). RT-PCR cycle threshold (Ct) values were normalized and analyzed with 2-delta delta Ct method[28]. Both forward and reverse primer sequences are listed in Supplementary Table 1.

Statistics

All statistical analyses were conducted using GraphPad Prism 9 software and R Studio. False discovery rate adjusted (FDR) Student's t-test or two-way analysis of variance (ANOVA) with Šídák's multiple comparison test was performed to determine statistical differences between groups. A p-value under 0.05 was considered to be significant. All data were expressed as mean ± SEM.

3.3. Results

TPH2 is specifically ablated in adipocytes and increased adiposity induces TPH2 upregulation in DIO.

To investigate the effect of Adipocyte-specific TPH2 loss on the development of DIO, we generated the mice lack *Tph2* expression in adipocytes by using Cre-loxp system. $TPH2^{loxP/loxP}$ with or without Adipoq-Cre mice were randomly divided into 4 groups and fed an either Chow or HFD. We determined eWAT *Tph2* expression level to evaluate whether genetic ablation of adipocyte-specific was successful. Indeed, Chow-KO mice exhibited very low gene expression levels of *Tph2*, while HFD feeding significantly upregulated the expression of *Tph2*. In HFD-KO mice, the mRNA level of *Tph2* was reduced by approximately 0.5-fold compared to HFD-Fl mice (Fig.1a). While, genetic ablation of TPH2 abolished the *Tph2* mRNA level in Chow-KO, HFD-KO eWAT only showed 50% reduction of *Tph2* mRNA level with genetic ablation of adipocyte TPH2. To further determine the origin of *Tph2* mRNA in eWAT, we isolated epididymal adipocytes and SVF to analyze *Tph2* gene expression level. Surprisingly, HFD-KO adipocytes showed ~0.2-fold reduction in *Tph2* expression level compared to adipocytes from HFD-Fl mice. While in SVF, there was no difference between HFD-Fl and HFD-KO, but compared to adipocytes, SVF had ~4-fold higher *Tph2* gene expression level (Fig.1b). Furthermore, we sought to address the question of what triggers the dramatic upregulation of *Tph2* expression in DIO. Specifically, we aimed to determine whether it is the HFD itself or the increased adiposity that leads to the dramatic upregulation in *Tph2* expression. We determined the *Tph2* mRNA level of isolated epididymal adipocytes and SVF in C57BL6 mice fed an either Chow or HFD

and Chow fed *ob/ob* mice. HFD feeding significantly increased *Tph2* gene expression level in both epididymal adipocytes and SVF (Fig1.d & e). In epididymal adipocytes from obese ob/ob mice fed a chow diet, we observed a significant increase in *Tph2* expression compared to Chow-fed C57BL6 mice (Fig.1f). Also, in isolated brown adipocytes, *Tph2* mRNA levels were upregulated in both HFD fed mice and *ob/ob* mice (Fig.S1a & b). These findings suggest that the upregulation of *Tph2* in DIO occurs independently of HFD feeding, emphasizing the role of adiposity in driving *Tph2* expression changes.

MRI analysis revealed that adipocyte-specific deficiency of *Tph2* did not alter body weight between mice fed a same diet (Fig.2a). HFD-KO mice had a slightly decreased fat mass compared HFD-Fl, but not statistically significant (Fig.2b). HFD feeding increased the lean mass, but there were no differences in lean mass between mice with same genotype (Fig.2c). After 12-week of diet feeding regimen, mice were euthanized, and collected tissue weights were measured. As expected, there were no significant differences in weights of iWAT, mWAT, liver and BAT between genotypes, however eWAT mass was significantly decreased in HFD-KO mice compared to HFD-Fl mice (Fig.2d & e).

Adipocyte-specific ablation of TPH2 improves glucose tolerance and insulin sensitivity in obese mice.

Considering the role of peripheral 5-HT on regulating energy metabolism, we evaluated the effect of adipocyte-specific Tph2 loss on glucose homeostasis and insulin sensitivity in HFD fed mice. There were no alterations in Chow fed mice, but

HFD-KO mice had significantly reduced fasting blood glucose level compared to HFD-Fl mice (Fig.3a). In HFD-KO mice, fasting plasma insulin level was also significantly lower than HFD-Fl mice, indicating adipocyte-Tph2 loss improved DIO induced insulin resistance (Fig.3b). We performed IPGTT and IPITT to further explore the glucose tolerance and insulin sensitivity in HFD fed mice. HFD-KO mice had significantly improved glucose tolerance and insulin sensitivity compared to HFD-Fl mice, suggesting adipocyte-specific Tph2 ablation protected mice against DIO induced glucose intolerance and insulin resistance (Fig.3b & c).

Genetic ablation of adipocyte-specific TPH2 reduces eWAT adiposity through upregulation of lipolysis gene expression, and reduces pro-inflammatory and p53 signaling gene expressions.

Since HFD-Ko mice had significantly reduced eWAT mass compared to HFD-Fl mice, we performed H&E staining to determine eWAT adiposity. There were no differences between Chow-Fl and Chow-KO, while epididymal adipocyte size of HFD-KO mice was significantly smaller than HFD-Fl (Fig.4a & b). Furthermore, we assessed eWAT 5-HT level to evaluate whether loss of adipocyte-specific *Tph2* expression affected adipocyte 5-HT production. Remarkably, 5-HT level in eWAT of HFD-KO mice were significantly reduced compared HFD-Fl mice, and it was similar with the 5-HT level of Chow fed mice (Fig.4c).

To explore how adipocyte-specific deletion of *Tph2* altered molecular biology of eWAT, we analyzed gene expression profile of eWAT from HFD fed mice. Both *Tph1* and *Maoa* mRNA level was not altered, demonstrating specific abolition of *Tph2*

(Fig.5a). We also checked both lipogenic and lipolysis related gene expression levels. While lipogenesis related genes were not altered, both *Atgl* and *Hsl* were significantly upregulated in HFD-KO mice (Fig.5b). To investigate decreased eWAT adiposity affected DIO induced inflammation, pro-inflammatory gene expression levels were measured. Both *Tnfa* and *Il1b* mRNA levels were downregulated in eWAT of HFD-KO mice, showing signs of reduced eWAT inflammation (Fig.5c). Additionally, we determined gene expression levels of p53 signaling which induces adipocyte death, and both *p53* and *Cdkn1a* mRNA levels were significantly decreased in HFD-KO eWAT (Fig.5d). Also, HFD-KO eWAT had significantly increased *Adipoq* gene expression level, suggesting increased production of adiponectin with loss of adipocyte-specific TPH2 (Fig.5e).

Loss of adipocyte TPH2 derived 5-HT protected mice from DIO induced hepatic steatosis and liver damage.

Previous studies reported the link between adipocyte-derived peripheral 5-HT and hepatic lipid accumulation. Thus, we evaluated hepatic steatosis and liver function in HFD fed mice. H&E staining of liver sections from both HFD-Fl and HFD KO mice revealed that liver from HFD-KO mice had significantly less lipid accumulation. (Fig.6a & b). Furthermore, HFD-KO mice had significantly reduced levels of ALT and AST, liver function makers (Fig.6c & d). However, plasma lipid profile, such as total cholesterol, TG and NEFA levels were not different between HFD-Fl and HFD-Ko mice (Fig. S2a). These results suggest that adipocyte-specific TPH2 deletion protected mice from DIO induced developing hepatic steatosis and liver damage.

Abolishing TPH2 expression in epididymal adipocytes increases systemic energy expenditure and BAT activation through upregulation of *Ucp-1* and *Prdm16*.

Although HFD-KO mice showed no differences in whole body composition, decreased eWAT mass and improved glucose homeostasis were observed in HFD-Ko mice. Previously, it was shown that adipocyte derived 5-HT regulate BAT thermogenesis and increase systemic energy expenditure[20,21]. Therefore, we used indirect calorimetry to determine systemic energy expenditure in HFD fed mice. During the experiment, systemic energy expenditure was calculated by collecting oxygen consumption and carbon dioxide production (Fig. S3a & b). Results from the indirect calorimetry further analyzed by using CalR, and surprisingly HFD-KO mice had significantly higher systemic energy expenditure than HFD-Fl mice[26] (Fig. 7a & b). The amount of diet consumed was same between HFD-Fl and HFD-KO mice during the indirect calorimetry experiment (Fig.7c). Moreover, both groups of mice had similar RER and moved similar distance during the experiment, indicating the group difference in energy expenditure is not due to the physical activity (Fig. S3c and Fig. 7d).

To verify increase in systemic energy expenditure associated with BAT activation, we used thermal imaging technique to determine the surface temperature of interscapular region of mice. Remarkably, we found that interscapular surface temperature of HFD-Ko mice was significantly higher than HFD-Fl mice (Fig.8a & b). We further assessed molecular changes in BAT with qPCR analysis. BAT Tph2 mRNA level was downregulated in HFD-Ko mice, and thermogenesis related genes Ucp-1

and Prdm16 were highly upregulated with absence adipocyte *Tph2* (Fig.8c &d). Similar to eWAT, *Adipoq* gene expression level was increased in HFD-KO BAT compared to BAT of HFD-Fl mice (Fig.8e).

Adipocyte-specific loss of TPH2 increases gut transit time, and reduces fecal energy loss, resulting in enhanced energy absorption.

Paradoxically, even though the adipocyte-specific deficiency of TPH2 induced BAT thermogenesis and significantly increased systemic energy expenditure, HFD-KO mice still become obese when fed a HFD. Surprisingly, the amount of diet consumption was not different between HFD-Fl and HFD-KO, suggesting energy loss from increased thermogenesis is compensated from other sources. Thus, we hypothesized that reduced 5-HT production from adipocyte TPH2 could decreased gut motility and enhance energy harvest efficiency in gastrointestinal system. To test this hypothesis, we measured total gastrointestinal transit time. The mice were orally administered a carmine red solution, and the time taken for the first appearance of feces with carmine red was recorded. HFD-KO mice had significantly increased total gastrointestinal transit time compared to HFD-Fl mice, suggesting possible role of adipocyte derived 5-HT in regulating gut motility (Fig.9a). In order to evaluate the fecal calorie content, the mice were transferred to wire-bottom cages, and fecal samples were collected over a period of 5 days following a 3-day acclimation period. Surprisingly, during fecal collection period, HFD-KO mice produced significantly less amount of feces than HFD-Fl mice (Fig.9b). Bomb calorimetry analysis of fecal samples revealed that calorie level in same amount feces were not different between

groups, indicating energy harvesting capacity is not altered (Fig.9c). Nonetheless, HFD-KO mice exhibited a significantly lower caloric loss through feces compared to HFD-FI mice, due to their reduced daily fecal output (Fig.9d). We also measured daily energy intake level during the fecal collection, and there was no statistical difference in daily energy intake level between two groups (Fig.9e). However, to our surprise, HFD-KO mice displayed a significantly higher daily caloric absorption level, calculated by subtracting the daily fecal energy excretion from the daily energy intake (Fig.9f). This observation suggests that HFD-KO mice are effectively absorbing more calories from HFD compared to HFD-FI mice. Then, we measured the *Tph2* gene expression level in mWAT, and found significant downregulation in HFD-KO mice, suggesting a possible link between mWAT TPH2-derived 5-HT and intestinal energy absorption (Fig.9g).

Overall, this study provides the novel finding that genetic ablation of adipocyte-specific TPH2 protects mice from developing DIO induced insulin resistance and hepatic steatosis. We demonstrated that the absence of adipocyte TPH2 increases the systemic energy expenditure through inducing BAT thermogenesis. However, the specific loss of TPH2 in adipocytes resulted in decreased gut motility and increased daily caloric absorption, compensating for the elevated systemic energy expenditure. These findings provide a deeper understanding on the molecular mechanisms of adipocyte TPH2 on regulating systemic metabolism, which may facilitate the development of therapeutic approaches to obesity and its metabolic complications.**3.4. Discussion**

Adipocyte TPH1 derived peripheral 5-HT promotes the progression of metabolic disorders through inducing hepatic steatosis and reducing systemic energy expenditure[20–22]. We found that increased adiposity of WATs dramatically upregulates the *Tph2* expression in both epididymal and brown adipocytes, indicating the possible association between adipocyte TPH2 and obesity induced metabolic complications. However, to the best of our knowledge, contribution from adipocyte-specific TPH2 produced 5-HT on the metabolic physiology has never been explored. Thus, we generated the mice line deficient in adipocyte-specific TPH2 expression using Cre-loxP system. In isolated epididymal adipocytes of HFD-Fl and HFD-KO mice, we confirmed HFD-KO mice had more than 80% reduction in *Tph2* mRNA level compared to that of HFD-Fl mice. Interestingly, *Tph2* mRNA level of SVF from HFD fed mice were higher than adipocyte *Tph2* level in same mice. WAT derived SVF contains pre-adipocytes, immune cells, fibroblasts, stem cells and nerve cells from sympathetic nervous system[29,30]. Thus, high level of *Tph2* mRNA in eWAT SVF could be explained by the presence of nerve cells, which predominantly express TPH2.

Adipocyte TPH1 knockout mice are resistant to the development of DIO and its associated complications, such as insulin resistance and hepatic steatosis without any changes in circulating 5-HT levels[20–22]. The proposed molecular mechanism of this protective effects was increased BAT thermogenic activity with loss of adipocyte Tph1[20,21]. Genetic or pharmacological inhibition of Tph1 promoted BAT thermogenesis, but it did not prevent the development of DIO or alter thermogenesis in Ucp-1 knockout mice. This suggests that the metabolic benefits derived from Tph1 inhibition are dependent on UCP-1 induced thermogenesis in BAT[20]. Additionally, Oh et al.

demonstrated that the specific deletion of adipocyte 5-HTR$_{3a}$ protects mice against the development of DIO and enhanced insulin resistance by promoting increased BAT thermogenesis, demonstrating that peripheral 5-HT regulates BAT thermogenesis by binding to 5-HTR3a receptors[21]. Furthermore, intestine-specific ablation of TPH1 significantly decreased circulating 5-HT level and prevented DIO induced glucose intolerance and hepatic steatosis in mice. However, mice lacking intestinal TPH1 still developed DIO when fed a HFD and exhibited similar levels of energy expenditure compared to control mice[31]. These conflicting results suggest that peripheral 5-HT not only regulates thermogenesis and systemic metabolism by binding to 5-HTRs, but also could modulate them via alternate molecular pathways. In our study, we found that loss of adipocyte-specific TPH2 decreased eWAT 5-HT level and contributed to the protection against DIO induced insulin resistance and hepatic steatosis. However, HFD-KO mice still exhibited obesity with HFD feeding, while adipocyte-specific absence of TPH2 stimulated thermogenesis in BAT and notably raised systemic energy expenditure. We checked the daily energy intake levels of mice, and there was no significant difference between groups. The similar weight gain observed between HFD-FI and KO mice is not physiologically possible, unless HFD-KO mice are compensating for the energy loss resulting from increased BAT thermogenesis. Collectively, these findings describe a novel role of adipocyte TPH2 in regulating whole body energy homeostasis, including systemic energy expenditure and energy harvesting.

Previous studies reported that obese individuals have increased circulating 5-HT levels and alterations in gastric motility and also genetic ablation of

enterochromaffin cell specific-TPH1 resulted in significant reduction in both circulating and gut 5-HT levels which lead to decreased gastrointestinal motility and slowed gastric emptying in mice[32–35]. Based on these findings, we hypothesized that that loss of adipocyte TPH2 derived 5-HT decreased gastrointestinal motility, which led to enhanced energy harvesting efficiency, and compensation of the energy loss from increased systemic energy expenditure. Remarkably, we found that HFD-KO mice showed significantly increased total gastrointestinal transit time, demonstrating the possible role of adipocyte TPH2-dervied 5-HT in regulating gut motility. In HFD-KO mice, decreased gut motility resulted in significantly reduced fecal output and fecal energy loss compared to HFD-Fl mice. However, fecal energy density was not different between groups, indicating macronutrient absorption efficiency was not altered by decreased gut motility. These observations imply that increased 5-HT production from adipocyte TPH2 in obesity affects the caloric balance via regulation of gut motility. Furthermore, when the fecal transit time is prolonged, the gut microbiome has increased opportunities to digest and ferment fibers that the host organism could not process, leading to the production of short-chain fatty acids (SCFA) that are readily absorbed by the host's endothelial cells[36,37]. Depending on the type of SCFA, absorbed SCFAs could be utilized as an energy source for colonocytes or transported to liver or other peripheral tissues for gluconeogenesis or lipogenesis[38–40]. Additionally, with development of DIO, the gut microbiome profile also changed into a more obesogenic profile, and fecal transplantation of these microbes to germ-free mice caused obesity in the absence of HFD feeding, indicating the crucial role of gut microbes in energy harvesting[41,42]. Moreover, recent lines of evidence highlighted the

association between mWAT and inflammatory bowel diseases, suggesting the possible role of mWAT in modulating gut physiology[43,44]. Considering these findings, adipocyte-specific deletion of TPH2 reduces 5-HT production from mWAT, which could decrease gut motility and led to enhanced energy preservation and gut microbiome produced SCFA, resulting in extra caloric supply for the host organism.

Increased level of circulating 5-HT has been associated with the development and progression of hepatic steatosis[18]. Adipocyte-specific TPH2 deletion improved hepatic steatosis and liver damage in DIO. Choi et al. demonstrated that the genetic or pharmacological inhibition of liver 5-HTR_{2a} significantly downregulated hepatic lipogenesis and improved hepatic steatosis in obese mice without affecting systemic energy expenditure[45]. Taken together, adipocyte-specific Tph2 deletion may decrease 5-HTR_{2a} signaling and prevent DIO induced hepatic lipid accumulation and damage.

Overall, our study presents compelling evidence that adipocyte Tph2 expression is dramatically upregulated with increased adiposity in obesity, and abolishing adipocyte Tph2 could improve DIO induced insulin resistance and hepatic steatosis by activation of BAT thermogenesis. To our knowledge, this is the first study that demonstrated the possible role of adipocyte TPH2 in regulating whole body energy homeostasis, which encompasses both energy expenditure and preservation. These findings further support recent research emphasizing the significance of adipocytes in regulating energy balance and suggest that targeting adipocyte TPH2 could be a potential therapeutic strategy for addressing obesity-related issues.

3.5. Figures

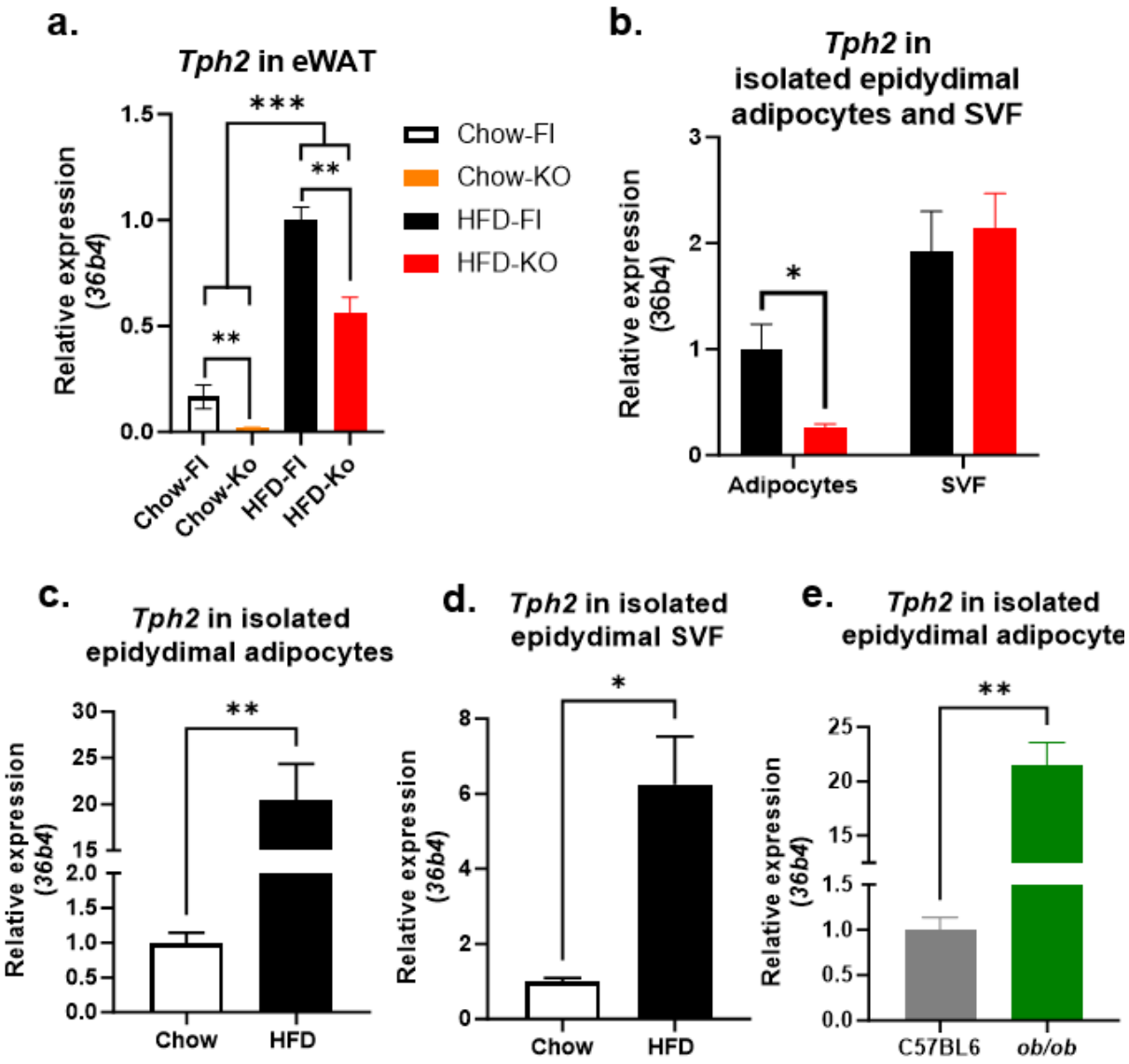
a.
Tph2 in eWAT
Relative expression (36b4)
1.5
1.0
0.5
0.0
***
**
**
Chow-FI
Chow-KO
HFD-FI
HFD-KO
Chow-FI
Chow-Ko
HFD-FI
HFD-Ko
b.
Tph2 in isolated epididymal adipocytes and SVF
Relative expression (36b4)
3
2
1
0
*
Adipocytes
SVF
c.
Tph2 in isolated epididymal adipocytes
Relative expression (36b4)
30
25
20
15
2.0
1.5
1.0
0.5
0.0
**
Chow
HFD
d.
Tph2 in isolated epididymal SVF
Relative expression (36b4)
8
6
4
2
0
*
Chow
HFD
e.
Tph2 in isolated epididymal adipocyte
Relative expression (36b4)
25
20
15
1.5
1.0
0.5
0.0
**
C57BL6
ob/ob

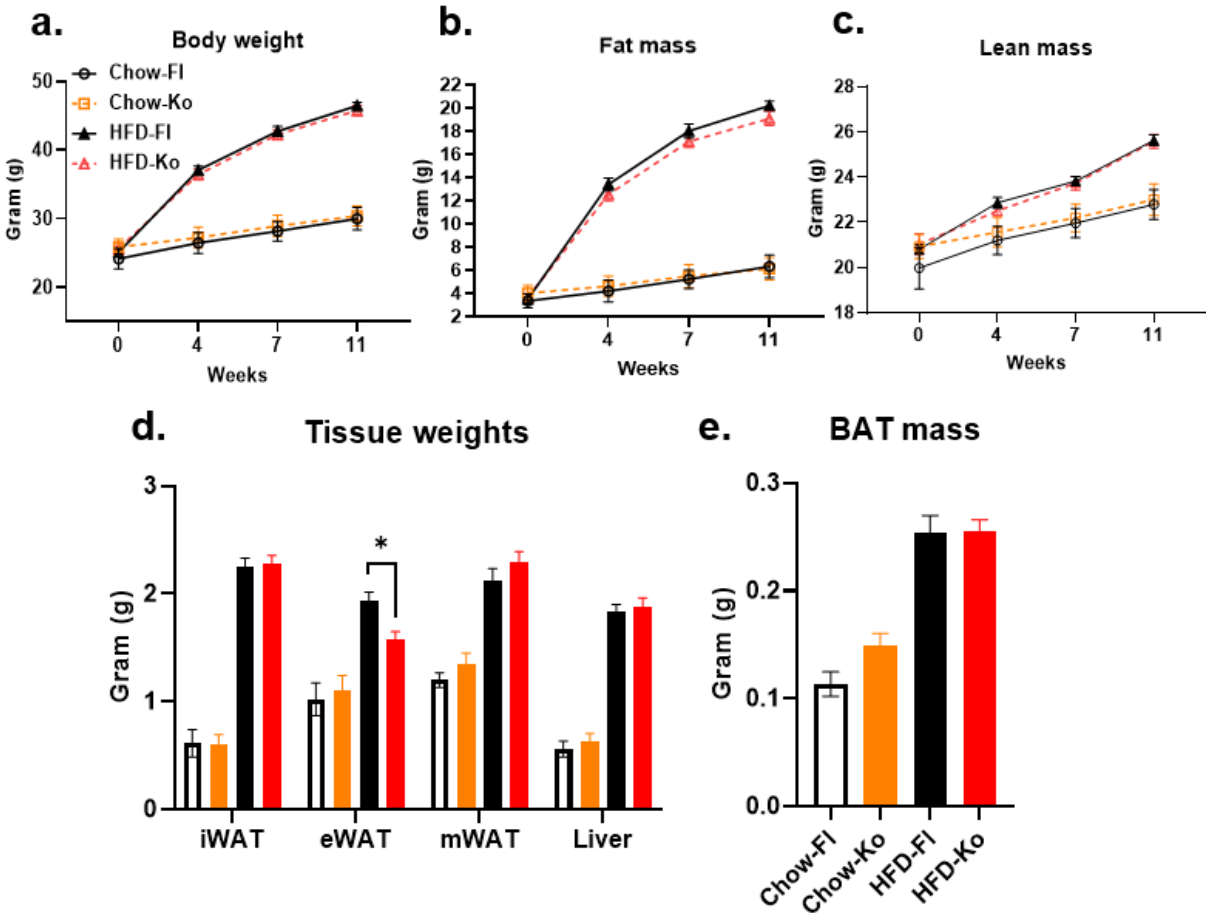
a.
Body weight
Chow-FI
Chow-Ko
HFD-FI
HFD-Ko
Gram (g)
Weeks
b.
Fat mass
Gram (g)
Weeks
c.
Lean mass
Gram (g)
Weeks
d.
Tissue weights
Gram (g)
*
iWAT
eWAT
mWAT
Liver
e.
BAT mass
Gram (g)
Chow-FI
Chow-Ko
HFD-FI
HFD-Ko

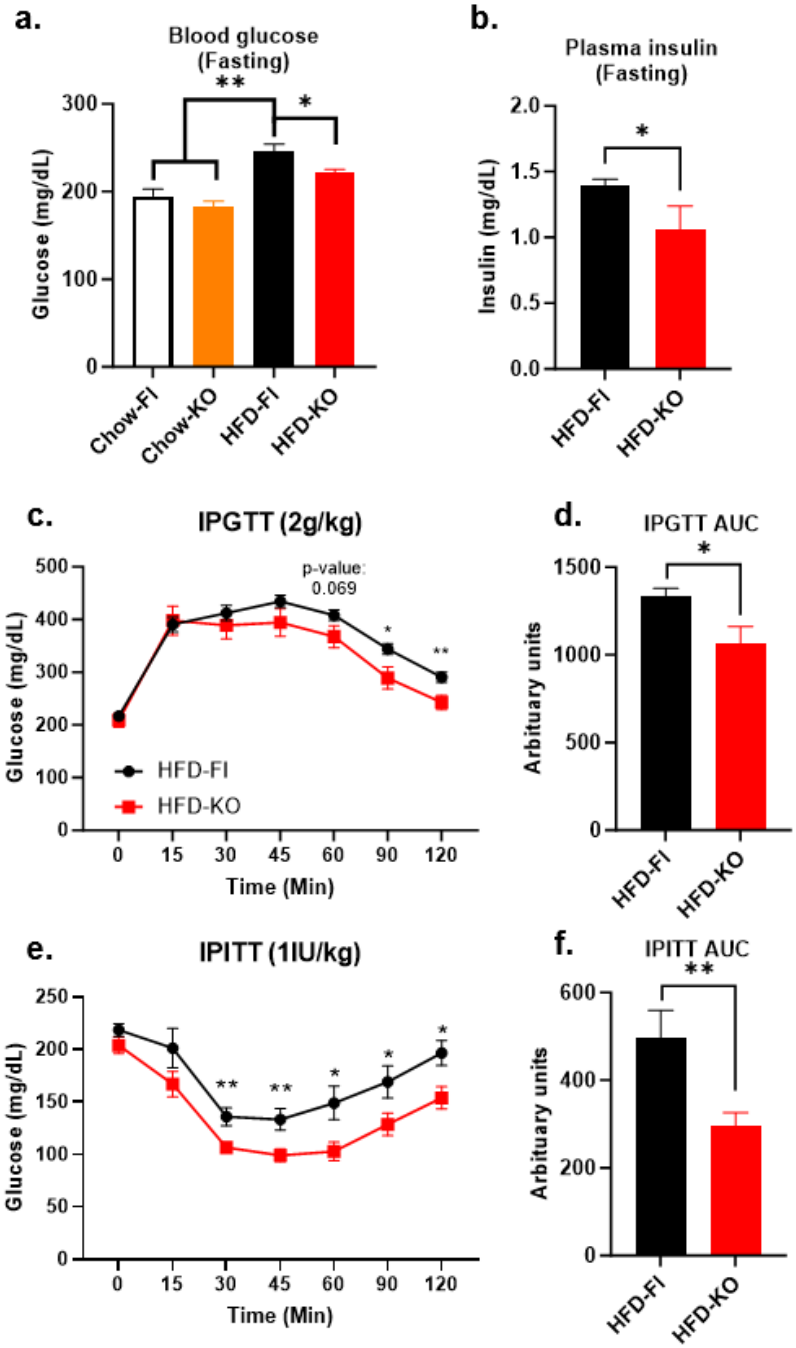

Figure 3. HFD-KO Mice Exhibit Decreased Fasting Blood Glucose and Insulin Level, Glucose Intolerance and Insulin Resistance. **(a)** Fasting state blood glucose level of all mice after 12-week of Chow or HFD feeding, n=8~21. **(b)** Fasting plasma insulin level of HFD-FI and KO mice after 12-week of HFD feeding, n=8~21 per group. **(c)** IPGTT in mice after 6-h fasting at week 6. Each data point represents mean glucose level at each time point, n=8 per group. **(d)** AUC for IPGTT was calculated after normalization with the lowest glucose level. **(e)** IPITT in mice after 6-h fasting at week 9. **(f)** AUC for IPITT was calculated after normalization with the lowest glucose level. Each data point represents mean glucose level at each time point., n=8 per group. All data are expressed as mean ± SEM via Student's t-test or one-way ANOVA followed by Tukey's post-hoc analysis. *p<0.05; **p<0.01.

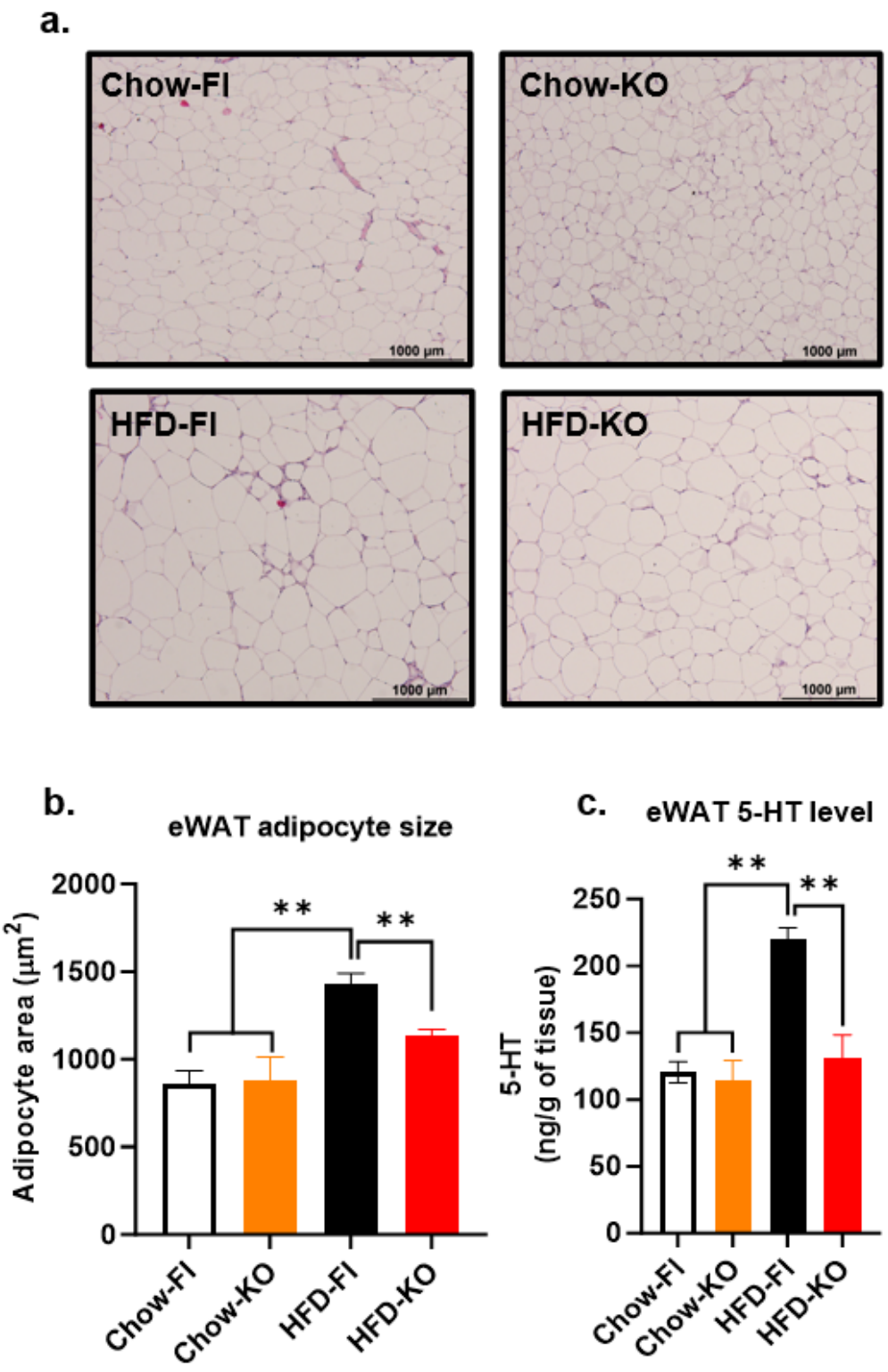

Figure 4. Adipocyte-specific Deficiency of TPH2 Induces Changes in eWAT Adiposity and 5-HT level. **(a)** Representative images of H&E staining of eWAT from both Chow-fed and HFD-fed mice. **(b)** Average adipocyte size calculated from eWAT H&E staining images, n=5 per group **(c)** 5-HT levels in eWAT, n=7~12 per group. All data are expressed as mean ± SEM via one-way ANOVA followed by Tukey's post-hoc analysis. *p<0.05; **p<0.01.

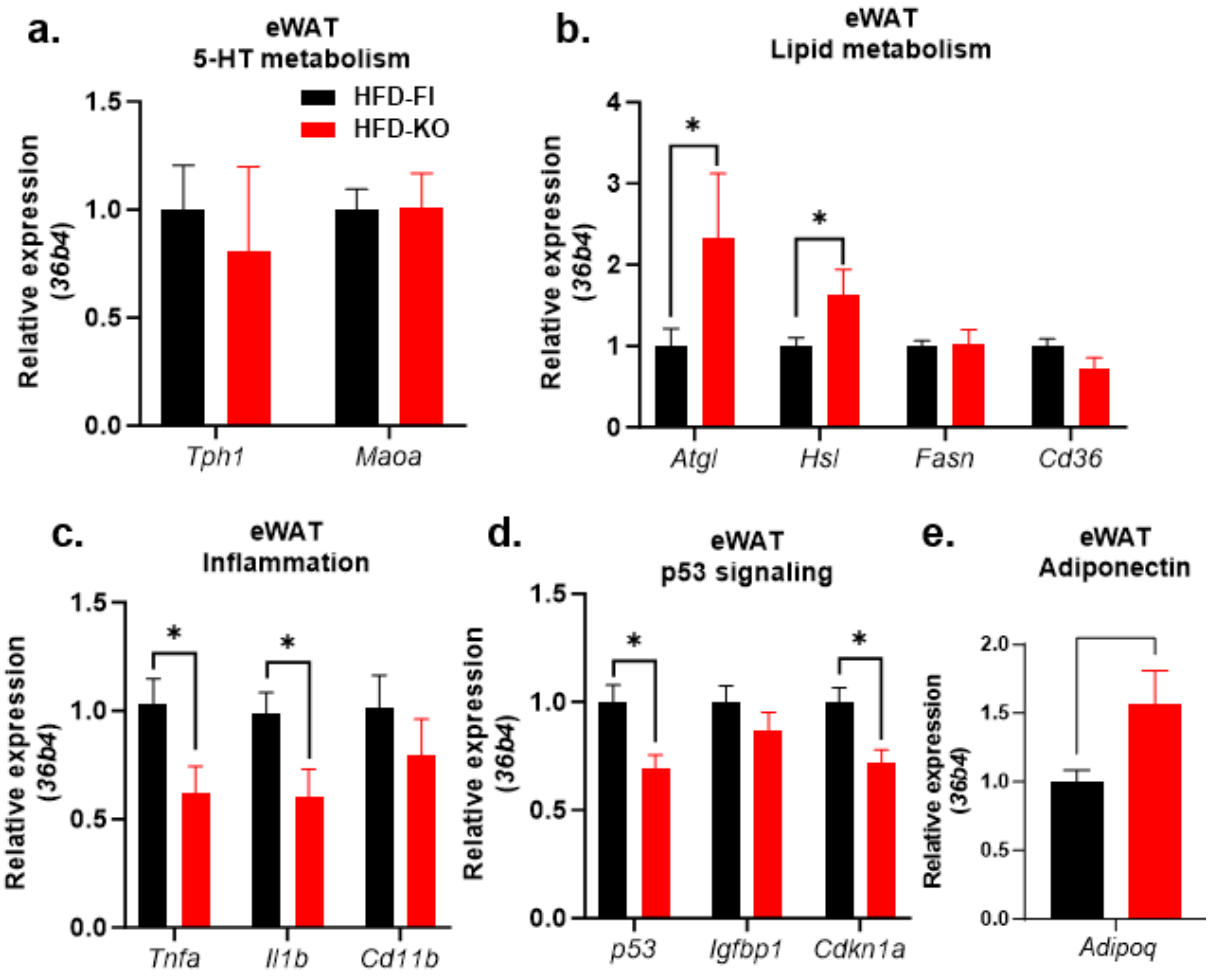

Figure 5. Adipocyte-specific Deficiency of Tph2 Induces Changes in eWAT Gene Expression Profile. **(a)** Expression profile of 5-HT metabolism related genes in eWAT, n=8~ 21 per group. **(d)** Expression profile of lipid metabolism related genes in eWAT, n=8~21 per group **(c)** Expression profile of inflammation related genes in eWAT, n=8~21 per group **(d)** Expression profile of p53 signaling related genes in eWAT, n=8~21 per group. **(e)** *Adipoq* mRNA level in eWAT, n=8~21 per group. All data are expressed as mean ± SEM via Student's t-test. *p<0.05.

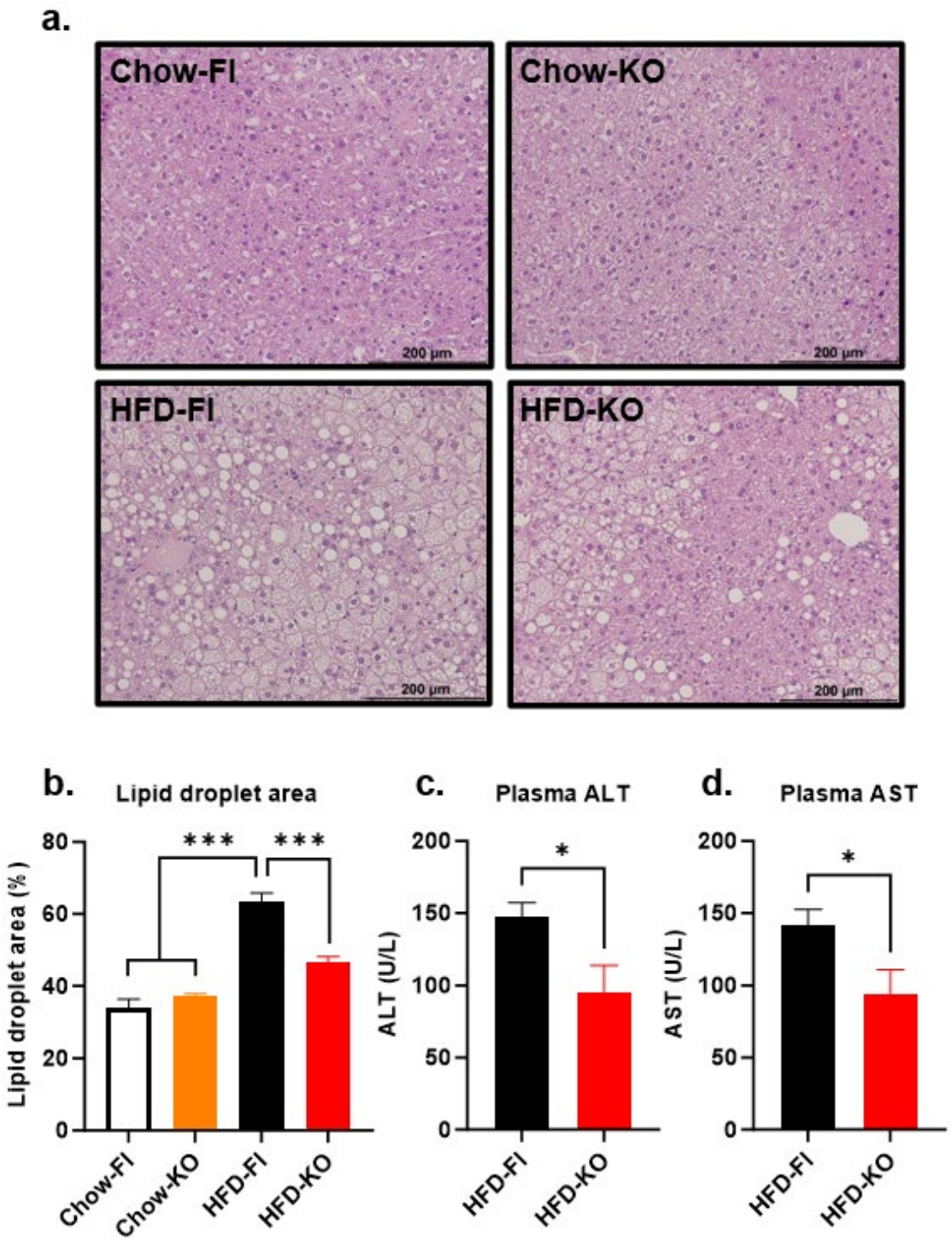

Figure 6. Adipocyte-specific Deficiency of TPH2 Induced Changes in Hepatic Steatosis and Liver Damage. (a) Representative images of H&E staining of liver from both Chow-fed and HFD-fed mice. **(b)** Average lipid droplet area calculated from liver H&E staining images, n=5 per group **(c)** Plasma ALT and **(d)** AST levels in HFD-FI and KO mice n=4~8 per group. All data are expressed as mean ± SEM via student's t-test or one-way ANOVA followed by Tukey's post-hoc analysis. *p<0.05; **p<0.01; ***p<0.001.

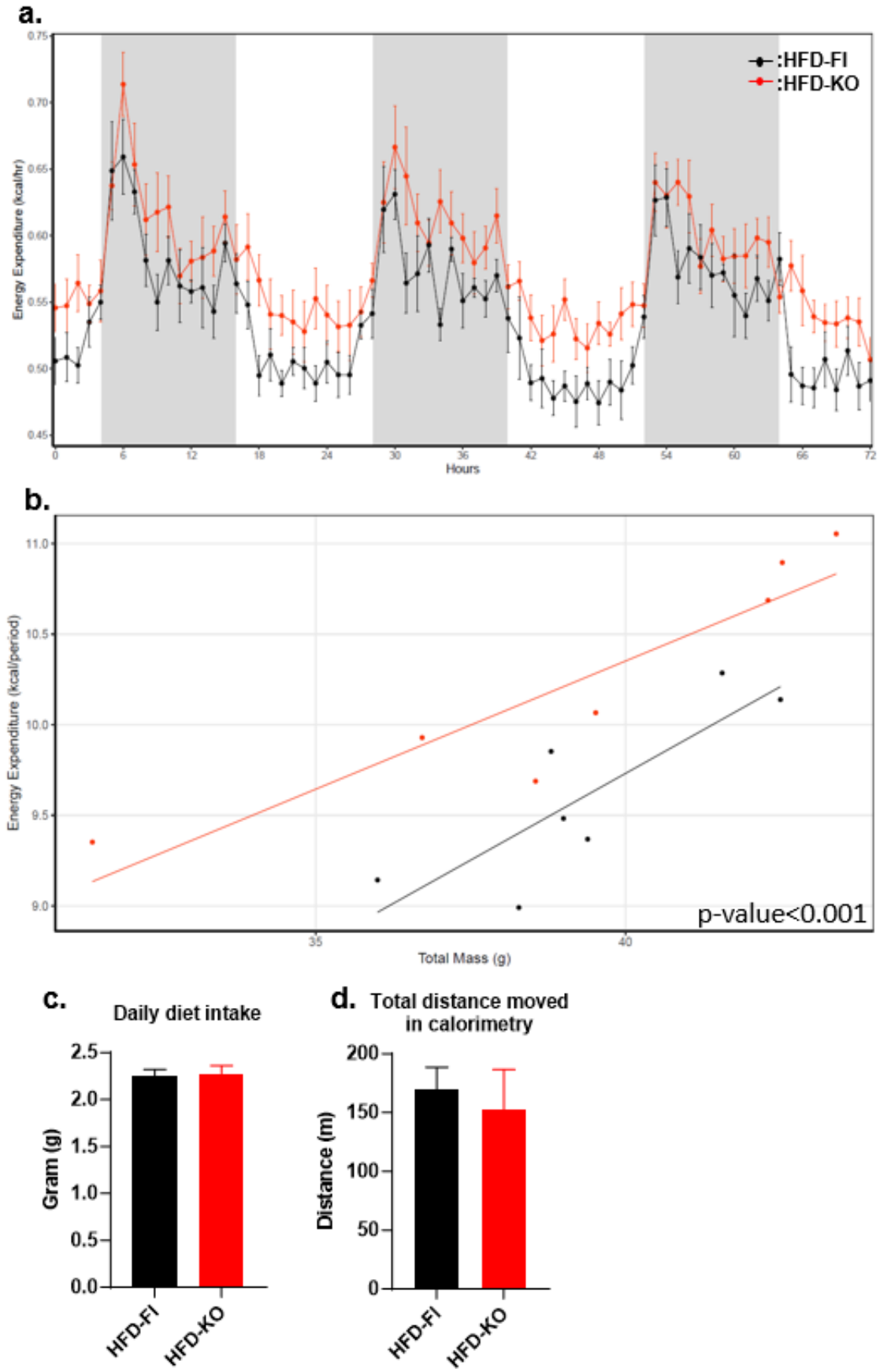
a.
:HFD-FI
:HFD-KO
Energy Expenditure (kcal/hr)
Hours
b.
Energy Expenditure (kcal/period)
Total Mass (g)
p-value<0.001
c.
Daily diet intake
Gram (g)
HFD-FI
HFD-KO
d.
Total distance moved in calorimetry
Distance (m)
HFD-FI
HFD-KO

Figure 7. Genetic Ablation of Adipocyte-specific TPH2 Increases Systemic Energy Expenditure. **(a)** Time course energy expenditure during the indirect calorimetry analysis **(b)** Regression model of average energy expenditure for 72-hour, analyzed by the generalized linear model using body mass as a covariate, n=7~8 per group. **(c)** Average food intake per day, n=8~11. **(d)** Total distance moved during the indirect calorimetry, n=7~8 per group. All data are expressed as mean ± SEM.

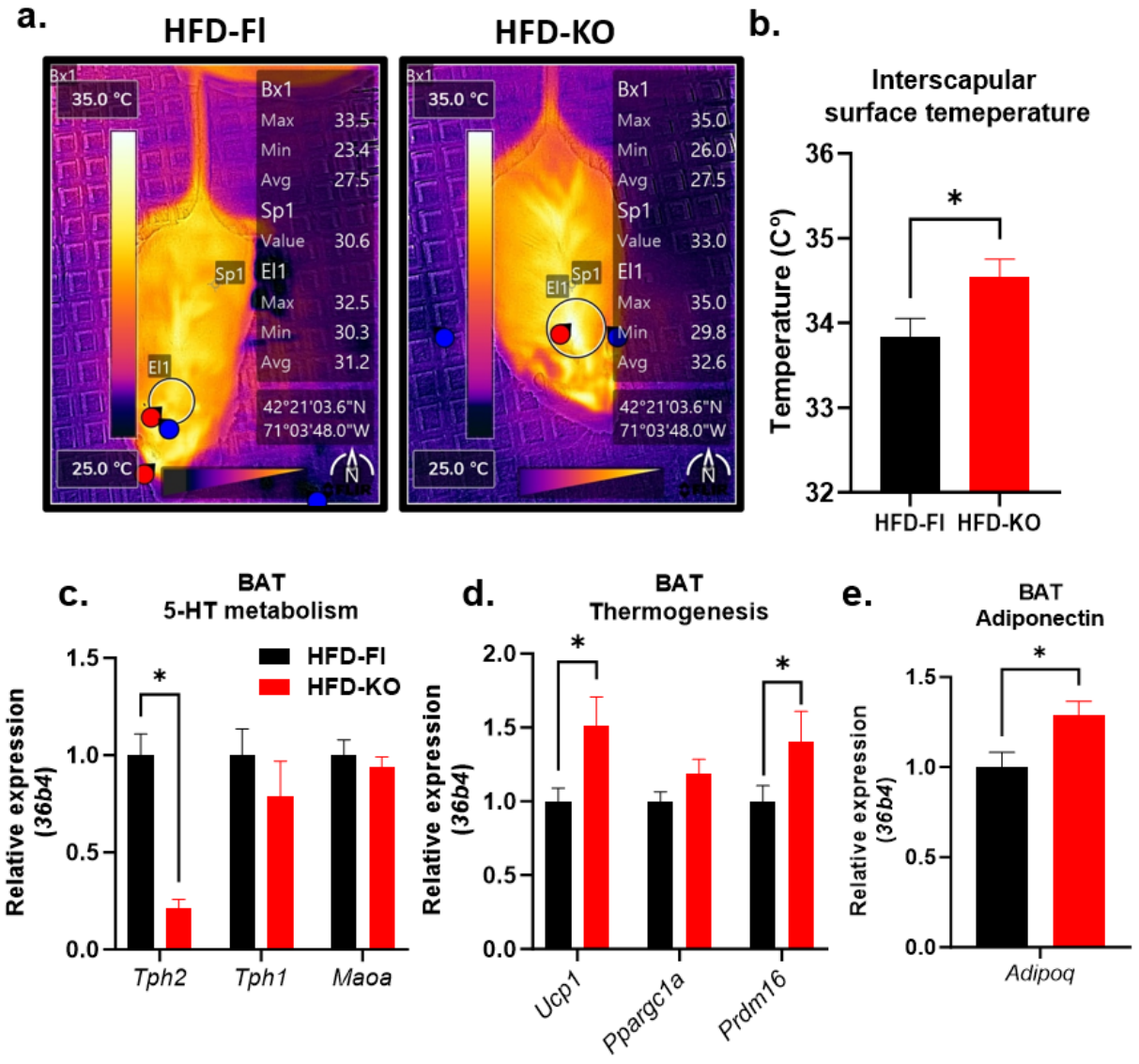

Figure 8. HFD-KO Mice Exhibit Increased BAT Activation and Altered Gene Expression Profile. **(a)** Representative thermal images of the experimental animals, n=10~14 per group **(b)** Interscapular temperature calculated from thermal images, n=10~14 per group. **(c)** Expression profile of 5-HT metabolism related genes in BAT, n=8~21 per group. **(d)** Expression profile of thermogenesis related genes in BAT, n=8~21 per group. **(e)** *Adipoq* mRNA level in BAT, n=8~9 per group. All data are expressed as mean ± SEM via Student's t-test. *p<0.05; **p<0.01; ***p<0.001.

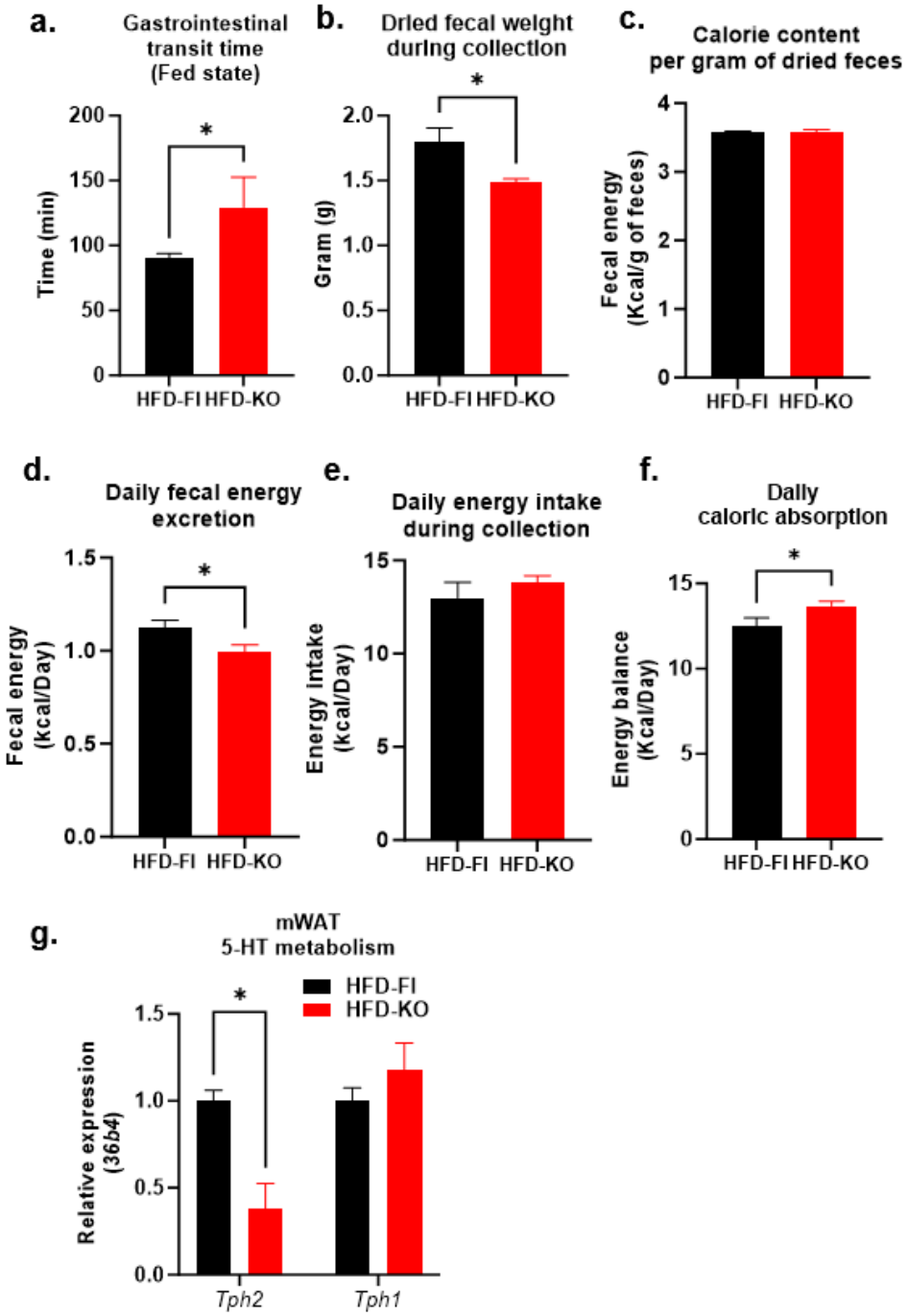

Figure 9. Adipocyte-specific TPH2 Deletion Reduce Gut Motility and Fecal Energy Loss. **(a)** Gastrointestinal transit time measured at week-12 of HFD feeding, n=10~14 per group **(b)** Freeze-dried weight of fecal samples collected for 5 days, n=9~10 per group. **(c)** Calorie level in a gram of freeze-dried fecal samples, n=9~10 per group. **(d)** Daily caloric loss through fecal excretion calculated by multiplying daily fecal output and fecal caloric level, n=9~10 per group. **(e)** Daily energy intake level during fecal collection, n=9~10 per group. **(f)** Daily caloric absorption in HFD-FI and KO mice, calculated by subtracting daily fecal energy loss from daily energy intake, n=9~10 per group. All data are expressed as mean ± SEM via Student's t-test. *p<0.05; **p<0.01; ***p<0.001; ****p<0.0001.

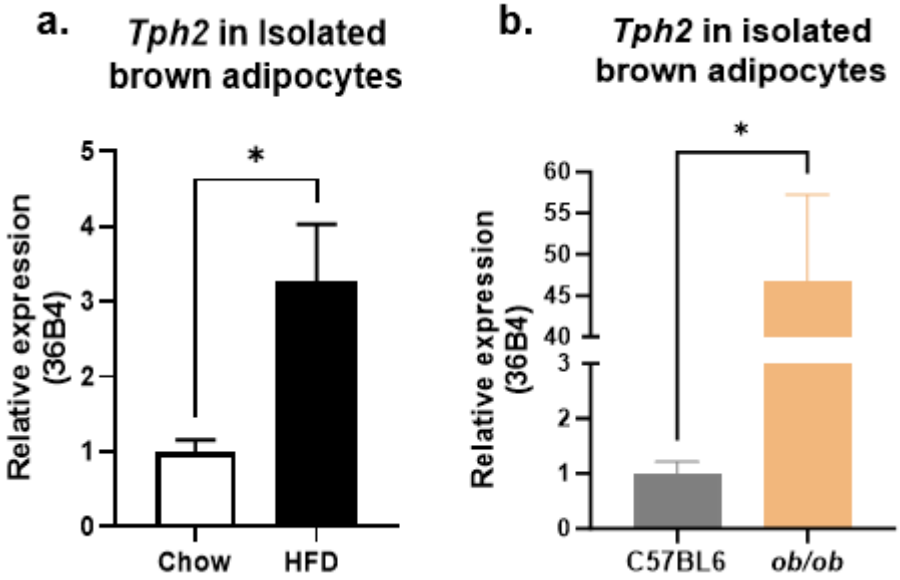

Figure S1. *Tph2* Gene Expression in Isolated Brown Adipocytes with HFD Feeding and Over-eating. (a) *Tph2* gene expression levels in isolated brown adipocytes after 6-week of HFD feeding, n=5 per group. **(b)** *Tph2* gene expression levels in isolated brown adipocytes after 6-week of Chow feeding, n=5 per group. All data are expressed as mean ± SEM via Student's t-test. *p<0.05

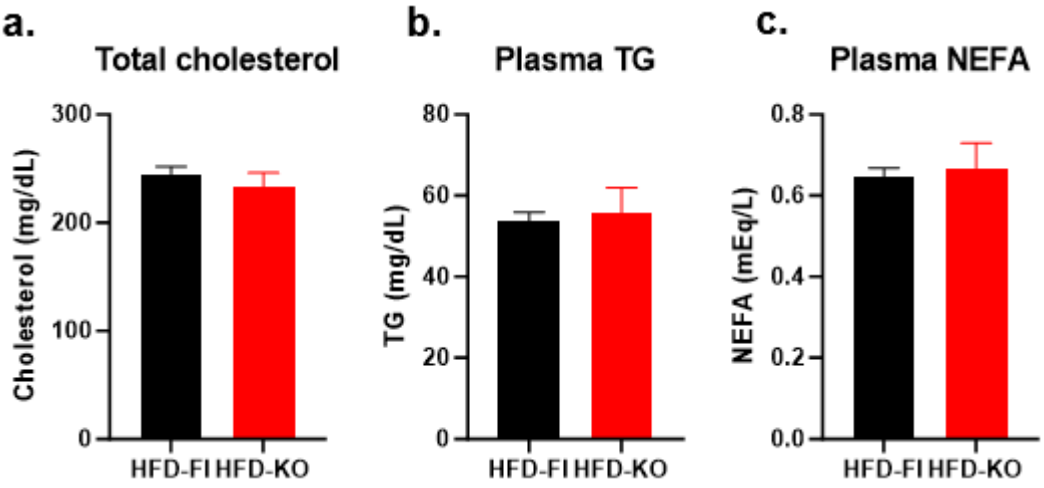

Figure S3. Fasting Plasma Lipid Profile of Each Group. **(a)** Plasma total cholesterol level in HFD-FI and KO mice, n=4~10. **(b)** Plasma NEFA level in HFD-FI and KO mice, n=4~10. **(c)** Plasma TG level in HFD-FI and KO mice, n=4~10. All data are expressed as mean ± SEM via Student's t-test.

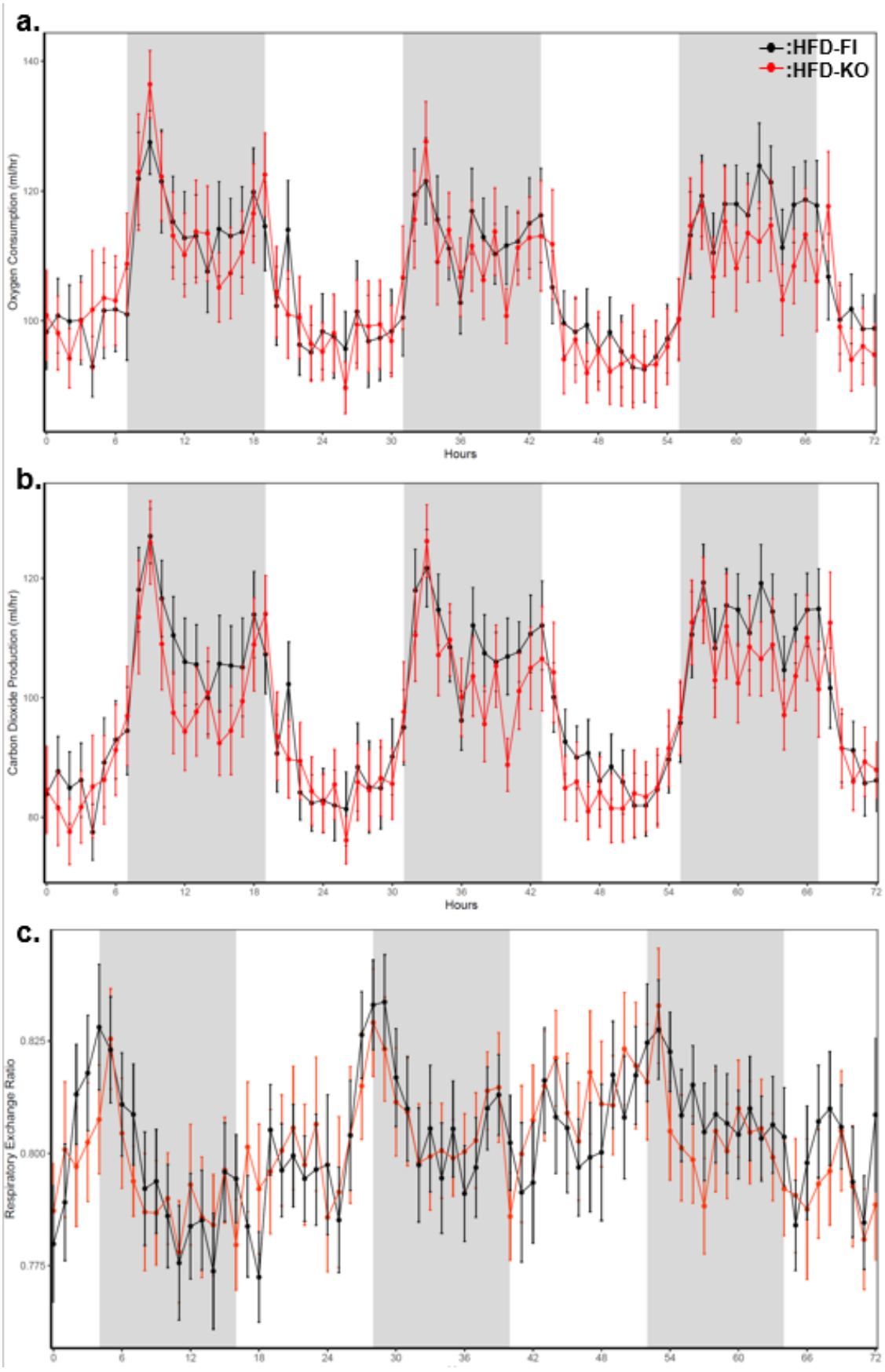
a.
:HFD-FI
:HFD-KO
Oxygen Consumption (ml/hr)
Hours
b.
Carbon Dioxide Production (ml/hr)
Hours
c.
Respiratory Exchange Ratio

Figure S4. Oxygen Consumption, Carbon Dioxide Production and RER in Indirect Calorimetry Analysis. **(a)** Time course oxygen consumption during the indirect calorimetry analysis, n=7~8. **(b)** Time course carbon dioxide production during the indirect calorimetry analysis, n=7~8. **(c)** Time course RER of mice during the indirect calorimetry analysis, n=7~8. All data are expressed as mean ± SEM.

Supplementary Table 1. Primer sequences used in this study.

Gene	Forward	Reverse
36b4	GAGGAATCAGATGAGGATATGGGA	AAGCAGGCTGACTTGGTTGC
Adipoq	CTCCACCCAAGGGAACTTGT	GGACCAAGAAGACCTGCATC
Atgl	TGTGGCCTCATTCCTCCTAC	TCGTGGATGTTGGTGGAGCT
Cdkn1a	CACAGCTCAGTGGACTGGAA	ACCCTAGACCCACAATGCAG
Cidea	GCCGTGTTAAGGAATCTGCTG	TGCTCTTCTGTATCGCCCAGT
Cd11b	CACTCAGTGACTGCCCAAAA	CCTCAAGACAGGACATCGCT
Cd36	TGGCCAAGCTATTGCGACAT	ACACAGCGTAGATAGACCTGC
Cd68	ACCGCCATGTAGTCCAGGTA	ATCCCCACCTGTCTCTCTCA
Fasn	GCTGCGGAAACTTCAGGAAAT	AGAGACGTGTCACTCCTGGACTT
F4/80	CTTTGGCTATGGGCTTCCAGTC	GCAAGGAGGACAGAGTTTATCGTG
Hsl	GGAGCACTACAAACGCAACGA	TCGGCCACCGGTAAAGAG
Igfbp3	TGTTTTCTGGTCCAGCCTCT	CAAGCCACTCCTCTTTCCTG
Il1b	CTGGTGTGTGACGTTCCCATT	CCGACAGCACGAGGCTTT
Maoa	GCGGTACAAGGGTCTGTTCC	CAGCCAATCCTGAGATGCCG
Mcp1	AGGTCCCTGTCATGCTTCTG	TCTGGACCCATTCCTTCTTG
Ppargc1a	GCCCAGGTACGACAGCTATG	ACGGCGCTCTTCAATTGCTT
Ppara	AGAAGTTGCAGGAGGGGATT	TCGGACTCGGTCTTCTTGAT
Pparg	GGTGTGATCTTAACTGCCGGA	GCCCAAACCTGATGGCATTG
Prdm16	AGCCCTCGCCCACAACTTGC	TGACCCCCGGCTTCCGTTCA
p53	TGGCTCCTCCCCAACATCTTATC	CTTCCTCTGTCCGACGGTCTCTC
Srebp1c	GGAGGGGTAGGGCCAACGGCCT	CATGTCTTCGAAAGTGCAATCC
Tnfa	ATGGGCTTTCCGAATTCAC	GAGGCAACCTGACCACTCTC
Tph1	ACCATGATTGAAGACAACAAGGAG	TCAACTGTTCTCGGCTGATG
Tph2	GCCATGCAGCCCGCAATGATGATG	CAACTGCTGTCTTGCTGCTC
Ucp1	CTTTGCCTCACTCAGGATTGG	CTTTGCCTCACTCAGGATTGG

3.6. References

1. James, W. P. T. The epidemiology of obesity: The size of the problem. *J. Intern. Med.* **263**, 336–352 (2008).

2. Wang, Y., Beydoun, M. A., Liang, L., Caballero, B. & Kumanyika, S. K. Will all Americans become overweight or obese? Estimating the progression and cost of the US obesity epidemic. *Obesity* **16**, 2323–2330 (2008).

3. Lega, I. C. & Lipscombe, L. L. Review: Diabetes, Obesity, and Cancer-Pathophysiology and Clinical Implications. *Endocr. Rev.* **41**, (2020).

4. Waddell, T. *et al.* Greater ectopic fat deposition and liver fibroinflammation and lower skeletal muscle mass in people with type 2 diabetes. *Obesity* **30**, 1231–1238 (2022).

5. Keszthelyi, D., Troost, F. J. & Masclee, A. A. M. Understanding the role of tryptophan and serotonin metabolism in gastrointestinal function. *Neurogastroenterol. Motil.* **21**, 1239–1249 (2009).

6. Namkung, J., Kim, H. & Park, S. Peripheral serotonin: A new player in systemic energy homeostasis. *Mol. Cells* **38**, 1023–1028 (2015).

7. Tidemand, K. D., Peters, G. H., Harris, P., Stensgaard, E. & Christensen, H. E. M. Isoform-Specific Substrate Inhibition Mechanism of Human Tryptophan Hydroxylase. *Biochemistry* **56**, 6155–6164 (2017).

8. Mohammad-Zadeh, L. F., Moses, L. & Gwaltney-Brant, S. M. Serotonin: A review. *J. Vet. Pharmacol. Ther.* **31**, 187–199 (2008).

9. Berger, M., Gray, J. A. & Roth, B. L. The expanded biology of serotonin. *Annu. Rev. Med.* **60**, 355–366 (2009).

10. Yabut, J. M. *et al.* Emerging Roles for Serotonin in Regulating Metabolism: New Implications for an Ancient Molecule. *Endocrine Reviews* vol. 40 1092–1107 (2019).

11. Paulmann, N. *et al.* Intracellular serotonin modulates insulin secretion from pancreatic β-cells by protein serotonylation. *PLoS Biol.* **7**, e1000229 (2009).

12. Young, R. L. *et al.* Augmented capacity for peripheral serotonin release in human obesity. *Int. J. Obes.* **42**, 1880–1889 (2018).

13. Gallagher, T. K., Geoghegan, J. G., Baird, A. W. & Winter, D. C. Implications of altered gastrointestinal motility in obesity. *Obes. Surg.* **17**, 1399–1407 (2007).

14. Margolis, K. G. *et al.* Pharmacological reduction of mucosal but not neuronal serotonin opposes inflammation in mouse intestine. *Gut* **63**, 928–937 (2014).

15. Sikander, A., Rana, S. V. & Prasad, K. K. Role of serotonin in gastrointestinal motility and irritable bowel syndrome. *Clin. Chim. Acta* **403**, 47–55 (2009).

16. Gullikson, G. W., Loeffler, R. F. & Virina, M. A. Relationship of serotonin-3 receptor antagonist activity to gastric emptying and motor-stimulating actions of prokinetic drugs in dogs. *J. Pharmacol. Exp. Ther.* **258**, 103–110 (1991).

17. Zha, W., Ho, H. T. B., Hu, T., Hebert, M. F. & Wang, J. Serotonin transporter deficiency drives estrogen-dependent obesity and glucose intolerance. *Sci. Rep.* **7**, (2017).

18. Chen, X., Margolis, K. J., Gershon, M. D., Schwartz, G. J. & Sze, J. Y. Reduced serotonin reuptake transporter (SERT) function causes insulin resistance and hepatic steatosis independent of food intake. *PLoS One* **7**, 32511 (2012).

19. Zha, W., Hu, T., Hebert, M. F. & Wang, J. Effect of pregnancy on paroxetine-induced adiposity and glucose intolerance in mice. *J. Pharmacol. Exp. Ther.* **371**, 113–120 (2019).

20. Crane, J. D. *et al.* Inhibiting peripheral serotonin synthesis reduces obesity and metabolic dysfunction by promoting brown adipose tissue thermogenesis. *Nat. Med.* **21**, 166–172 (2015).

21. Oh, C. M. *et al.* Regulation of systemic energy homeostasis by serotonin in adipose tissues. *Nat. Commun.* **6**, (2015).

22. Shong, K. E., Oh, C. M., Namkung, J., Park, S. & Kim, H. Serotonin regulates de novo lipogenesis in adipose tissues through serotonin receptor 2a. *Endocrinol. Metab.* **35**, 470–479 (2020).

23. Hageman, R. S. *et al.* High-fat diet leads to tissue-specific changes reflecting risk factors for diseases in DBA/2J mice. *Physiol. Genomics* **42**, 55–66 (2010).

24. Choi, M. S. *et al.* High-fat diet decreases energy expenditure and expression of genes controlling lipid metabolism, mitochondrial function and skeletal system development in the adipose tissue, along with increased expression of extracellular matrix remodelling- and inflamm. *Br. J. Nutr.* **113**, 867–877 (2015).

25. El-Merahbi, R., Löffler, M., Mayer, A. & Sumara, G. The roles of peripheral serotonin in metabolic homeostasis. *FEBS Letters* vol. 589 1728–1734 (2015).

26. Mina, A. I. *et al.* CalR: A Web-Based Analysis Tool for Indirect Calorimetry Experiments. *Cell Metab.* **28**, 656-666.e1 (2018).

27. Murphy, E. F. *et al.* Composition and energy harvesting capacity of the gut microbiota: Relationship to diet, obesity and time in mouse models. *Gut* **59**, 1635–1642 (2010).

28. Livak, K. J. & Schmittgen, T. D. Analysis of relative gene expression data using real-time quantitative PCR and the 2-ΔΔCT method. *Methods* **25**, 402–408 (2001).

29. Singhal, M. *et al.* Serotonin Transporter Deficiency is Associated with Dysbiosis and Changes in Metabolic Function of the Mouse Intestinal Microbiome. *Sci. Rep.* **9**, (2019).

30. Giordano, A. *et al.* White adipose tissue lacks significant vagal innervation and immunohistochemical evidence of parasympathetic innervation. *Am. J. Physiol. - Regul. Integr. Comp. Physiol.* **291**, (2006).

31. Sumara, G., Sumara, O., Kim, J. K. & Karsenty, G. Gut-derived serotonin is a multifunctional determinant to fasting adaptation. *Cell Metab.* **16**, 588–600 (2012).

32. Wei, L. *et al.* Serotonin Deficiency Is Associated With Delayed Gastric Emptying. *Gastroenterology* **160**, 2451-2466.e19 (2021).

33. Akiho, H. The role of serotonin in irritable bowel syndrome. *Constipation Irrit. Bowel Syndr. Causes, Treat. Prev.* **10**, 109–121 (2012).

34. Xing, J. & Chen, J. D. Z. Alterations of gastrointestinal motility in obesity. *Obes. Res.* **12**, 1723–1732 (2004).

35. Al Mushref, M. & Srinivasan, S. Effect of high fat-diet and obesity on gastrointestinal motility. *Ann. Transl. Med.* **1**, 1–11 (2013).

36. Topping, D. L. & Clifton, P. M. Short-chain fatty acids and human colonic function: Roles of resistant starch and nonstarch polysaccharides. *Physiol. Rev.* **81**, 1031–1064 (2001).

37. McNeil, N. I., Cummings, J. H. & James, W. P. T. Short chain fatty acid absorption by the human large intestine. *Gut* **19**, 819–822 (1978).

38. Venter, C. S., Vorster, H. H. & Cummings, J. H. Effects of Dietary Propionate on Carbohydrate and Lipid Metabolism in Healthy Volunteers. *Am. J. Gastroenterol.* **85**, 549–553 (1990).

39. McNeil, N. I., Cummings, J. H. & James, W. P. T. Short chain fatty acid absorption by the human large intestine. *Gut* **19**, 819–822 (1978).

40. Reilly, K. J. & Rombeau, J. L. Metabolism and potential clinical applications of short-chain fatty acids. *Clin. Nutr.* **12**, S97–S105 (1993).

41. Turnbaugh, P. J. *et al.* An obesity-associated gut microbiome with increased capacity for energy harvest. *Nature* **444**, 1027–1031 (2006).

42. Sanmiguel, C., Gupta, A. & Mayer, E. A. Gut Microbiome and Obesity: A Plausible Explanation for Obesity. *Curr. Obes. Rep.* **4**, 250–261 (2015).

43. Gonçalves, P., Magro, F. & Martel, F. Metabolic inflammation in inflammatory bowel disease: Crosstalk between adipose tissue and bowel. *Inflamm. Bowel Dis.* **21**, 453–467 (2015).

44. Peyrin-Biroulet, L. *et al.* Mesenteric fat in Crohn's disease: A pathogenetic hallmark or an innocent bystander? *Gut* **56**, 577–583 (2007).

45. Choi, W. *et al.* Serotonin signals through a gut-liver axis to regulate hepatic steatosis. *Nat. Commun.* **9**, (2018).

Chapter 4. Limitations and future directions

4.1. Limitations

The projects presented in this dissertation utilized both AAV induced over-expression and Cre-loxP knockout mice model to comprehensively investigate the role of adipocyte-specific Tph2 on systemic and adipocyte physiology and metabolism, which provided a novel insight into pathogenesis of obesity-induced metabolic complications. Yet, there are noteworthy limitations that must be considered.

Chapter 2

In this chapter, we explored the role of epididymal adipocyte-specific Tph2 on developing adipocyte dysfunction and impaired metabolic homeostasis. However, some mice developed malocclusion during the experimental period, we had to remove those mice from the whole experiment, resulting in inadequate power for several analyses. Another key limitation is that we used the whole eWAT for molecular analysis, but cell population in WAT is very heterogeneous, which could confound the results from certain experiments. Tph2 Oex eWAT had significantly reduced mRNA levels of Atgl and Hsl, suggesting decreased lipolysis. However, we did not determine phosphorylation of these enzymes to provide direct evidences for decreased lipolytic activity. We demonstrated that Tph2 Oex mice had higher 4-HNE formation in eWAT, liver and plasma, but not in iWAT, demonstrating possible 4-HNE trafficking from eWAT to liver. However, it is possible that liver 4-HNE could be derived from hepatic steatosis induced oxidative stress, not from eWAT. Also, we proposed that hydrogen peroxide produced from 5-HT degradation contributed to the formation of 4-HNE, but we did not

present direct evidence for this process. Previous literatures well documented the association between 4-HNE and p53 signaling, and we also observed increased p53 signaling in Tph2 Oex eWAT. However, it is possible that increased adiposity or inflammation in eWAT activated p53 signaling, not 4-HNE. Adipocyte p53 signaling is strongly correlated with adipocyte dysfunction and formation of crown-like structures. We provided some evidence for adipocyte dysfunction with TPH2 over-expression, but none on the formation of crown-like structures. We also reported the significant decrease of *adipoq* gene expression level in BAT, however we did not show this decrease actually connected to reduced level of BAT or circulating adiponectin. Furthermore, we reported that pro-inflammatory cytokine mRNA levels in eWAT and BAT were significantly increased, however we did not determine the actual cytokine levels or infiltration of immune cells to confirm Tph2 over-expression induced inflammation.

Chapter 3

In this chapter, we generated adipocyte-specific TPH2 knockout mice to investigate the role of TPH2 on developing DIO and obesity-associated pathologies. We showed that Tph2 gene expression was diminished in Chow-Ko eWAT, however in HFD-Ko eWAT, the mRNA level of *Tph2* was reduced by approximately 0.5-fold compared to that of HFD-Fl mice. We further analyzed *Tph2* mRNA levels in isolated epididymal adipocytes and observed an 80% reduction, although complete ablation was not achieved. HFD-KO mice gained body and fat mass with HFD feeding, while their eWAT mass was significantly lower than HFD-Fl mice. We proposed that increase

in lipolysis gene expression contributed to decrease in eWAT mass, however decreased mRNA levels of *Atgl* and *Hsl* are indirect evidence for reduced lipolysis. Furthermore, in HFD-KO eWAT, we observed decreased pro-inflammatory cytokine, p53 signaling and adiponectin gene expression levels, however we did not provide the data that prove direct changes in reduced inflammation, inhibited p53 signaling or increased adiponectin level., which could be possible molecular mechanisms for the beneficial effect of TPH2 deficiency. HFD-KO liver had significantly less hepatic lipid accumulation and liver damage. It is evident that the loss of adipocyte TPH2 improved DIO induced liver dysfunction, however the underlying molecular mechanism for this effect is not elucidated. Furthermore, we observed the increased BAT activation and systemic energy expenditure with the loss of adipocyte TPH2. Previous studies reported the role of adipocyte-derived 5-HT on inhibition of BAT thermogenesis via 5-HTR_{3a}. We speculated that this is also the molecular mechanism of BAT activation in HFD-KO mice, however we did not quantify circulating or BAT 5-HT levels, or stimulate BAT 5-HTR_{3a} signaling to see whether this reduces BAT activation in HFD fed $TPH2^{loxP/loxP}$ with Adipoq-Cre mice. We provided evidences that demonstrates the role of adipocyte TPH2 in regulating gut motility and fecal energy loss. Energy loss from fecal output was significantly lower in HFD-KO mice, suggesting possible caloric compensation for increased systemic energy expenditure. We proposed these changes were mediated by reduced 5-HT from HFD-KO mWAT, however the molecular mechanisms for this effect are not identified.

4.2. Future directions

Chapter 2

To overcome aforementioned limitations, it would be worthwhile to repeat the AAV induced epididymal adipocyte-specific TPH2 over-expression model to ensure adequate power for the analyses. We demonstrated the impaired systemic glucose tolerance and insulin sensitivity with TPH2 over-expression, however the relative contribution to this impairment from adipose tissue, liver and muscle is not determined. To delineate the role of each tissue on developing adipocyte TPH2 induced glucose intolerance and insulin resistance, hyperinsulinemic/euglycemic clamp should be performed to identify tissue-specific effect of TPH2 over-expression. We demonstrated epididymal adipocyte TPH2 over-expression altered gene expression profiles in various tissues. We did not determine that the changes in gene expression level actually translated into protein or activation of pathways. To circumvent this, western blot analysis should be performed to evaluate phosphorylated protein levels of ATGL, HSL, and UCP1 and p53 protein levels. Furthermore, we hypothesized that eWAT 5-HT derived 4-HNE could be transported to liver and induce hepatic dysfunction and steatosis. Immunostaining revealed that Tph2 Oex liver had elevated 4-HNE fluorescence, however this is not the direct evidence for 4-HNE trafficking between eWAT and liver. To investigate this association, radiolabeled 4-HNE could be injected into mice and analyze the presence of radiolabeled 4-HNE in liver and other tissues. We found significant downregulation of *Adipoq* gene expression level in Tph2 Oex BAT. It would be interesting to verify whether this change connected to the alterations in BAT and systemic adiponectin levels. Lastly, we hypothesized that peripheral 5-HT not

only regulates energy metabolism via 5-HTR signaling, but also intracellular pathways such as 4-HNE formation and p53 signaling. To delve deeper into this hypothesis, we could induce over-expression of ALDH2 in TPH2 over-expressing adipocytes to examine whether inhibition of 4-HNE accumulation could reverse the observed adipocyte dysfunctions in Tph2 Oex mice.

Chapter 3

Current project demonstrated that dramatic upregulation of Tph2 expression in obese WATs are mediated by increased adiposity, however we still don't know the adiposity induced molecular changes which drive Tph2 upregulation. We should perform single cell RNAseq analysis to identify the regulatory pathway of Tph2 expression. HFD-KO mice had significantly reduced 5-HT levels in eWAT, demonstrating the contribution of adipocyte TPH2 in producing 5-HT. Previous studies have demonstrated that while adipocyte-specific knockout of TPH1 significantly reduced 5-HT levels in adipose tissues, it did not result in any alterations to circulating 5-HT levels. We also need to determine 5-HT levels in BAT, mWAT and blood to systemically assess the contribution of adipocyte TPH2 in peripheral 5-HT levels. The regulatory roles of 5-HT in glucose homoeostasis in liver and eWAT is extensively explored. However, the effect of 5-HT on mWAT and muscle metabolism is poorly understood. Thus, it would be worthwhile to investigate TPH2 derived 5-HT induced molecular changes in mWAT and muscle tissues. Moreover, in Tph2 Oex mice, we demonstrated that the loss of adipocyte TPH2 could reduce the fecal output, resulting in decreased fecal calorie loss. It is well established that 5-HT modulates smooth

muscle contraction through 5-HTR_4 signaling. It would be helpful to conduct selective pharmacological activation of 5-HTR_4 in HFD-KO mice and evaluate gut motility and fecal output. HFD-KO mice exhibited significant improvement in hepatic steatosis and liver damage compared to HFD-Fl mice. However, the underlying molecular mechanism of this improvement is not fully understood. Other groups demonstrated that peripheral 5-HT promotes hepatic lipid accumulation through 5-HTR_{2a} signaling. However, we still lack the direct evidence that shows the loss of adipocyte TPH2 reduced 5-HTR_{2a} signaling. It would be worthwhile to investigate the effect of 5-HTR_{2a} agonist on HFD-KO liver function to identify the molecular mechanism of this protective effects. Additionally, we observed significantly increased systemic energy expenditure in HFD-KO mice. Previous studies reported that peripheral 5-HT could inhibit BAT thermogenesis by binding to 5-HTR_3. However, in chapter 2, we also found that adipocyte TPH2 derived 5-HT could affect systemic metabolism through alternative pathways, such as 4-HNE and p53 signaling. Thus, it would be logical to investigate the effect of 5-HTR_3 agonist on the BAT of HFD-KO mice, and also 4-HNE levels in WATs and plasma of HFD-KO mice. Lastly, adipocyte-specific loss of TPH2 decreased gut motility in mice, which could significantly affect the gut microbiome profile. Furthermore, host and gut microbes 5-HT metabolism have close relationship, thus it would be worthwhile to assess the changes in gut microbiome profile with the loss of adipocyte TPH2 expression.